UNIVERSITÀ DEGLI STUDI DEL PIEMONTE ORIENTALE

Dipartimento di Medicina Traslazionale

Corso di Dottorato di Ricerca in Scienze e Biotecnologie Mediche

Ciclo XXIX

Defining the causal association between human beta papillomavirus infection, keratinocyte stem cells expansion and skin cancer development

Coordinatore

Prof.ssa Marisa Gariglio

Tutor

Prof.ssa Marisa Gariglio

Dottoranda

Carlotta Olivero

1. SUMMARY **2**
2. INTRODUCTION **7**
2.1 PAPILLOMAVIRUSES **8**
2.1.1 General features **8**
2.1.2 Classification, evolution, tropism and disease association **9**
2.1.3 HPV structure, genomic organization and life cycle **13**
2.1.4 High-risk α-HPVs and cervical carcinogenesis **18**
2.2 β-HPV AND KERATINOCYTE CARCINOMAS **20**
2.2.1 Epidermodysplasia verruciformis **21**
2.2.2 β-HPV infection in the immunocompromised host **24**
2.2.3 Molecular mechanisms underling β-HPV-induced skin cancer **27**
2.2.4 Mouse models to investigate β-HPV role in keratinocyte carcinoma development **30**
2.3 KERATINOCYTE STEM CELLS **32**
2.3.1 General characteristics of keratinocyte stem cell (KSC) **32**
2.3.2 Hair Follicle-Keratinocyte Stem Cells (HF-KSC) features **35**
2.3.3 Interfollicular epidermis - keratinocyte stem cells (IFE-KSC) features **38**
3. AIMS **41**
4. RESULTS **44**
4.1 HPV8 Field Cancerization in a Transgenic Mouse Model is due to Lrig1+ Keratinocyte Stem Cell Expansion (Accepted for publication in Journal of Investigative Dermatology, April 2017) **45**
4.2 Understanding the natural history of β-HPV infection in skin lesions and their malignant progression using tumourgraft models **60**
4.3 Establishment of an immunodeficient HPV8tg mouse model that recapitulates the events occurring in OTR **72**
5. CONCLUSIONS **79**
6. REFERENCES **85**

1. SUMMARY

1. Summary

Human papillomaviruses (HPVs) are small non-enveloped viruses with a double-stranded DNA genome that infect cutaneous or mucosal squamous stratified epithelia of different body sites. They can establish infections that usually remain latent in healthy individuals but also be responsible for the development of benign or neoplastic proliferative lesions, depending on the specific oncogenic properties of the different types. To date, more than 180 HPV types have been completely sequenced and classified into five genera based on phylogenetic analyses. The Alpha genus (α-HPVs) is the best characterized and comprises mucosa-tropic types associated with the development of genital cancer (e.g. HPV 16, 18). HPVs belonging to the skin-tropic Beta genus (β-HPVs, e.g. HPV 5 and 8) appear to cause widespread unapparent asymptomatic infections without associated disease in the general population. In patients with epidermodysplasia verruciformis (EV), an inherited primary immunodeficiency characterized by a high susceptibility to β-HPV infection, these viruses replicate very efficiently and reveal their full transforming potential, inducing disseminated wart-like lesions and driving their progression to Keratinocyte Carcinomas (KC).

Although their involvement in skin carcinogenesis in both immunocompetent and non-EV immunocompromised patients (either primary or acquired immunocompromised) is still a matter of debate, both experimental and epidemiological evidence suggests a carcinogenic role of these viruses in the skin that takes place at the early stages and contribute to the pathogenesis of KC. Previous studies from our group shown detection of viral gene products and viral genome amplification in precancerous skin lesion derived from OTR (Organ Transplant Recipient). These results greatly strengthen the evidence for an involvement of β-HPVs in the pathogenesis of KC.

Based on these finding, we focused on understanding the molecular mechanisms underlying β-HPV-induced KC in immunocompromised patients through different approaches, including the HPV8 transgenic mouse model and in vivo tumorigenicity assays of tumours from OTRs.

When considering the involvement of β-HPV in the development of KC, it is important to examine where β-HPV is localized. The current hypothesis is that the reservoir for β-HPV resides within long-lived hair follicle keratinocyte stem cells (HF-KSC), however, the precise HF-KSC populations involved in β-HPV latent infection remain to be defined. To determine the role of HF-KSC in β-HPV induced skin carcinogenesis, we utilized a transgenic mouse model in which the keratin 14 promoter drives expression of the entire HPV8 early region

(HPV8tg). HPV8tg mice developed thicker skin in comparison to wild type littermates consistent with a hyperproliferative epidermis. HF keratinocyte proliferation was evident within the Lrig1+ KSC population (69 vs 55%, $p<0.001$, n=6), and not in the CD34+, LGR5+ and LGR6+ KSC populations. This was associated with a 2.8-fold expansion in Lrig1+ keratinocytes and 3.8 fold increased colony forming efficiency. Consistent with this, we observed nuclear p63 expression throughout this population and in the HF infundibulum and adjoining IFE, associated with a switch from p63 TA isoforms to ΔNp63 isoforms in HPV8tg skin. EV keratosis and in some cases actinic keratoses demonstrated similar histology associated with β-HPV virus reactivation and nuclear p63 expression within the HF infundibulum and perifollicular epidermis. These findings would suggest that β-HPV field cancerization arises from the HF junctional zone and predispose to squamous cell carcinoma (SCC).

In addition, we have established an *in vivo* orthotopic humanized xenograft model using skin tumours from OTR. This technique allow to increase the availability of the tumours -that is usually a limitation in skin cancer research-, to investigate detailed molecular mechanisms of the events driving tumorigenesis and to identify β-HPV infection/expression in these lesions. Therefore, this methodology provides a highly promising *ex vivo* environment in which to study the progression of the disease from pre-malignancy to malignancy, e.g. from an AK to a SCC as reported in this thesis, which cannot be documented in the human beings due to the necessary excision of such tumours.

However, it remains to be determined whether immunosuppression also facilitates carcinogenesis by inhibiting tumour immune surveillance and killing. To test this hypothesis and generate a mouse model recapitulating the events occurring in OTR, we have crossed the HPV8 transgenic mice (FVB/N genetic background) with Rag2 deficient mice (which lack B and T cells; C57BL/6 genetic background). The results so far obtained with the F2 generation indicate that immunosuppression facilitates carcinogenesis by inhibiting tumour immune surveillance, as the number of skin lesions and their degree of dysplasia in HPV8+:$Rag2^{-/-}$ mice was found increased when compared to the HPV8tg+:$Rag2^{+/+}$ mice.

Overall, the results obtained in this study advance our understanding of the molecular mechanisms underlying β-HPV infection and strengthen the hypothesis of a causative role for these viruses in keratinocyte carcinoma development.

1. Sommario

I papillomavirus umani (HPV) sono piccoli virus nudi contenenti un genoma a doppia elica di DNA circolare di 8 kb che infettano gli epiteli squamosi stratificati cutanei e mucosali di differenti distretti corporei. Gli HPV possono stabilire infezioni latenti in individui sani, ma inducono anche lesioni neoplastiche benigne o maligne in base alle proprietà oncogene specifiche dei differenti genotipi. Fino ad oggi sono stati identificati più di 180 genotipi differenti di HPV che sono stati classificati in 5 generi sulla base dell'analisi filogenetica. Il genere Alpha (α-HPV) è il più caratterizzato e comprende i genotipi a tropismo mucosale associati all' insorgenza di carcinoma a livello genitale (ad esempio HPV16 e 18). Gli HPV appartenenti al genere β (β-HPV) sono evoluzionisticamente distinti dal genere α e causano infezioni inapparenti o asintomatiche molto diffuse nella popolazione generale. Nei pazienti affetti da epidermodisplasia verruciforme (EV), una immunodeficienza primaria caratterizzata da un'alta suscettibilità all'infezione da β-HPV, questi virus replicano con alta efficienza, sviluppano il loro pieno potenziale trasformante, inducendo numerose lesioni simil verrucose con alto rischio di progressione a carcinoma cutaneo .

Sebbene il loro coinvolgimento nel processo di carcinogenesi cutanea in pazienti immunocompetenti e immunosoppressi non-EV (con immunosoppressione primaria o acquisita) è ancora materia di dibattito, numerose evidenze epidemiologiche e sperimentali suggeriscono un ruolo carcinogenico di questi virus che inizia nelle fasi precoci e contribuisce alla patogenesi del carcinoma cutaneo. Il nostro gruppo ha dimostrato precedentemente la presenza di prodotti dei geni virali e l'amplificazione del genoma virale in lesioni cutanee precancerose derivate da pazienti trapiantati d'organo (OTR, Organ Transplant Recipient). Questi risultati rafforzano l'evidenza di un coinvolgimento dei β-HPVs nella patogenesi del carcinoma cutaneo.

Sulla base dei dati già acquisiti, abbiamo studiato i meccanismi molecolari alla base dell'induzione del carcinoma cutaneo indotto da β-HPV in pazienti immunocompromessi attraverso differenti approcci, quali il modello di topo transgenico HPV8 e il saggio di tumorigenicita' *in vivo* di tumori derivati da OTR.

Pe capire il ruolo di β-HPV nello sviluppo del carcinoma cutaneo, è importante conoscere dove questo virus naturalmente si localizza. L'ipotesi attuale è che il reservoir di β-HPV risieda in cellule staminali con ciclo cellulare rallentato presenti nel follicolo pilifero (HF-KSC); tuttavia, la precisa popolazione di HF-KSC coinvolta nell'infezione latente di β-HPV è ancora sconosciuta. Per determinare il ruolo delle HF-KSC nel carcinoma cutaneo indotto da β-HPV,

abbiamo utilizzato un modello di topo transgenico nel quale il promotore della cheratina 14 guida l'espressione della regione precoce di HPV8 (HPV8tg). I topi HPV8tg presentano uno spessore della cute piu' ampio rispetto ai topi wild type e mostrano una cute iperproliferante. La proliferazione dei cheratinociti del follicolo pilifero è evidente nella popolazione di cellule staminali Lrig1+ (69 vs 55%, p<001, n=6), ma non lo è nelle popolazioni CD34+, LGR5+ e LGR6+. Questo è in linea con l'osservazione dell'espanzione dei cheratinociti Lrig1+ di 2,8 volte e dell'efficienza di formare colonie di 3.8 volte. In accordo con questi risultati, abbiamo osservato l'espressione nucleare di p63 in questa popolazione, nell'infindibulum e nella cute interfollicolare fiancheggiante, associata a un cambiamento di espressione tra la forma TA di p63 in ΔNp63 nella cute dei topi HPV8tg. Le cheratosi dei pazienti EV e alcune cheratosi attiniche (AK) di pazienti non EV mostrano un istologia simile associata alla riattivazione di β-HPV e all'espressione nucleare di p63 nell' infindibulum e nella cute perifollicolare. Questi dati suggeriscono che il campo di cancerizzazione indotto da β-HPV inizia dalla "junctional zone" e predispone al carcinoma cutaneo..

Inoltre abbiamo realizzato un modello umanizzato di xenotrapianto ortotopico utilizzando tumori cutanei derivati da OTR. Questa tecnica permette di aumentare la disponibilità dei tumori cutanei – che è una delle limitazioni nell'ambito della ricerca sui tumori cutanei-, analizzare in dettaglio i meccanismi molecolari coinvolti nella tumorigenesi e identificare l'infezione e l'espressione di β-HPV in queste lesioni. Inoltre, questa tecnica permette di studiare la progressione della malattia da una situazione pre-cancerosa a una cancerosa, ad esempio da AK a SCC come riportato in questa tesi, che non può essere studiato a livello umano per la naturale necessità di rimuovere la lesione prima dell'evoluzione maligna.

In questo contesto, rimane da stabilire se l'immunosoppressione faciliti la carcinogenesi anche attraverso la riduzione dell'immunosorveglianza. Per verificare questa ipotesi e generare un modello murino che ricapitolasse gli eventi che si verificano nei pazienti trapiantati, abbiamo incrociato i topi transgenici HPV8 (background genetico FVB/N) con i topi deficienti per il gene RAG2 (background genetico C57BL/6), che non producono cellule B e T. I risultati ottenuti fino ad ora con la generazione F2 indicano che l'immunosoppressione facilita la carcinogenesi anche inibendo l'immunosorveglianza del tumore, come dimostrato dai dati ottenuti; infatti,il numero di tumori cutanei nella cute dei topi HPV8+:Rag2$^{-/-}$ e il loro grado di displasia è risultato significativamente maggiore rispetto ai topi HPV8+:Rag2$^{+/+}$.

Nell'insieme, i risultati ottenuti in questo studio contribuiscono a chiarire la storia naturale dell'infezione da β-HPV e rafforzano l'ipotesi di un ruolo di questi virus nello sviluppo del tumore cutaneo.

2. INTRODUCTION

2.1 PAPILLOMAVIRUSES

2.1.1 General features

Papillomaviruses (PV) are small non-enveloped viruses with an icosahedral capsid and a circular double-stranded DNA genome of 8Kb in length. They are species-specific and exhibit a strict tropism for the squamous stratified epithelia where they can induce cutaneous and mucosal hyperplastic lesions in a broad spectrum of vertebrates, including humans, other mammalians, birds and reptiles (Doorbar et al., 2012).

Human Papillomaviruses (HPV) can infect different body sites, such as the upper respiratory, oral and genital mucosae, and the skin according to the specific tropism of the different viral species. HPV prevalence has increased in many parts of the world during the past few decades. They typically establish persistent infections which can either remain in an unapparent silent status or cause clinical manifestations after a latency period of variable duration; reactivation of latent HPVs seems to be favored by several conditions affecting the host, such as immune status, genetics, environmental and unknown factors. HPVs can be responsible not only for benign hyperproliferative lesions (papillomas) in mucosal and cutaneous sites, but also for malignancies (especially squamous cell carcinoma, SCC) depending on their ability to establish chronic infections and stimulate cellular proliferation (Akgül et al., 2006).

HPVs have been implicated in cancers at several sites; in particular, the best documented HPV oncogenic activity concerns cervical cancer, where the association between HPV infection and the onset of precancerous lesions that can subsequently progress to high-grade tumours is well defined. Roughly 610000 new cancer cases per year (among these, 530000 cervical cancer cases) have been attributed to HPV infection, of which more than 80% in developing countries (Crosbie et al., 2013).

Although the causal association of HPV infection with cervical carcinogenesis is epidemiologically and experimentally ascertained, its implication in the development of precancerous skin lesions that can evolve to high-grade tumors of epithelial origin – comprehensively grouped into the Keratinocyte Carcinomas (KCs: basal and squamous cell carcinomas) – has been much less clear to date; such uncertainties partly come from the fact that cutaneous HPVs have been shown to be ubiquitously present in the skin in the general healthy population. Nevertheless, several epidemiologic and experimental evidences are in

favour of their potential oncogenic role in the insurgence of skin lesions (Knipe & Howley, "Fields Virology, 4th edition", 2001; Pfister, 2003).

2.1.2 Classification, evolution, tropism and disease association

Papillomaviruses were originally grouped together with Polyomaviruses (PyVs) in a family called Papovaviridae; this classification was based on similarities in the capsid proteins and some proteins involved in viral replication and on the fact that these were the only viruses with circular double-stranded DNA genomes anxd a non-enveloped icosahedral capsid. Subsequently PVs and PyVs were split into two different viral families (Papillomaviridae and Polyomaviridae) because of substantial differences in genomic sequence, organization and size (de Villiers et al., 2004; Bernard, 2013).

After many years of research and genomic sequencing of thousands of PV isolates, PV classification was based on phylogenetic criteria following hierarchical taxonomic levels (family, genus, species, types, subtypes and variants). The L1 gene, encoding the major capsid protein, represents the most conserved gene of the PV genome, showing clusters of sequence similarity throughout its whole length among different PVs; for this reason, L1 nucleotide sequence is used to perform comparative alignments for PV identification and classification. By this approach, more than 200 PV types have been discovered to date, encompassing more than 180 HPV types and 103 animal PV types (Figure 1; http://pave.niaid.nih.gov/#home).

A novel PV type is established when L1 nucleotide sequence exhibits at least 10% diversity from the closest known PV type; 2-10% diversity define a PV subtype, while less than 2% diversity introduce a PV variant. Different PV genera share less than 60% sequence identity and different PV species belonging to the same genus share 60-70% sequence identity; finally, PV types belonging to the same species share 71-89% sequence identity (de Villiers et al., 2004; Forslund, 2007; Bernard et al., 2010; Bernard, 2013).

PV phylogenetic analyses indicate that PV evolution is linked to their hosts. A major part of PV evolutionary diversification must have proceeded clearly through mechanisms that restrict PVs to their host species; these host-virus associations strongly suggest that PV phylogenetic trees reflect a time scale similar to the host phylogenetic trees and that specific events in host evolution may have created new ecological niches for PV to adopt. However, it has also always been a generally accepted view that beyond host-linked evolution yet other evolutionary mechanisms drive PV diversification, as there exist remotely related PV taxa in

the same species, but in part separated by diverse target tissues (skin vs. mucosa); PVs and their hosts have not gone through an identical evolutionary path, even though initial niche sorting followed by host-virus co-speciation was a key determinant of the PV evolutionary history. Recombination may have played an important role during PV evolution, however it is likely that these events mainly occurred early in the evolutionary process; in addition, further mechanisms may have contributed to the current PV diversity, including host-switching and possible extinction of the PV lineage in some hosts. The tight host-virus interactions that have underlain PV evolution are thought to have led over time to a balance between viral replication and immune tolerance, allowing the viruses to become well adapted to their hosts where in most instances can complete their life cycle and be maintained without causing any overt disease (Doorbar et al., 2012).

PV molecular evolution progresses several orders of magnitude slower than that of RNA viruses, possibly even approaching the slow speed of the genome of the host species. This property is shared with other double-stranded DNA viruses infecting vertebrates such as Polyomaviruses and Herpesviruses, reflecting the fact that these viral genome sequences are stabilized by the high-fidelity proof-reading capability of host DNA polymerases; for these reasons, mutations are fixed at a very slow rate in the PV genome, which is therefore highly stable (Bernard, 2013; Van Doorslaer, 2013)

On the basis of L1 nucleotide sequences, HPVs are divided into five genera (Figure 1), with the different species and types exhibiting different sites of infection, life cycle characteristics and functions of specific viral gene products and different disease association: Alpha (α-HPV), Beta (β-HPV), Gamma (γ-HPV), Mu (μ-HPV) and Nu (ν-HPV) (Bernard et al., 2013).

The Alpha genus is the most represented one and comprises both mucosal and cutaneous species. Based on their oncogenic potential and association with the development of malignancies, mucosal α-HPVs are further subdivided into low-risk and high-risk groups.

The World Health Organization has defined 12 mucosal α-HPV types (HPV 16, 18, 31, 33, 35, 39, 45, 51, 52, 56, 58, 59) as being high-risk cancer-causing types; they are mainly responsible for the development of cervical cancer and can also be associated with cancers at other sites with much lower incidence (head and neck carcinomas such as oropharyngeal cancers, and cancers of the penis, anus, vagina and vulva). Nevertheless, high-risk α-HPVs do not cause cancer in the vast majority of the individuals they infect.

Low-risk α-HPVs cause benign mucosal lesions. Certain types (e.g. HPV 6 and 11) are associated with the development of respiratory papillomatosis (especially HPV 11), which is a laryngeal disease often occurring in children, and with benign external ano-genital warts

(especially HPV 6); these types are sometimes occasionally found to be associated with cancers in these sites especially in individuals with immune defects, where such infections are more difficult to manage. Other low-risk α-HPV types (e.g. HPV 13 and 32) are responsible for the development of oral papillomas as it occurs in the case of oral focal epithelial hyperplasia.

Cutaneous α-HPVs (e.g. HPV 2, 3, 7, 10, 27, 28, 57) are associated with the development of different types of benign skin warts arising on various sites of the hands, face, elbows and knees.

The Beta genus comprises to date 43 types, which exhibit cutaneous tropism (e.g. HPV 5, 8, 9, 14, 17, 20, 21, 23, 36, 38, 47, 49). β-HPVs are evolutionarily distinct from the Alpha genus and establish widespread unapparent asymptomatic infections that remain latent without any clinical manifestation in the general healthy population. In subjects with impaired immune function, it seems that these viruses can spread unchecked and they have been implicated in the development of KCs. In particular, in individuals suffering from epidermodysplasia verruciformis (EV), a primary immunodeficiency associated with abnormal susceptibility to β-HPV infection, they are responsible for the development of disseminated wart-like lesions that often undergo malignant progression; there is also increasing evidence for their involvement in the onset of precancerous skin lesions with potential to evolve to KCs in other immunosuppressed populations (e.g. OTRs, organ transplant recipients). Their involvement in the pathogenesis of KC in immunocompetent individuals is more controversial.

Gamma (e.g. HPV 4), Mu (e.g. HPV 1) and Nu (HPV 41) genera comprise a smaller number of types, exhibiting cutaneous tropism; they are associated with the development of benign palmar and plantar skin warts (de Villiers et al., 2004; Pfister, 2003; Doorbar et al., 2012).

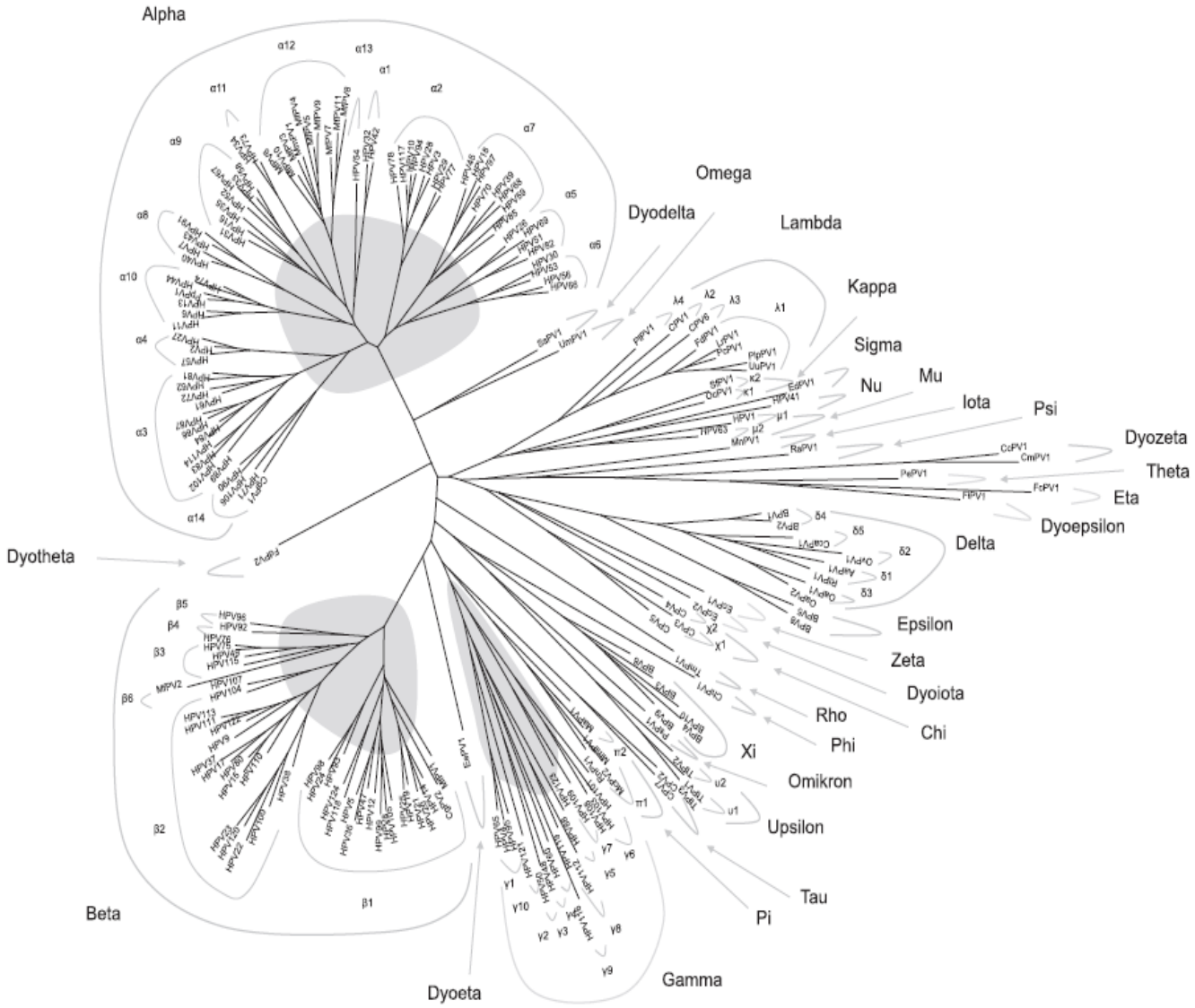

Figure 1. The phylogenetic tree of Papillomaviruses, obtained from multiple comparative alignments of the L1 gene. Symbols at the end of each branch define PV types; the external half circles refer to PV genera, while the internal half circles surround PV species (Bernard et al., 2013).

2.1.3 HPV structure, genomic organization and life cycle

HPV virions have a 52-55 nm diameter. The icosahedral capsid is made of the two structural proteins L1 and L2, repeated and organized in 72 capsomers. L1 is the major coat protein and accounts for 80% of the total amount of viral proteins; L2 is the minor coat protein and seems to favor the assembly of new viral particles amplifying their infectious ability. The two capsid proteins enclose the double-stranded DNA genome, which is about 8 kb in size (Knipe & Howley, "Fields Virology, 4th edition", 2001). Genomic organization is highly conserved among all HPV family members (Doorbar, 2007), with 7-8 open reading frames (ORFs) on a single transcriptionally active DNA strand encoding a larger number of gene products as a result of mRNA splicing (Figure 2). In the HPV genome, three regions can be distinguished:

- the early region coding for functional proteins (E1, E2, E4, E5, E6 and E7 for AlphaPV and E1, E2, E4, E6, E7 for BetaPV) expressed in all the phases of the viral life cycle, which are responsible for the persistence of the viral genome in a cell, its replication and the stimulation of cell proliferation necessary to support viral replication itself;
- the late region, coding for the structural coat proteins L1 and L2 that are expressed in the final phases of the productive viral life cycle;
- the long control region (LCR), a non-coding fragment regulating the expression and replication of the viral genome.

The L1 and L2 proteins are conserved across widely divergent PVs, and along with E1 and E2 are key viral gene products that are thought to have been present in the common ancestor of all PVs; other viral genes, such as E6, E7, E4 and E5, have been acquired or significantly modified during evolution and are not necessarily present or may not have the same function in all PVs. Because of such evolutionary mechanisms, different HPV genera have some exclusive features despite the highly conserved structure of the genome. For instance, the β-HPV genome is relatively short compared with that of the mucosal α-HPVs, ranging from 7.4 kb to 7.7 kb; this is due to the considerably reduced size of the LCR, about 400 bp compared with 650–900 bp in other HPVs. β-HPVs also display some differences in the coding region: most of them lack a functional E5 ORF and the E2 and E4 ORFs of all the β-HPV types are much longer compared with the other HPVs. Similarly to β-HPVs, also γ-HPVs lack the E5 gene (Tommasino, 2014; Ciesielska et al., 2012; Quint et al., 2015).

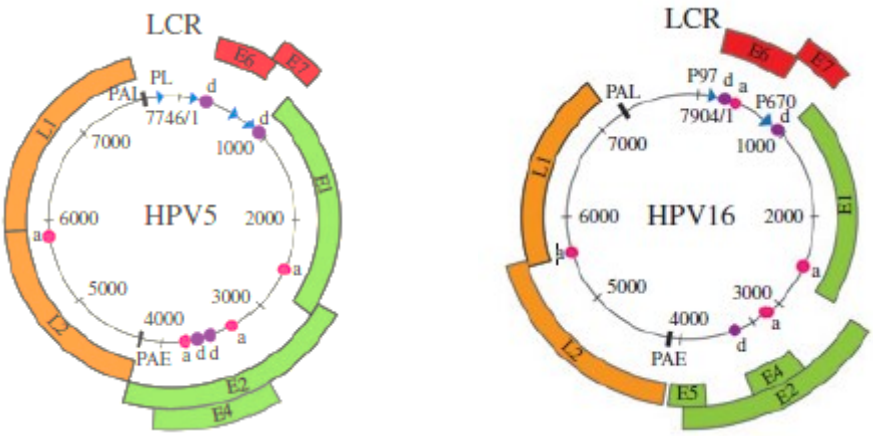

Figure 2. The genome organization of the prototype Beta HPV5 and Alpha HPV16. The HPV genome comprises a long control region (LCR) and seven or eight genes that are necessary for different stages of the virus life cycle. These genes encode a larger number of gene products as a result of mRNA splicing. The LCR contains binding sites for cellular transcription factors (e.g., SP1, AP1, Oct1), as well as for the viral E1 and E2 proteins that control viral replication and gene expression. BetaPV types lack an E5 ORF and have a much longer E4 ORF than the AlphaPV types. The positions of major promoters and splice donor/acceptor sites are indicated by arrows (promoters) and circles (d, donor; a, acceptor), respectively, alongside the positions of the early (PAE) and late polyadenylation sites (PAL) (Quint et al, 2015).

The LCR is a significant non-coding fragment of viral DNA located between the L1 and E6 ORFs, accounting for about 10% of the entire genome. It contains an origin of replication and cis-responsive elements for regulatory transcription and replication factors of viral genetic material; in detail, there are binding sites for cellular transcription factors (e.g. SP1, AP1, Oct1), as well as for the viral E1 and E2 proteins that control viral replication and gene expression (Figure 2) (Doorbar et al., 2012). All the LCR regions contain enhancers that provide the virus with specific tropism to the stratified squamous epithelial cells. Other regulatory enhancer elements are positioned within genes. The LCR harbours one of the two well-characterized promoter elements, namely the early promoter upstream of the E6 ORF, while in many HPV types the late promoter is located within the E7 ORF; these promoters regulate the expression of differentially spliced mostly polycistronic mRNAs, being trans-activated in a timely and coordinated differentiation-dependent fashion in specific epithelial layers where the different phases of the viral life cycle take place. The early promoter mainly drives E6 and E7 expression, while the late promoter regulates the expression of all the other viral genes (Ciesielska et al., 2012; Doorbar, 2013; Tommasino, 2014).

The E1 protein, an ATP-dependent DNA helicase, is the only enzyme encoded by the PV genome. E1 is essential for the maintenance, replication and amplification of the viral episome in the nucleus of infected cells; it does so by interacting with cellular DNA replication factors and assembling with E2 to the origin of replication to trigger viral DNA replication.

The E2 protein acts both as repressor and activator of viral gene transcription by binding to multiple sites in the LCR; in particular, it negatively modulates the expression of E6 and E7 by down-regulating the activity of the early promoter. Furthermore, E2 recruits E1 to a specific E1-binding motif in the origin of replication and is implicated in the maintenance of the viral genome in its episomal (extrachromosomal) form.

The E4 protein is the most abundant viral gene product and is expressed later than the other early proteins. E4 is thought to be involved in viral genome amplification and suppression of cellular proliferation in the late phases of the productive life cycle; it seems also to be able to form multimers that assemble into amyloid-like fibres that can destabilize the cytokeratin network of the host epithelial cells facilitating the extracellular release of new viral particles (Bergvall et al., 2013; McBride, 2013; Doorbar, 2013).

HPVs encode three proteins with transforming properties: the E5, E6 and E7 oncoproteins. Through combined and cooperative action, they abrogate the activity of tumour suppressor factors, promoting evasion of all cell cycle checkpoints and inducing a deregulated progression of the cell cycle; the result is a stimulation of cell growth, survival and proliferation and a delay of terminal cell differentiation (Doorbar, 2007).

E5 is a transmembrane protein localizing to cell membranes - predominantly to the endoplasmic reticulum and also to the Golgi apparatus and nuclear membrane - suggesting that its activity must be related to the trafficking of membrane proteins through different cellular compartments; it can dimerize in these sites and in certain HPV species trigger cell fusion. It is absent in HPV types from the Beta genus. (Connolly et al., 2014).

E6 and E7 are multimeric proteins with potential to associate with multiple cellular partners. Such functional differences contribute to the respective transforming abilities of various HPV species and types. In the best characterized HPV species, E7 binds and targets for ubiquitin-dependent proteasomal degradation the hypophosphorylated form of members of the Rb family (pRb, p107, p130). In uninfected epithelium, cell cycle entry and cell division in the basal and parabasal cell layers is controlled by growth factors that stimulate the activity of G1 cyclins including cyclinD/Cdk, which phosphorylates Rb family members and displace them from transcriptional activators of the E2F family allowing the trans-activation of genes necessary for S-phase progression (e.g. minichromosome maintenance protein 7 (MCM7), PCNA, Ki67,

cyclins); the continual stimulation of these cells physiologically allows renewal of the epithelium as surface cells exfoliate (Tommasino, 2014).

E6 interferes with DNA damage repair, growth arrest and apoptosis. The function of E6 complements that of E7. The efficient binding of Rb proteins by E7 can lead to inhibited cell growth and apoptosis through a p53-dependent pathway; as a result, E6 proteins of many HPV types have evolved to target the tumour suppressor p53 for ubiquitin-dependent proteasomal degradation or other forms of inactivation, resulting in the abrogation of its activity that plays an essential role in protecting genomic integrity. (Akgül et al., 2006; Ciesielska et al., 2012; McLaughlin-Drubin et al., 2012; Moody et al., 2010).

The HPV replicative cycle (summarized in Figure 3) is tightly linked to the differentiation program of stratified squamous epithelia. Most viruses infect a target cell and produce progeny virus from that same infected cell; conversely, in HPV infections, the synthesis of new virions occurs only after the infected cell has undergone mitosis and one of the infected daughter cells has differentiated. HPV replication requires the timely and coordinated expression of the different viral gene products as the infected cell moves towards the epithelial surface; this highly regulated pattern of gene expression allows the different stages of the life cycle to be completed appropriately. For this reason, HPV life cycle takes 2-3 weeks, the time necessary for an epithelial cell to migrate from the basal to most superficial layers, mature, undergo senescence and die. (Doorbar, 2007; Moody et al., 2010; Roman et al, 2013; Crosbie et al., 2013; Doorbar et al., 2012).

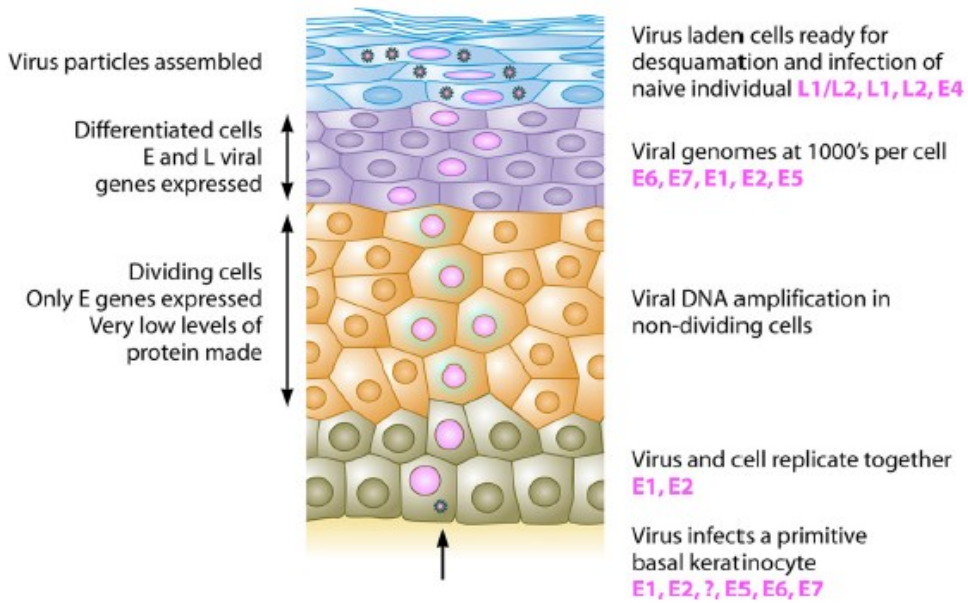

Figure 3. Productive HPV life cycle. HPVs replicate only in fully differentiating squamous epithelia. The life cycle involves both temporal and spatial separation of viral protein expression. The virus first

infects a cell in the basal layer of the epithelium where access is naturally facilitated (e.g. microtrauma, epithelial transitional zones, hair follicles). In the lower proliferative compartments of the epithelium, there is a phase of viral episome maintenance al low copy number, in which viral and cellular DNA replicate together. As long as the cell is dividing, HPVs control the expression of their viral proteins very tightly; the E6 and E7 oncogenes are thus expressed at very low levels, along with the genes coding for E1 and E2 replication factors. When the host cells stop dividing and begin to differentiate into mature epithelial cells, this provides a signal to the virus to activate all of its genes to amplify the viral genome copy number to the thousands. In the top layers of the epithelium, all of the viral genes, including those encoding the L1 and L2 proteins, are expressed, and many thousands of viral genomes are encapsidated; finally, the newly assembled infectious viral particles exit the cells in the context of epithelial surface desquamation. The time taken from infection to the generation of new virions is at least 2-3 weeks (Stanley, 2012).

Experimental models suggest that infection requires access of virus particles to the basal lamina and the interaction with heparin-sulphate proteoglycans and possibly also laminin. Structural changes in the virion capsid, which includes cleavage of L2, facilitate transfer to a secondary receptor on the basal keratinocyte, which is necessary for virus internalization and subsequent transfer of the viral genome to the nucleus; although the α-6 integrin and growth factor receptors have been implicated in this process, the precise nature of the entry receptor remains somewhat controversial (Doorbar et al., 2012). Once internalized by a clathrin-dependent endocytic pathway, virions undergo endosomal transport, uncoating and cellular sorting. The L2 protein-DNA complex ensures the correct nuclear entry of the viral genomes, while the L1 protein is retained in the endosome and ultimately subjected to lysosomal degradation (Doorbar et al., 2012).

In many cases, infection is thought to require epithelial wounding or micro-wounding to allow access of the virus to the basal lamina, and a role for the wound healing response in simulating the lateral expansion of the infected cells has been suggested. Some HPV species are thought to infect sites where access to the basal layer is naturally facilitated, such as the base of the hair follicle (HF) for cutaneous HPVs, or sites where columnar and stratified squamous epithelial cells meet each other, such as the cervical or anal squamo-columnar junctions for high-risk α-HPVs. It is thought that lesion formation begins with the infection of a long-lived, slow-cycling keratinocyte stem cell (KSC) and that the longevity of the keratinocyte stem cells is a key factor in the formation of a persistent lesion, with these cells being a reservoir for the infection (Doorbar, 2007; Quint et al., 2015).

Infection of the stem cells is followed by the early non-productive stage of the life cycle, consisting of an initial phase of genome amplification and then by maintenance of the viral episome al low copy number (100-200 copies per cell) (Doorbar et al., 2012).

The HPV genome does not encode polymerases or other enzymes necessary for viral DNA replication, which depends on the presence of the cellular DNA replication machinery, with viral DNA replication accompanying cellular DNA replication as the cells progress through S-phase (Stanley, 2012). The only viral proteins that are thought to be necessary for this initial amplification phase are E1 and E2, which are expressed from the late promoter and ensure viral DNA replication and transcription (Doorbar, 2007).

Viral proteins are not readily detectable prior to the onset of genome amplification during normal productive infection; the low level expression of viral proteins in the basal layer is thought to reflect, at least in part, the need of the virus to avoid detection by the host's immune system (Doorbar et al., 2012). After an initial increase in viral copy number, the infected 'differentiating' cells move from an S-like to a G2-like phase, with viral genome amplification occurring primarily in G2 after cellular DNA replication has been completed; the virus at this point fully recruits the cellular DNA replication machinery for its own replication (Doorbar et al., 2012).

A key function of the E6 and E7 proteins in most HPVs is not to promote basal cell proliferation, but rather to stimulate cell cycle re-entry in the mid-upper epithelial layers in order to allow genome amplification (Stanley, 2012). To complete the late productive stage of the life cycle, the infected cells must undergo terminal differentiation in the most superficial epithelial layers. The completion of the life cycle ultimately involves the expression of the minor coat protein L2, the exit of the cell from the cell cycle and the expression of the major coat protein L1 to allow genome packaging (Doorbar, 2007).

2.1.4 High-risk α-HPVs and cervical carcinogenesis

Genital α-HPV infection is the most common sexually transmitted viral infection all over the world, with a peak of incidence in young individuals between 15-25 years of age following the onset of sexual activity and a progressive fall with age; over 80% of sexually active women become infected at some stage in their life with one or several high-risk and low-risk α-HPV types (Crosbie et al., 2013).

The frequency of high-risk α-HPV-associated cervical cancers is of around 30-40 people per 100000 and over 99% of cervical lesions harbor viral sequences, although the proportion associated with specific high-risk α-HPV types is different in different countries and shows demographic, ethnic and socio-economic variation. HPV 16 and 18 cause approximately 50%

and 20% of the cases of cervical SCC – arising in the stratified squamous cells of the ectocervix - respectively, and both types are equally associated with around 35% of the cases of cervical adenocarcinoma – arising in the columnar glandular cells of the endocervix and more aggressive (Doorbar, 2007).

Cervical precancerous lesions are named cervical intraepithelial neoplasia (CIN) and are histologically classified for diagnostic purposes according to the grade of dysplasia: CIN1 (mild dysplasia), CIN2 (moderate dysplasia), CIN3 (in situ carcinoma); CIN1 lesions are low-grade lesions (LSIL, low-grade squamous intraepithelial lesions), while CIN2 and CIN3 lesions are high-grade lesions (HSIL, high-grade squamous intraepithelial lesions). The accurate identification of lesion grade has prognostic significance, as it has been estimated that around 20% of CIN1 will progress to CIN2, and that around 30% of CIN2 will progress to CIN3 if left untreated; CIN3 are generally considered to be the direct precursors of cervical cancer, and it has been suggested that around 40% of CIN3 lesions will progress to cervical cancer in the absence of intervention. In general, more regions with different histological grade can be found in the context of a cervical lesion; different high-risk α-HPV types are usually associated with discrete areas of disease except at junction regions (where lesions abut or are in close proximity) where more than one type may be detected (Doorbar, 2007).

Most cervical cancers develop in the transformation zone, corresponding to the squamo-columnar junction - the transitional site where the columnar glandular cells of the endocervical canal meet the stratified squamous cells of the ectocervix. The particular susceptibility of the transformation zone to cancer onset and progression may also be linked to the increased accessibility and proliferation of the basal cell layers at this metaplastic epithelial site, particularly around the time of puberty and the onset of sexual activity; in this case, we can hypothesize that the primary preferential target cells for high-risk α-HPV infection may be cells close to the squamo-columnar junction, such as the epithelial reserve cells, which lie immediately underneath the columnar epithelium of the endocervix, and eventually form the stratified epithelial layers of the transformation zone as the cervix matures (Doorbar et al., 2012). Early acquisition of high-risk α-HPV infections, also facilitated by the low levels in antigen-presenting cells in this site, can disturb the metaplastic changes occurring at this time in the transformation zone and increase the risk of cervical cancer in the future (Cubie, 2013; Tommasino, 2013; Moody et al., 2010).

2.2 β-HPV AND KERATINOCYTE CARCINOMAS

While the causative relationship between HPV infection and genital SCCs is well established, the role of HPV in the development of cutaneous malignancy is, as yet, unclear. However, there are an increasing body of evidence suggesting the involvement of cutaneous β-HPV in the development of KC. To demonstrate that a pathogen causes cancer, convincing epidemiologic evidence of association and a plausible biological mechanism for oncogenesis are necessary; while this has been achieved for high-risk α-HPVs and cervical cancer, such requirements have not yet been satisfied for β-HPVs and KC, as there is great lack of consistency among epidemiological studies and no molecular role for these viruses in cutaneous tumorigenesis has been certainly proven so far.

KC is the most common cancer type among Caucasians, where it accounts for around 30% of all malignancies and its rates are increasing by 4–8% yearly. Although the majority of KC cases can be treated surgically and do not usually exhibit high aggressiveness, these cancers are associated with high morbidity and represent a significant burden on the healthcare system. Immunosuppression and UV exposure are the main risk factors for KC – these tumours mostly arise in sun-exposed skin sites (Akgül et al., 2006: Aldabagh et al. 2013).

The major histological types of KCs are basal cell carcinoma (BCC) and cutaneous squamous cell carcinoma (SCC), associated with different underlying mutational patterns. BCC is more common in fair-skinned individuals and originates from transformation of basal epidermal cells. SCC, which is more aggressive than BCC, is more common among darker skin population and arises from transformation of squamous epidermal cells; it is usually preceded by precancerous lesions, namely actinic keratosis (AK), with high potential to undergo malignant progression; other forms of skin tumours that are histologically related to SCC are keratoacanthoma (KA) – a low-grade SCC subtype originating from the hair follicles, able to regress spontaneously and representing a midpoint between a benign wart and invasive SCC – and Bowen's disease – an early stage in situ intraepidermal form of SCC (Nindl et al., 2007; Knipe & Howley, "Fields Virology, 5th edition", 2007; Pfister, 2003).

The epidemiological demonstration of a possible causal link between β-HPV infection and KC development is complicated by the fact that these viruses are also present in non-affected skin areas of patients and even ubiquitously widespread in the general healthy population, establishing persistent, asymptomatic latent infections without apparent disease; it is thought that everybody is positive for multiple β-HPV types. With increasing age, the number of infecting β-HPV types seems to rise; β-HPV persistence with the same types is common, and

family members often share the same types ("β-HPV signature"). Different studies using different sampling techniques have shown that the most commonly detected β-HPV types are HPV 5, 8 and 23; different ethnicities may harbour different β-HPV types, with HPV5 being the most prevalent type and the only type common to all countries studied (Aldabagh et al., 2013).

β-HPV infection seems to be acquired very early in infancy, with exposure beginning soon after birth; the presence of the viruses on the skin surface of the mother and other people in close contact with the newborn is the most likely source of infection. β-HPV transmission probably occurs by contact with infected skin or its ubiquitously present remnants (e.g. scales, dandruff); the likelihood of a prenatal vertical transmission from mother to fetus has also been proposed. Transmission in later stages of postnatal life is thought to be limited; this may be due to the fact that in the first postpartum days, the thinner horny layer facilitates access to the basal layer, or to the fact that after the sites available to infection have been occupied, the settlement of other β-HPV types is more difficult because of the occurrence of a cross-reactive antiviral response following initial infection. In immunocopetent individuals, this early infection seems to persist in a latency status and without clinical manifestations (Harwood et al., 2002; Bouwes Bavinck et al., 2008; Akgül et al., 2006; Feltkamp et al., 2008).

2.2.1 Epidermodysplasia verruciformis

Epidermodysplasia verruciformis (EV), which is considered to be a primary immunodeficiency (PID), is the only setting where the association between β-HPV infection and skin carcinogenesis has been ascertained. It is a rare autosomal recessive condition, in which selective depletion of specific T-cell clones - although the immunophenotype might be normal in some patients - is associated with an abnormal susceptibility to persistent infection restricted to a subset of about 20 β-HPV types, often with more than one infecting type. It arises in early childhood with the development of disseminated benign plane warts and occurring mainly on the trunk, neck and extremities, and persist lifelong. EV patients also develop wart-like lesions (Figure 4A) that are intraepidermal proliferative lesion that display the typical cytopathic effects of EV skin lesions, including acanthosis, koilocytosis, the presence of enlarged cells with prominent blue–grey pallor and occasional perinuclear halos, with greater malignant potential on light-exposed areas (Figure 4B, left panel). These lesions are associated with HPV 5 and 8, often with more than one β-HPV type being detected, and contain high β-HPV episome copy numbers per cell – indicating a high level of viral replication – and abundant E6 and E7

transcripts – indicating viral gene expression in the lesional tissue. In the fourth decade of life, around 30-60% of EV patients develop malignant tumours in sun-exposed sites (Quint et al., 2014), which are usually low grade in situ carcinomas with some features in common with Bowen's disease, but others are more aggressive SCC; HPV 5 and 8 account for 90% of the tumours with HPV 14, 17, 20 and 47 accounting for the remainder; β-HPV load can reach 100-300 genome copies per cell, even though in a limited number of tumour cells and always in episomal form. β-HPV-induced EV skin tumours are associated with productive infections: the high level of viral replication and subsequent active oncogene expression underlies skin carcinogenesis in these patients.

Our group has throughly studied the association between β-HPV infection and EV patient's lesions by mapping the β-HPV life cycle events. The data have suggested a progression pattern from benign keratotic skin lesion to Bowen's Disease and SCC, in which the β-HPV life cycle is progressively disrupted. In addition, our group has demonstrated that the abundant β-HPV seen in some lesions was the result of genome amplification within the carcinoma tissue. E4 protein of β-HPV was very abundant and could be easily visualised either in superficial cells supporting viral genome (cytoplasmic) or in the more basal proliferating cells (nuclear) (Figure 4B, right panel). The loss of staining at the tumour border has suggested that E4 staining could be exploited as a marker of viral expression during β-HPV-associated skin cancer progression (Borgogna et al., 2012; Borgogna, Landini et al., 2014).

A

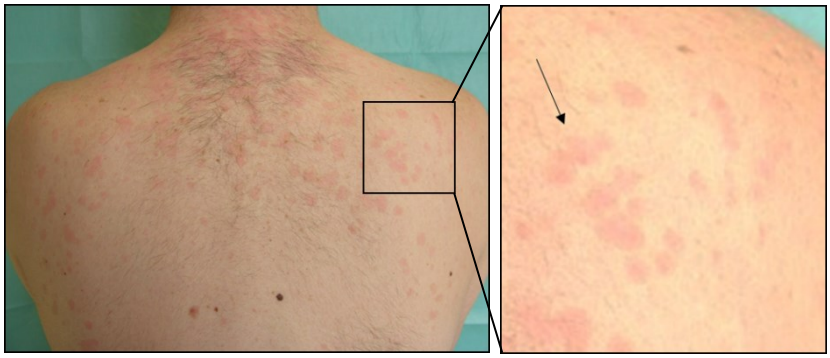

B

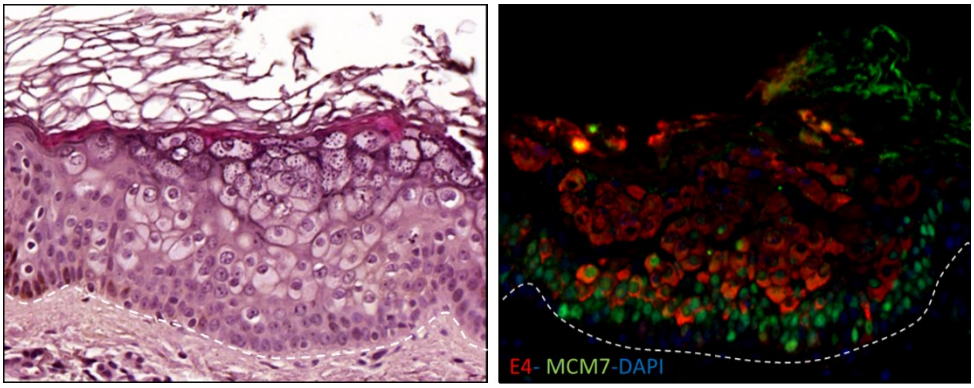

Figure 4. (A, left panel) Clinical manifestation of epidermodysplasia verruciformis on the back of an EV patient. The area surrounded by the black square is enlarged in the right panel. The black arrow shows the characteristic lesions. (B, left pannel) H&E staining of a wart-like lesion displays the typical cytopathic effects of EV skin lesions. The section was double stained in immunofluorescence using antibodies to E4 of β-HPV (red) and the proliferation marker MCM7 (green). The broken lines indicate the position of the basal layer.

Homozygous truncating mutations in the EVER1 or EVER2 genes have been reported in approximately 50% of EV patients; these two genes encode transmembrane proteins expressed in a variety of cells types, including mostly blood cells. These proteins form a complex localized to the endoplasmic reticulum, where they seem to control intracellular zinc homeostasis and in particular to decrease the nuclear zinc concentration, reducing the activity of zinc-regulated transcription factors necessary for viral gene expression (e.g. AP1). Thus, the EVER proteins may act as restriction factors for β-HPV gene expression and replication in keratinocytes, even though the exact underlying mechanisms are still unclear. EVER mutations disrupt zinc transport between cell compartments; it is thought that this leads to up-regulation of transcription factors that can induce β-HPV transcription and stimulate keratinocyte proliferation, which in turn further amplifies β-HPV oncoprotein expression (Quint et al., 2015; Lazarczyk et al., 2008) (Figure 5)

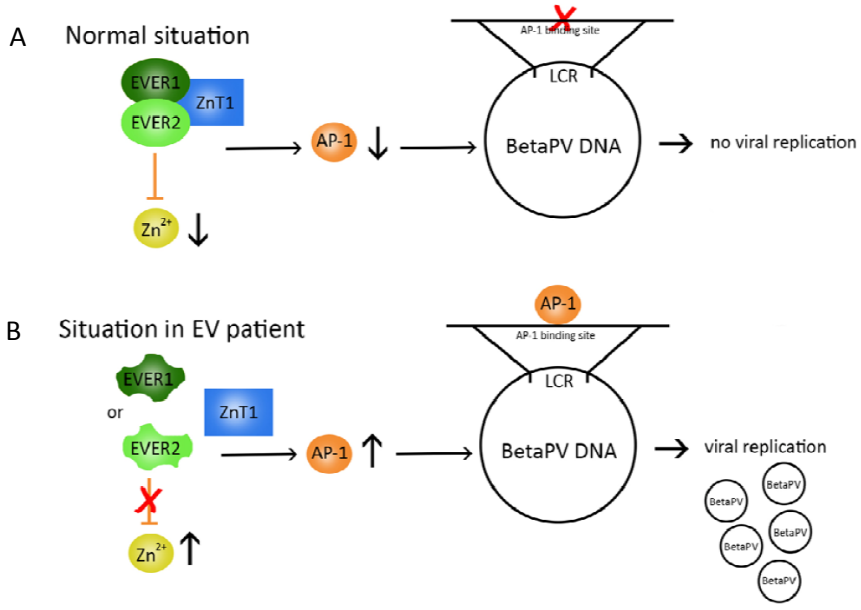

Figure 5. A. Normally, the EVER/ZnT-1 complex is responsible for a low level of free intracellular Zn2+. This low level of free Zn2+ tonically inhibits the activity of AP-1 transcription factors necessary for BetaPV replication in keratinocytes. B. In EV patients, a dysfunctional EVER/ZnT-1 complex leads to a higher Zn2+ concentration, which causes increased activity of the AP-1 transcription factors, thereby initiating BetaPV replication (Quint et al., 2015)

Other HPV species may counteract EVER protein function through different mechanisms in order to facilitate viral gene expression; HPV16 E5 has been reported to be able to bind and inhibit the EVER complex. It has also been postulated that EV-associated imbalance in zinc homeostasis contributes to HPV-specific immune deficiency through the same mutations.
However, in a substantial proportion of patients clinically diagnosed with EV, EVER genes are not mutated; it is likely that unknown mutations affecting other genes are involved in the genetic background of the disease (Akgül et al., 2006; Pfister, 2003, Leiding et al., 2012; Cubie, 2013; Arron et al., 2011).

2.2.2 β-HPV infection in the immunocompromised host

The association of cutaneous HPV infection with the development of skin lesions is well established in the case of EV. More recently, mutations in other two genes, RHOH – encoding a Rho-GTPase expressed predominantly in hematopoietic cells involved in intracellular transduction form T-cell and B-cell receptors – and MST1 – encoding a kinase involved in many biological processes in various cell types, including apoptosis, negative regulation of cell growth and proliferation, and differentiation - have been identified in PID patients associated with high susceptibility to β-HPV infections exhibiting an EV-like phenotype. RHOH and MST1 deficiencies lead to T-cells defects, which probably play a role in the pathogenesis of chronic active β-HPV infections (Crequer, Troeger et al., 2012; Crequer, Picard et al., 2012).

Other PID syndromes (e.g. SCID, WHIM), whose genetic backgrounds have been described and affect various aspects of immune function, are characterized by recurrent severe bacterial and viral infections since infancy. As a result, these patients have a number of subsequent clinical manifestations, among which diffuse HPV-associated warts and also carcinomas; β-HPV infections have also been reported in EV-like skin lesions from these individuals and might be implicated in their onset and development, leaving open the possibility that these viruses play a role in cutaneous carcinogenesis affecting many of these subjects. Our group reported a patient with an unclassified primary T-cell immunodeficiency (characterized by a low number of naïve T cells) that did not carry any of the genetic mutations associated with EV or WHIM syndrome, but displayed remarkable and specific susceptibility to α and β HPV infection. The HPV susceptibility involved both cutaneous and genital sites as the patient developed either βHPV-positive wart-like lesions or αHPV-positive anal-penile

condylomas. This pattern is slightly different from the clinical picture of canonical EV patients where the susceptibility is considered to be restricted to the β genus (Landini et al., 2014).

Similarly to PID patients, individuals with acquired T-cell immunodeficiencies, whether secondary (e.g. hematological malignancies, AIDS) or iatrogenic (e.g. OTRs undergoing long-term immunosuppressive therapy to prevent graft rejection) are all at increased risk of developing extensive, persistent and recurrent HPV-associated warty and keratotic skin lesions especially on sun-exposed sites (Leiding et al., 2012; Cubie, 2013; Aldabagh et al., 2013). In the particular case of OTRs, although suppression of T-cell immunity and immunosuppressant drugs per se can exert carcinogenic effects, the most obvious mechanism of post-transplant tumorigenesis is that iatrogenic down-regulation of cell-mediated immunity unmasks the transforming activity of infectious agents resulting in the development of virus-related malignancies (Connolly et al., 2014).

Several epidemiological studies have demonstrated statistically significant associations between β-HPV infection and KC development. For instance, large international case-control studies in OTR and in immunocompetent individuals observed an association between the presence of β-HPV DNA in eyebrow hairs and the development of KC, as well as between β-HPV serum antibodies and KC (Bavinck et al., 2010). The BCC:SCC ratio is inverted in OTRs compared to the general population, with SCC occurring 4 times more often than BCC; SCC represents the most common de novo malignancy in the OTR setting, who exhibit a risk 60-250-fold as great as that of immunocompetent subjects with a SCC frequency over 50% at 10 years and over 80% at 20 years post-transplantation – while BCC is increased 10-40 fold (Euvrard et al., 2003; Tessari et al., 2010). In addition, SCC arising in OTRs can be multiple and highly aggressive, with increased rates of recurrence and metastasis; they usually develop within the first decade post-transplantation in sun-exposed sites co-localizing with other precancerous lesions, suggesting that their persistence favors malignant progression, and affects large skin areas in a process called field cancerization.

The major weakness of the available studies is that the proposed association is mostly based on the presence of viral DNA in tumour tissues or positive antibody responses. Very few studies have addressed whether the β-HPV detected in these cases are actually localized within the malignant cells or whether they are transcriptionally active, the confirmation of which would greatly strengthen the evidence for a carcinogenic role of these pathogens.

Studies from our group have demonstrated that detection of the abundant viral E4 protein of β-HPV was helpful for the visualization of active β-HPV infection in skin tumours from EV patients (Borgogna et al., 2012; Borgogna, Landini et al., 2014). Based on these finding, our

group has decided to investigate whether detection of β-HPV gene products, as defined in EV skin cancer, could also be observed in lesions from OTRs. Using a combination of antibodies against the viral proteins E4 or L1 of the β-genotypes and fluorescent in situ hybridisation (FISH) to detect the viral genome, we were able to visualise viral infection in premalignant lesions, such as actinic keratosis and keratoakantoma as well as in the pathological hyperplastic edges of either SCC or BCC from OTRs. Increased expression of the cellular proliferation marker MCM7, that extended into the upper epithelial layers, was a common feature of all the E4-positive areas, indicating that cells were driven into the cell cycle in areas of productive viral infection (Borgogna, Lanfredini et al., 2014; Figure 6).

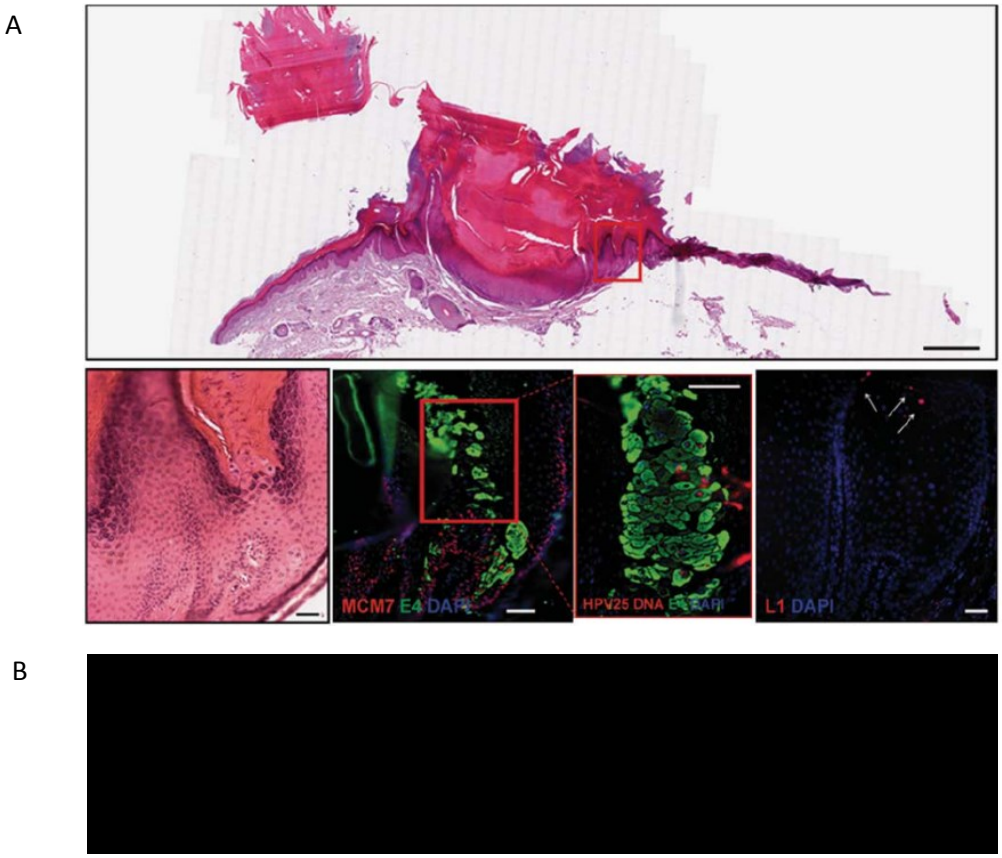

Figure 6. (A) Distribution of the viral and cellular markers E4, L1, human papillomavirus 25 (HPV25) DNA and MCM7 in a case of hypertrophic actinic keratosis from a hand from a kidney transplant recipient. The top picture (scale bar: 1000 mm) shows the scan of the tissue section of the actinic keratosis using hematoxylin and eosin (H&E) staining. The region shown in the lower panels corresponds to the red square highlighted in the over H&E image, reproduced in the lower left-hand picture. The same section was double stained using antibodies to E4 (green) and MCM7 (red) (second picture); serial sections were double stained for the presence of viral genome amplification by HPV25 DNA-fluorescent in situ hybridization (FISH) (red) and for E4 expression (green) (third picture), and also stained with antibodies to L1 (red) (fourth picture). The white arrows indicate nuclear L1 staining. All sections were counterstained with DAPI (blue) to visualize cell nuclei. Scale bars: 50 mm

(Borgogna, Lanfredini et al., 2014). (B) Schematic table of skin tumours derived from our OTRs cohort analysed by immunofluorescence for detect the presence of β-HPV markers.

These data demonstrated that β-HPV transcription occurs at the site of skin transformation in the organ transplant recipient setting and also point to its possible involvement in the process of skin carcinogenesis (Borgogna et al., 2014).

Based on these results, we have decided to investigate the association between β-HPV infection and OTRs KCs using an orthotopic tumourgraft model developed by Patel et al at the NCI-Bethesda by xenografting fresh skin tumours from OTRs onto a "humanized" stromal bed repopulated with human fibroblasts in nude mice (Patel et al., 2012). This methodology provides advantages in our study for the following reasons: i) skin tumours are usually very small, thus the material left from the routine diagnostic procedure is often insufficient and does not allow for the storage of fresh tissues; ii) the xenograft is usually bigger than the original tumour, it can be exploited in its entirety for molecular investigation and split in half for fresh and fixed storage; iii) this is currently the only way to allow premalignant lesions continue their natural malignant progression once they have been removed from the patient, thus it provides a unique opportunity to analyse them. In addition, in order to recapitulate the events occurring in OTRs and analyse how their immune defects increase virus-induced skin carcinogenesis, we have decided to cross the HPV8 transgenic mice (a model of HPV8-induced skin carcinogenesis; Shaper et al., 2005) with Rag2KO mice (that lack B and T cells). If immunosuppression also facilitates carcinogenesis by inhibiting tumour immune surveillance, we would expect the greatest SCC frequency in the β-HPV8 Rag2KO mice.

2.2.3 Molecular mechanisms underling β-HPV-induced skin cancer

Although both experimental and epidemiological evidence suggests a carcinogenic role of β-HPV, little is known about the initial events of persistent infection. It is generally accepted that tumour initiation primarily involves a population of long-lived cells such as KSC. However, although some specific types of HPV were detected on plucked hairs from different body sites, supporting the idea that the HF (hair follicle) is an important site of infection for HPV, there is as yet no evidence to suggest which cells are initially infected by HPVs.

Recent work has suggested that overexpression of E6 and E7 oncoproteins from β-HPV types 5 and 8 can enhance the stem-like characteristics of transduced keratinocytes (Hufbauer et al., 2013). The capability of these viruses to increase the number of stem cell-like cells present during early carcinogenesis may enable the persistence and accumulation of DNA

damage necessary to generate malignant stem cells. These clinical and molecular observations suggest fundamental differences in the way that β types and high-risk α types cause cancers.

To initiate an infection, β-HPV need to gain access to the basal keratinocytes, and probably a KSC within the basal cell layer, which is normally protected by differentiated stratified epithelium. In many cases, it is thought that this is facilitated by an exogenous (micro) trauma or other localized break in the epithelial barrier. However, at particular epithelial sites, infection may be less dependent on epithelial damage. Current thinking suggests that β-HPV infects a long-lived, slow-cycling KSC, such as may be found in the HF bulge region (Figure 7 left panel). Division of these infected cells populates the surrounding basal layer with cells containing viral episomes, with completion of the β-HPV life cycle upon differentiation (Figure 7 right panel).

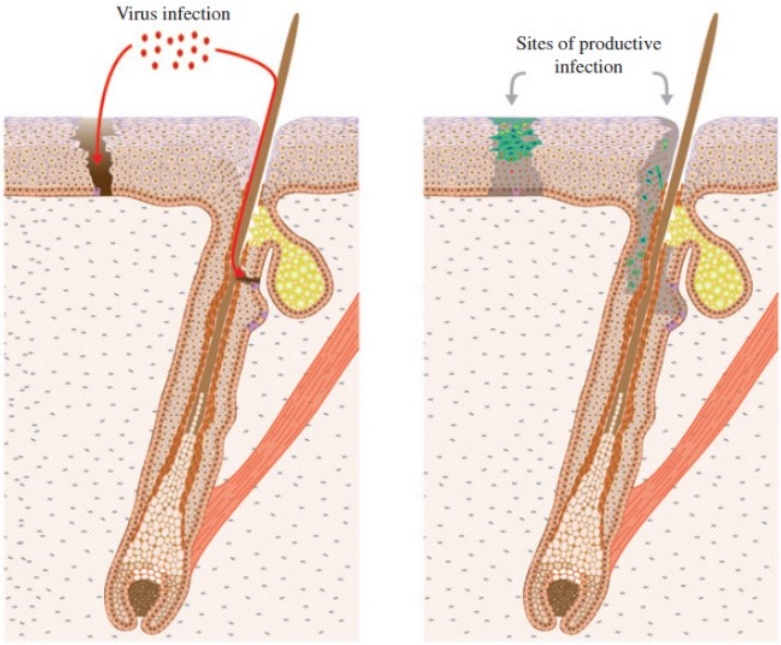

Figure 7. To initiate infection, HPV virions must gain access to the epithelial basal cells and probably an epithelial stem cell localized in the bulge region (coloured purple), either through a wound or possibly through the hair follicle (left pannel). Once the wound has been repaired and a β-HPV lesion has formed (right pannel), it is thought that the viral genome persists as a low copy number episome in the basal layer, often with limited viral gene expression. Cell cycle entry (cells with red nuclei) can be driven by the viral E6/E7 proteins, with E4 expression (green), genome ampification (dark blue) and L1 expression (yellow) occurring as the infected cell migrates towards the epithelial surface. It is thought that viral gene expression may become deregulated in EV and immunosuppressed individuals (Quint et al., 2015).

Based on the idea that β-HPVs have evolved to persist in a long-lived, slow-cycling stem cell, it is not surprising that, unlike the high-risk α types, the β-HPV episome is incapable of being

reliably maintained in faster-cycling cancer cells. This is consistent with the proposed 'hit and run' mechanism of carginogenesis. According to this model, the viruses might play a role in early stages of the pathogenesis of KC – particularly SCC, which appear to be the KC type with stronger association to β-HPV infection - as indirect and possibly transient carcinogens. β-HPV could being involved in tumour initiation in the presence of additional risk factors rather than in malignant progression or in the maintenance of the transformed phenotype as on the contrary occurs in high-risk α-HPV-driven cervical tumorigenesis (Borgogna, Lanfredini et al., 2014).

The "hit and run" hypothesis is supported by the following evidences:

- the lower transforming potential of β-HPV oncoproteins compared to high-risk α-HPV oncoproteins
- the low viral load and minimal gene expression in non-EV tumor tissues, and the fact that even in EV SCC the higher amount of viral DNA and gene expression is confined to few tumor cells
- the high prevalence of β-HPV DNA at high viral loads in AK precursor lesions
- the lack of evidence for β-HPV DNA integration in tumour cells, which on the contrary is a pivotal event in high-risk α-HPV-induced cervical cancer.

Taken togheter, these evidences suggest that β-HPV oncogene expression in early stages of SCC development could be a condition facilitating a transforming process previously triggered and subsequently carried on by other tumorigenic factors such as UV exposure, causing DNA damage, and immunosuppression, a condition that allows the reactivation of β-HPV.

It seems that β-HPVs, especially by means of the E6 oncoprotein, can inhibit either the apoptotic pathways triggered by UV-induced DNA damage or the repair of DNA damage itself, favouring a condition of genetic instability that may lead to the accumulation of mutations in proto-oncogenes and tumour suppressor genes and subsequently to host cell transformation (Akgül et al., 2006). In this picture, continuous β-HPV persistence could be no longer required when the cells are already initiated toward malignancy and, in more advanced stages of the carcinogenic process, the viruses might finally be lost, substained by the fact that β-HPV is not integrated into the human cellular DNA.

In conclusion, two important factors (UV radiation and immunosuppressive medication) contribute to the development of KC in OTR. In addition to this, a role for β-HPVs in the development of early premalignant lesions and KC has been proposed in individuals with compromised antiviral immune surveillance mechanisms. This might be due to an increased

viral replication and gene expression in the context of a reactivation of previously unapparent β-HPV infections kept under control by cell-mediated immunity rather than increased de novo β-HPV infections (Figure 8).

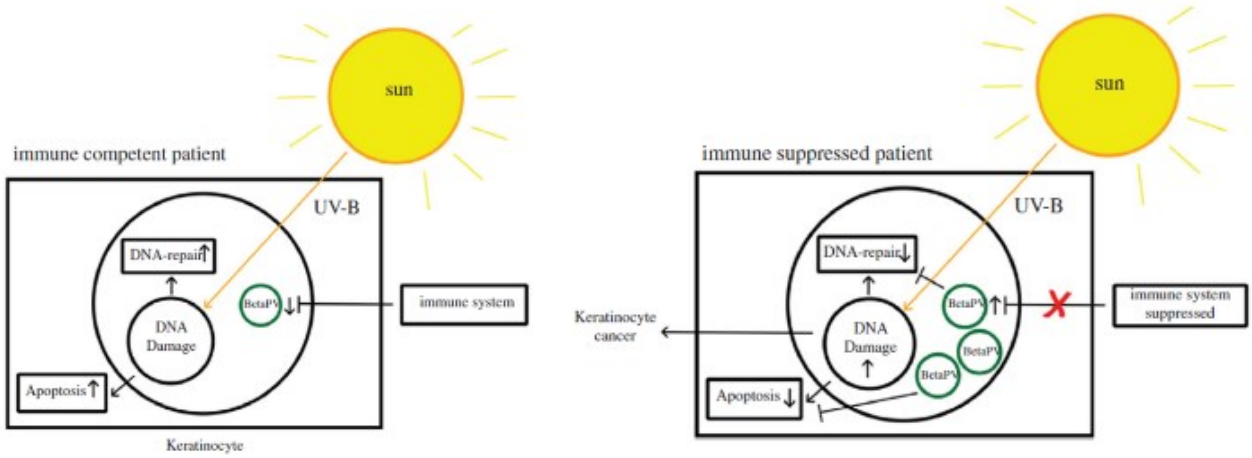

Figure 8. Proposed mechanism for β-HPV infection and keratinocyte carcinoma development. In immunocompetent individuals (left pannel), β-HPV infections are suppressed by the immune system. In this case, only low levels of β-HPV protein will be present to interact with host cell proteins involved in DNA damage repair and apoptosis, and genotoxic damage imposed by UV radiation will be managed adequately. In the presence of immunosuppression, however (right pannel), productive β-HPV infection occurs and sufficient amounts of β-HPV protein, particularly E6, are expressed, inhibiting DNA damage repair mechanisms and apoptosis. As a result, genomic instability develops in the infected keratinocytes, which may lead ultimately to the development of KC (Quint et al., 2015).

These proposed mechanisms may not be relevant in the above epidermal layers where cells have a short lifespan, but such effects could be significant in the KSC. Indeed, the persistent localization of β-HPVs in these cells – which may be the source of skin cancers – is likely to allow the acquisition of a condition of genetic instability that might transform them into cancers stem cells (Akgül et al., 2006; Quint et al., 2015).

2.2.4 Mouse models to investigate β-HPV role in keratinocyte carcinoma development

Different transgenic mice models have been developed so far for investigate the role of HPVs in skin cancer. The first transgenic mouse model for skin-associated HPVs was generated in 1992 at the University of Birmingham Medical School, by Searle's group. In this model the Mupapillomavirus HPV-1 early region was placed under the control of epidermis specific promoter-keratin 6 gene. Morphological alterations of the normal epithelial differentiation have been observed. The effect was greatest on the tail, where the epithelium

became hyperproliferative in appearance, with several layers of irregular or cuboidal cells above the basal layer and an increase in the total number of cell layers with abnormal cornification. A similar transient flaky appearance also associated with epidermal hyperplasia was observed on other regions of the skin around 7 days of age. It is worth mentioning that this transgenic mice were not able to develop any spontaneous skin lesion (Tinsley et al., 1992).

To further evaluate the possible contribution of β-HPV in skin carcinogenesis, Pfister and collegues established a transgenic mouse model where the complete early region of HPV8 (E1, E2, E4, E6, E7) was expressed under the control of the Keratin 14 promoter. In these transgenic mice, the first phenotypic alterations detectable started around 8 weeks after birth, showing the presence of spontaneous tumor like growth on the back with hair loss, hyperkeratosis, and ulceration. Almost all of these HPV8 transgenic mice (91%) developed single or multifocal benign tumors, without any treatment with physical or chemical carcinogens. These tumours are characterized by papillomatosis, acanthosis, hyperkeratosis, and varying degrees of epidermal dysplasia; furthermore 6% of this transgenic mice developed SCC. The rapidity of skin tumor development in these mice is no doubt related to the permanent expression of the HPV8 early genes in all proliferation competent keratinocytes driven by the K14 promoter. With this model it could thus be shown, for the first time, that expression of β-HPV proteins leads to skin cancer development without exposure to any further physical or chemical carcinogens (Schaper et al. 2005).

Using transgenic technology, several others mouse lines have been developed expressing HPV8 E2 protein or also E6/E7 from other β-genotypes, such as HPV38 and HPV20. The HPV38Tg mice had no spontaneous formation of tumours during the lifespan, but they developed actinic keratosis-like lesions after treatment with chronic UV radiation. The same phenotype was observed in HPV20 E6/E7 transgenic mice where again UV radiation was needed to enhance proliferation of the epidermal layers of the skin that was reflected in the higher rate of papilloma formation. Interestingly, E2 seems to act as an oncogene as E2-transgenic mice also develop skin lesions, even though to a lower extent, more slowly and with less severe malignant features. HPV8, so far, has been the only cutaneous HPV type found to induce skin cancer completely on its own in the absence of any additional co-carcinogenic treatment, making it a good candidate to investigate how β-HPV gene expression can influence the keratinocytes differentiation (Schaper et al. 2005; Akgül et al., 2006; Michel et al., 2006; Pfefferle et al., 2008; Viarisio et al. 2011; De Andrea et al. 2010).

2.3 KERATINOCYTE STEM CELLS

2.3.1 General characteristics of keratinocyte stem cell (KSC)

The skin of mammalian derives from a single layer of ectodermal progenitor cells, forms the outer covering of the body, and consists of two major areas: the upper area is an epithelium called the epidermis, and the lower area is a connective tissue called the dermis. The epidermis comprises a multi-layered epithelium, the interfollicular epidermis (IFE), and the pilosebaceous unit composed of hair follicles (HF) and sebaceous glands (SG) (Figure 9). The sweat glands are not part of this unit: they regulate the temperature of the skin and whole body by secreting an aqueous solution. The distribution of adnexal structures differs in different body sites, as does the thickness of the IFE (Solanas et al., 2013).

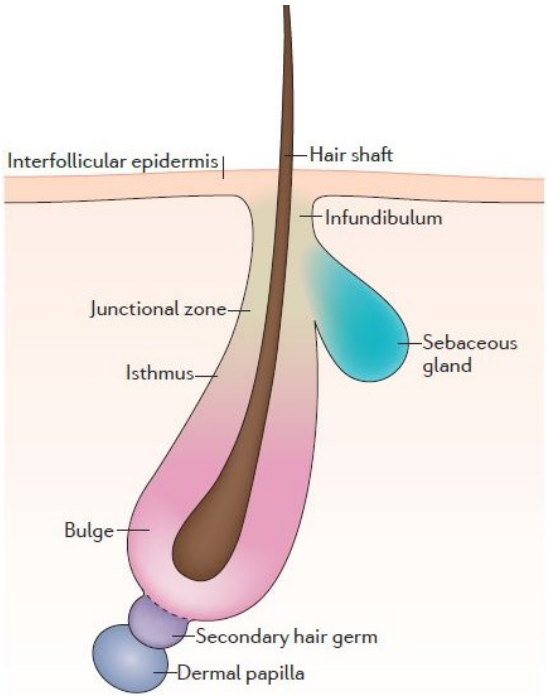

Figure 9. Generalized structure of the epidermis and the hair follicle. The interfollicular epidermis generates a protective barrier against dehydration and external aggressions. Hair follicles are scattered in the interfollicular epidermis and give rise to the hair shafts. The permanent portion of the hair follicle consists of the infundibulum, the junctional zone, isthmus and bulge. Attached to the side of the hair follicle is the sebaceous gland, which contributes to the generation of the isolating barrier of the epidermis with its secretions (Solanas et al., 2013)

Key functions of the epidermis are the formation of a protective interface with the external environment (e.g. prevents body dehydration; protects against radiation and penetration by microorganisms), lubrification of the skin with lipids, thermoregulation by hairs and sweat and

withstands mechanical stress. Each function depends on non-dividing, terminally differentiated keratinocytes that die and are shed from the body.

The skin is the tissue in which the existence of stem cells was first postulated. This is because the terminally differentiated cells are unable to divide and must be replaced throughout adult life by less differentiated cells, that both self-renew and generate differentiated progeny. These differentiated cells are replenished through a variety of keratinocytes stem cells (KSC) populations localized in different epidermal areas (Donati et al., 2015; Watt, 2014)

The epidermis contains three distinct classes of cells: KSC which are capable of infinite rounds of cell division, their immediate descendants, transient amplifying cells (TA) -which are capable of numerous but finite rounds of cell division-, and finally, non-dividing, and differentiating cells. Moreover, KSCs are relatively undifferentiated (ultra-structurally and biochemically) and posses many properties as follows: i) they have high proliferative potential and are responsible for long-term tissue maintenance; ii) they may be slow cycling presumably to conserve the proliferative potential and minimize the DNA replication error; iii) they are often located in close proximity to rapidly dividing cells, and in well-vascularized and well-protected area. Instead, the TA cells have the capability to withdraw from the cell cycle, migrate and differentiate into the distinctive suprabasal spinous, granular and stratum corneum layers of the epidermis.

Currently, there is also another hypothesis indicating that basal clones are not organized into these discrete functional unit, but, on the contrary, some clones were observed to increase their size parallel to the underlying basement membrane (lateral expansion), and their growth at the basal layer of the epidermis remained linear with time, constituting a unipotent population of cells, termed committed progenitors (Singh et al., 2012; Cangkrama et al., 2013; Solanas et al., 2013)

The proliferative hierarchy must be tightly regulated both temporally and spatially during epidermal development and homeostasis in order to prevent uncontrolled growth leading to hyperproliferative states and/or tumorigenesis (Strachan et al., 2008). Furthermore, the epithelium homeostasis is maintained by a balance in the stochastic cell fate specification following cell division (modified by the local microenvironment and mutations), which can lead to three possible outcomes: two proliferating cells, one proliferating and one differentiating cell, or two differentiating cells (Figure 10) (Kranjec et al., 2016).

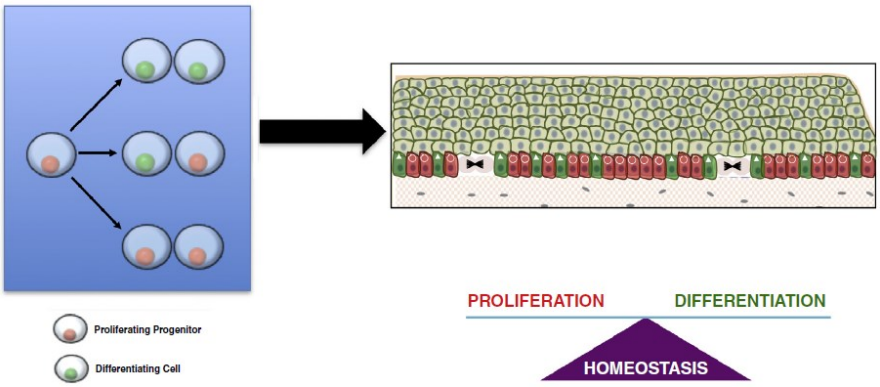

Figure 10. Cell dynamics in the homeostatic squamous epithelium. Each cell division can have one of the three possible outcomes: two differentiating cells, one differentiating and one proliferating progenitor and two proliferating progenitors (left panel). The fate of each division is stochastic and unpredictable, however across the total population the probabilities of having one of the three possible outcomes is balanced. As a result, in the basal layer there is the co-existence of proliferating progenitors (red cells with circles) which compensate for the loss of postmitotic cells by terminal differentiation (green cells with arrowhead) and stratification. Ultimately this ensures the regeneration and homeostatic maintenance of the epithelium (Kranjec et al., 2016).

In adult humans the renewal of the entire epidermis from the KSC populations takes approximately 4 weeks. Since the skin is the largest human organ (it is estimated to cover a surface area of approximately 1.8 m^2 on the average human body), this is a massive amount of continuously renewing tissue whose proliferation must be tightly controlled. KSC populations and their proliferative progeny are responsible for this remarkable feat of epidermal homeostasis by which a functional and even thickness epidermis is maintained (Strachan et al., 2008).

The first label-retaining experiments, that consist to label DNA in all dividing cells in the epidermis at a time point and then identify those cells that do not divide subsequently and thus retain the label DNA, described a population of slow-cycling cells residing at a protrusion below the sebaceous glands named the bulge region. These bulge label-retaining cells (LRC) were later shown to be able to regenerate the cycling portion of the HF after each growth cycle, confirming that they act as HF-KSC. However, bulge KSC do not contribute to the IFE proliferation, unless it has been damaged. These findings suggest the hypothesis that different KSC populations with specific properties and lineage preferences are responsible for the maintenance of the IFE and HF. Further experiments have been done for discovering new KSC markers using the lineage-tracing techniques: these consisted in the genetic tagging of a certain cell types that allows following its fate and that of its progeny during a particular process, such as development, homeostasis,or carcinogenesis.

Based on the latest advances, it arises the idea that KSC populations in the epithelium are highly compartmentalised and gradients expression of KSC surface markers are consistent with gradients of "stemness", as opposed to the idea of the existence of discrete stem and TA cell populations. The epidermis has resident KSC populations localized in the HF where KSC are activated at the start of a new hair cycle and upon wounding to provide cells for HF and IFE regeneration and repair, which ensures tissue renewal in the absence of injury (Watt 2014; Solanas et al., 2013; Donati et al., 2015).

2.3.2 Hair Follicle-Keratinocyte Stem Cells (HF-KSC) features

In murine skin, the first step of HF generation is the aggregation of a condensate of dermal fibroblasts around an area of the developing epidermis that secretes signals essential for HF formation. Embryonic HF-KSC are characterized by the expression of different factors that, in some cases, are later required to maintain HF stem cells throughout adulthood. These include the transcription factors SOX9 (LIM homeobox 2), NFATC1 (nuclear factor of activated T cells cytoplasmic 1), TCF3 (T cell factor 3) or TCF4 and TBX1 (T-box transcription factor 1), which are normally involved in developmental processes. Once morphogenesis is completed, approximately 18 days after birth, the first adult hair follicle cycle starts. Degeneration (catagen), resting (telogen) and regeneration (anagen) cycles will sequentially follow during the whole life of the mouse. Different pools of KSC are distributed along the longitudinal and vertical axes of the HF, which are defined by the expression of different superficial markers (Figure 11). These different pools have been shown to contribute to distinct temporal phases of the hair cycle and to different regions of the HF and IFE regeneration on wounding.

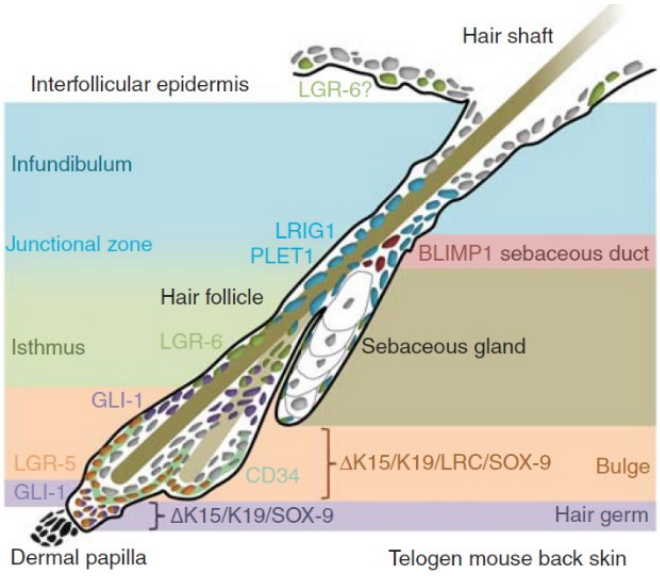

Figure 11. Markers of HF-KSC subpopulations in murine adult skin (Kretzschmar et al. 2014).

HF-KSC: bulge and germ region

In the bottom area of the mouse HF (lower portion of the bulge), the more proliferative cells are in close contact with the secondary hair germ and are enriched in the expression of the surface marker LGR-5 (Leu-rich repeat-containing G protein-coupled receptor 5) together with components of the Hedgehog signalling pathway, such as Sonic Hedgehog (SHH) and protein glioma-associated oncogene homologue 1 (GLI-1). GLI-1+ cells are found in the lower bulge and germ, as well as in the upper bulge. Interestingly, KSC expressing GLI-1 not only gave rise to differentiated cells in all layers of the lower HF, but were also found in the isthmus and junctional zone adjacent to the SG. In addition, GLI-1 contribute to IFE regeneration on wounding.

Among the bulge stem cell population, the first level of heterogeneity arise from the fact that only a portion of bulge KSC is activated during anagen and that different bulge KSC show distinct propensity to proliferate. The vertical axis in the bulge also distinguishes between KSC located in the mid-and upper bulge regions, which show lower levels of proliferation, and rapidly cycling KSC found in the lower bulge. Several markers have been identified in the HF bulge region. Significant overlap is found between expression of clusters of the differentiation marker CD34 and keratin 15 (K15), which is expressed at low levels throughout the epidermal basal layer and enriched in the bulge. There are two distinct layers of CD34+ bulge KSC, one of which expresses high levels of α6 integrin and is attached to the basement membrane, whereas the other, which appears only after the first hair cycle, is suprabasal and expresses low

levels of α6 integrin. Another KSC marker of the bulge region is SRY (sex determining region Y) - box 9 (SOX- 9). SOX-9 is expressed in the developing HF at embryonic day (E) 15.5 and marks slowly cycling and CD34+ HF-KSC that give rise to the entire pilosebaceous unit. As mention before, several other functional bulge KSC markers have been described, such as transcription factor 3 (TCF-3), LIM homeobox 2 (LHX2) and nuclear factor of activated T cells, cytoplasmic 1 (NFATC1).

Characterizing HF-KSC markers in human skin has been challenging because of the lack of robust tools for lineage tracing. Nevertheless, further analysis has been done and led to the identification that human bulge and hair germ KSC are enriched for both CD200 and K15, but negative for CD34 and CD271 (Kretzschmar et al., 2014)

HF-KSC: bulge upper region and sebaceous glands

HFs connect with the epidermis through the infundibulum, the junctional zone, and the isthmus which are positioned immediately above the bulge (Figure 9). These three areas have recently attracted much attention, as they seem to contain several subsets of specialized KSC.

In murine skin, the first pool of stem cells is located at the upper area of the bulge, although they can still be considered as part of it on the basis of their location. They differ from lower bulge populations in that they do not express CD34 and K15 and have high levels of GLI-1. Intriguingly, although hair germ and lower bulge cells are the first to contribute to hair cycling, upper bulge stem cells are as efficient as their lower counterparts in contributing to all the HF lineages during anagen. However, lower K15+ bulge cells contribute to the healing of IFE wounds in a transient way, whereas the progeny of K15– and GLI-1+ upper bulge cells stably remain at the wounded area long after it has been repaired. This suggests that upper bulge cells might constitute a long-term reservoir of KSC that contribute to the repair of the IFE in a stable manner.

The isthmus, a HF area just above the bulge, contains another KSC population marked by the *Lgr* family member LGR-6 (Figure 11). During postnatal hair morphogenesis, epidermal Lgr-6 expression is mainly detectable in the isthmus region, but LGR-6+ cells are also found in the IFE basal layer, periphery of the SG and the lower HF. Upon injury, LGR-6 stem cell progeny readily contribute to wound healing. LGR6+ cells show enriched expression of the epithelial stem cell marker MTS24, but do not express bulge KSC markers such as CD34 or K15. It is worth noting that the expression of MTS24 is broader than that of LGR6 and extends upwards into the junctional zone. This suggests that two distinct stem cell types coexist in the

junctional area, one in the lower territory (LGR6+) and the second in the upper region (MTS24+). However, the specific function of upper MTS24+ cells has not yet been described.

Climbing up along the vertical axis of the HF junctional zone (adjacent to the SG and infundibulum) there is a quiescent pool of cells that expresses the surface marker Lrig1+ (Leucine-rich repeats and immunoglobulin-like domain protein 1) (Figure 11). In mouse HF, Lrig1+ KSC defines the HF junctional zone adjacent to the sebaceous glands and infundibulum, whereas in adult human is located in the IFE. Lrig1+ stem cells are enriched for PLET1, but are negative for bulge stem cell markers such as CD34 or LGR-5 and only show low expression of α6 integrin. During normal homeostasis, Lrig1+ cells predominantly contribute to the junctional zone, the IFE and sebaceous glands but not to the HF. On wounding, progeny of Lrig1+ KSCs are rapidly recruited to the site of injury and contribute permanently to tissue regeneration. (Jensen et al., 2009)

To summarize, first, the maintenance of the junctional zone requires two types of KSC (LGR6+ and Lrig1+). Second, the progeny of both LGR6+ and Lrig1+ stem cells feeds into the IFE, although it is not known whether this contribution is random or restricted to specific areas. Another KSC markers localized in the upper area of the bulge region is the Placenta-expressed transcript protein 1 (PLET1), the first specific marker of HF KSC to be described outside the bulge. Besides expressing α6 integrin and K14, PLET1+ keratinocytes are negative for the KSC bulge markers CD34 and K15.

With regard to the sebaceous glands, there are at least three types of stem cells, Lrig1+, LGR6+ and bulge KSC that contribute to their maintenance. In addition to these, a fourth population of cells that expresses the transcription repressor BLIMP1 (B lymphocyte-induced maturation protein 1) (Figure 11) and localized adjacent to the SG contains sebocyte progenitors, suggesting a role for BLIMP1 in controlling the transition of quiescent stem cells to proliferative progenitor cells.

In human skin, no markers of KSC residing in either the junctional zone or SGs have been described so far (Singh et al., 2012; Solanas et al., 2013; Kretzschmar et al., 2014).

2.3.3 Interfollicular epidermis - keratinocyte stem cells (IFE-KSC) features

The IFE is defined as the region of stratified epidermis flanked by HFs. The classic hypothesis of IFE-KSC stem cell behaviour, based on label-retaining studies, pronounced that stem cells located at the basal layer give rise to short-lived progenitors that undergo several rounds of division, known as TA cells. These cells would amplify the keratinocyte population

and migrate upwards as they differentiate. Recent studies suggest, however, that the basal layer of the mouse IFE is heterogeneous and, other than basal cells that behave like committed progenitors, contain a reservoir of quiescent basal cells, it is predominantly implied in regenerative purposes, and is possibly compartmentalized around the HFs (Figure 12).

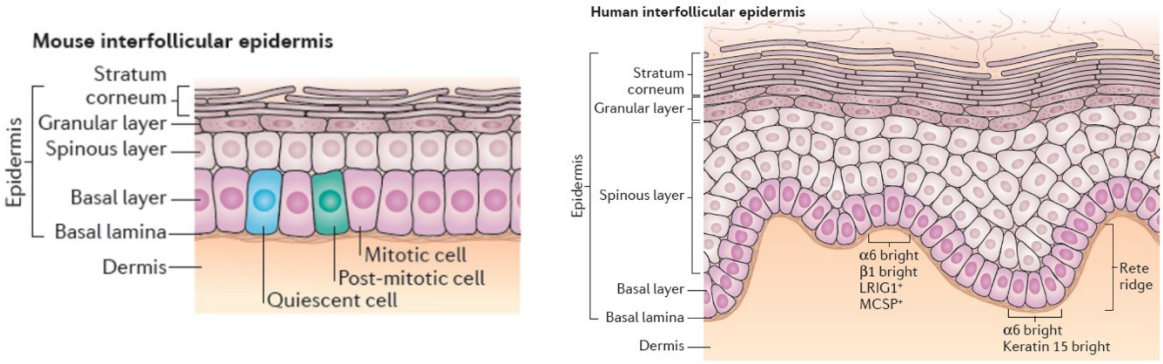

Figure 12. Left panel: the basal layer of the mouse IFE contains a unipotent population of cells termed committed progenitors that divide in a stochastic manner. In addition, the basal layer contains a quiescent population reserved for regeneration. Right panel: quiescent human IFE-KSC express high levels of α6 and β1 integrins, as well as Lrig1 (Leu-rich repeats and immunoglobulin-like domains 1) and MCSP (melanoma-associated chondroitin sulphate proteoglycan) (Solanas et al., 2013).

Molecular analysis of these two populations revealed that committed progenitors express lower levels of KSC markers, such as α6 and β1 integrin, and higher levels of proteins controlling the epidermal and keratinocyte differentiation programme, like Notch 3, GRHL3 and some members of the SPPR family. In addition, committed progenitors show higher rates of proliferation than the quiescent KSC population from which they originate. Interestingly, the higher expression of β1 integrin by quiescent mouse IFE-KSC has also been observed for human IFE-KSC, with quiescent and proliferative KSC populations being distinguished by several markers. For instance, quiescent human IFE-KSC not only express higher levels of α6 and β1 integrins, but also lower levels of the transferrin receptor CD71. Quiescence of human IFE-KSC also relies on the activity of Delta 1, MCSP (melanoma-associated chondroitin sulphate proteoglycan), Lrig1 (Leu-rich repeats and immunoglobulin-like domains 1), the polycomb protein CBX4 (chromobox protein homologue 4), or low levels of DSG3 (desmoglein 3) and EGFR (epidermal growth factor receptor).

However, the location of human quiescent IFE-KSC within the basal layer is still under debate, and three different hypotheses have been proposed. One of these suggests that the cells with the highest expression of α6 integrin and K15 located at the bottom of the rete ridges (structures

on the basal layer of the human IFE) are relatively quiescent and display a higher clonogenic potential than the more proliferative and K5 dimmer upper-rete ridge basal cells. However, there is also strong evidence indicating that the β1 integrin, MCSP and Lrig1+ quiescent KSC clustered at the top of the rete ridges harbour the highest stemness of all basal cells. Nevertheless, and contradicting both views, a third hypothesis based on lineage-tracing experiments in human grafts suggests that all epidermal basal cells, irrespective of their location, contribute equally to the maintenance of the epidermis. New approaches will be required to solve this problem, but regardless of whether quiescent stem cells reside at the tip or at the top of the ridges, it is important the information that the human epidermis does contain proliferative and quiescent pools of basal cells. This raises the possibility that the mechanisms ensuring its daily renewal might not differ greatly from those identified in the mouse IFE (Jensen et al., 2009; Kretzschmar et al., 2014)

Although epidermal stem cells reside in distinct locations and maintain homeostasis in a highly compartmentalized fashion, each stem cell population retains the capacity to differentiate into cells of all epidermal lineages, in response to wounding or genetic manipulation. This remarkable plasticity of adult epidermal stem cells has become apparent only recently and can be achieved by disrupting normal epidermal organization or altering key signaling pathways. A network of intracellular signalling pathways and reciprocal signaling with other cell types, such as melanocytes and dermal fibroblasts, maintain epidermal stem cell homeostasis (Strachan et al. 2008; Solanas et al. 2013, Watt et al., 2009; Page et al. 2013).

3. AIMS

3. Aims

Modern organ transplantation, which includes a multitude of different organs, is no longer encumbered by graft rejection but instead morbidity and mortality from cancer as a direct consequence of immunosuppressive therapy. The incidence of cancer in organ transplant recipients (OTRs) is at least double that of the general population, while the risk of skin cancer (notably squamous cell carcinoma, SCC) is x60-250 and is the most frequent form of malignant cancer in these individuals. In addition to the other well-known risk factors, numerous studies have also pointed to a possible causal role of *Betapapillomaviruses* (β-HPVs) in the pathogenesis of skin cancer. Nearly all adults are persistently infected in the skin with many viruses belonging to the β-HPV family. Although they appear not to cause overt clinical symptoms in a great majority of infected individuals, both experimental and epidemiological evidence suggests a carcinogenic role of these viruses in the skin that takes place at the early stages, particularly in subjects with impaired immune function. Borgogna and coworkers clearly showed that β-HPVs are actively replicating in precancerous lesions and in the vicinity of malignant tumours of kidney transplant recipients and can therefore cooperate with other carcinogenic agents, such as UVB, favouring skin cancer promotion (Borgogna, Lanfredini et al., 2014).

The aim of the present study was to unveil the molecular mechanisms underlying β-HPV-induced skin cancer through different approaches that can be summarized in three main objectives: 1) to demonstrate that the HPV8 oncoproteins target specific long-lived keratinocyte stem cell populations and provide a mechanistic model for the increased keratinocyte proliferation in HPV8 transgenic mice. We provide a model of β-HPV-induced skin carcinogenesis that is based on the aberrant expansion of Lrig1+ KSC in the upper hair follicle that spill out into the surrounding epidermis. Similarly expansion of the junctional zone HF KSC population was identified by p63 labelling in human EV keratosis and actinic keratosis; 2) establishment of an in vivo tumorigenicity assays of skin tumours from OTRs. We have generated in vivo orthotopic tumourgrafts in nude mice from human skin tumours and investigated β-HPV infection/expression in both original human tumours and tumourgrafts; and 3) to determine whether immunosuppression inhibits tumour immune surveillance and killing, leading to an increased/faster SCC formation in HPV8 transgenic mice. To this end, we have established a mouse model recapitulating the events occurring in OTR by crossing the β-HPV8 transgenic mice (HPV8tg) with Rag2 deficient mice (which lack

B and T cells). We have determined spontaneous SCC frequency in the following two cohorts: HPV8tg+:Rag2$^{-/-}$ and HPV8+:Rag2$^{+/+}$.

The results obtained during the three year period of my PhD program are reported in the results chapter that includes three parts as follows: 1) HPV8 Field Cancerization in a Transgenic Mouse Model is due to Lrig1 Keratinocyte Stem Cell Expansion (accepted for publication in Journal of Investigative Dermatology, April 2017); 2) Understanding the natural history of β-HPV infection in skin lesions and their malignant progression using tumourgraft models; 3) Establishment of an immunodeficient HPV8tg mouse model that recapitulate the events occurring in OTR.

4. RESULTS

4.1 HPV8 Field Cancerization in a Transgenic Mouse Model is due to Lrig1+ Keratinocyte Stem Cell Expansion (Accepted for publication in Journal of Investigative Dermatology, April 2017)

The HPV8tg mice skin displays HF proliferative epidermal hyperplasia

After birth, HPV8tg mice develop thicker skin in comparison to wild type (WT) littermates (Figure 13). Adult HPV8tg skin thickness of the ear was 0.6±0.1 vs 0.4±0.1 mm ($p<0.05$, $n=9$), there was no difference in weight and tail width. More keratinocyte layers were evident in the HF infundibulum and adjoining interfollicular epidermis (IFE) in HPV8tg, 4.2 ± 0.47 vs 2.0 ± 0.0 and 3.8 ± 0.49 vs 1.5 ± 0.43 respectively ($p<0.01$, $n=5$), but stratum corneum thickness measured on histological sections was not different.

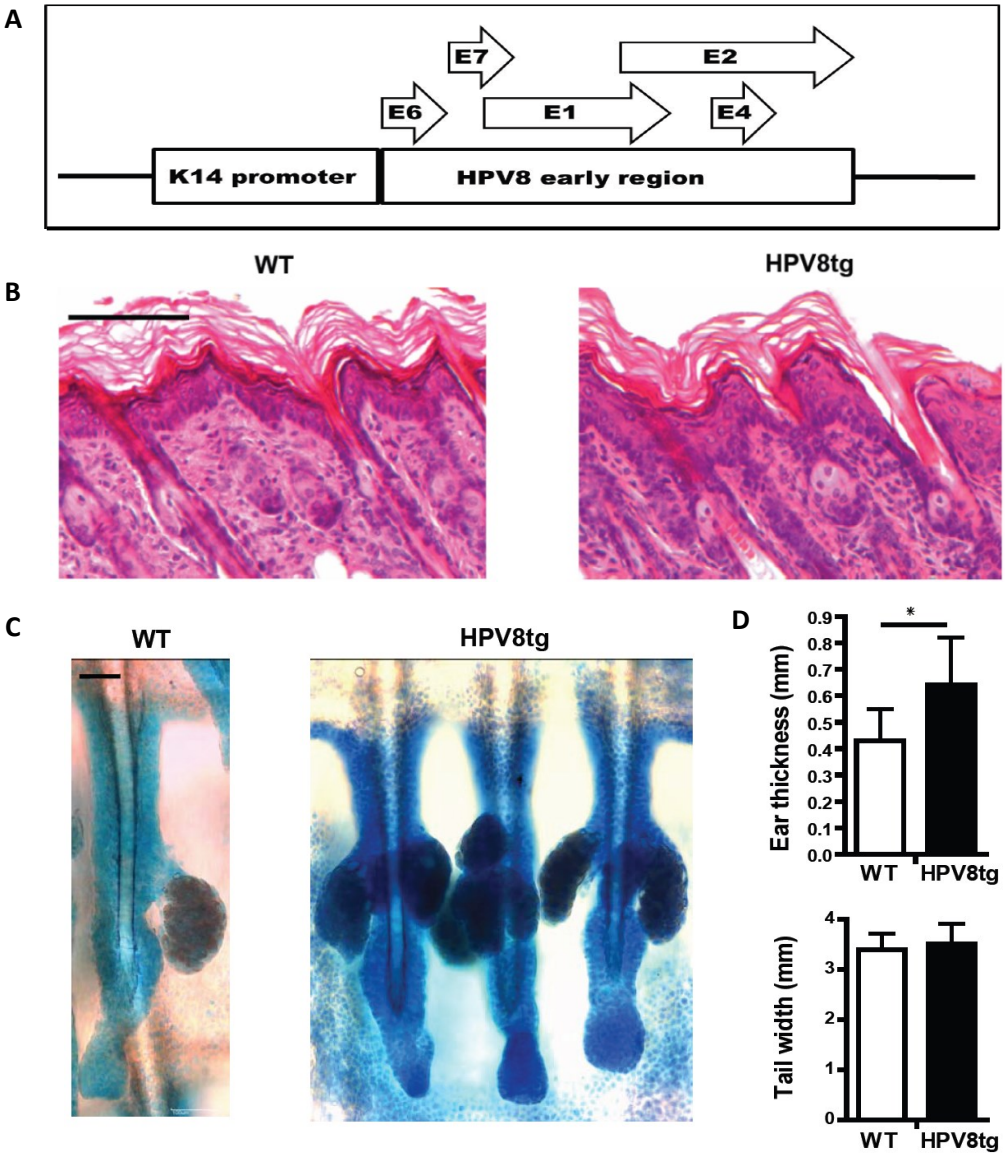

Figure 13: Phenotypic and histological characterization of HPV8tg mice.
A, Schematic representation of the HPV8 transgenes, showing the human cytokeratin-14 gene promoter upstream of the open reading frames of the HPV8 early region genes. **B,** Hematoxylin and eosin staining of paraffin embedded skin sections from WT (left panel) and HPV8tg (right panel) mouse skin. **C,** Toluidine blue staining of mouse whole mount skin including the hair follicle and overlying epidermis from WT (left panel) and HPV8tg (right panel) from the tail. **D,** Ear thickness (upper graph) and tail width (bottom graph) measured using calipers on age matched WT and HPV8tg littermates (n=8), with mean+/-SD (*,$p<0.05$; unpaired t test). All the images were processed using ImageJ software (NIH, USA). All scale bars =100µm.

Consistent with a hyperproliferative epidermis, keratinocyte proliferation assessed by Ki67 positive cells per basal keratinocyte was markedly increased within the HF (41± 10.9 vs 23 ± 11.8, n=7, p=0.01) and to a lesser extent the IFE (0.46± 0.18 vs 0.31 ± 0.11, n=15, p=0.01). The expression of HPV8 early region genes in this transgenic mouse model has been previously described (Schaper et al., 2005; De Andrea et al., 2010). While this HPV8tg mouse model yield spontaneous SCC formation, other similar β-HPV transgenic models driven by K14 promoter do not develop SCC spontaneously (Viarisio *et al*. 2011). Consistent with this, levels of E6 and E7 expression in HPV8tg mouse skin were similar to that observed in HeLa cells with natural HPV18 infection (Figure 14).

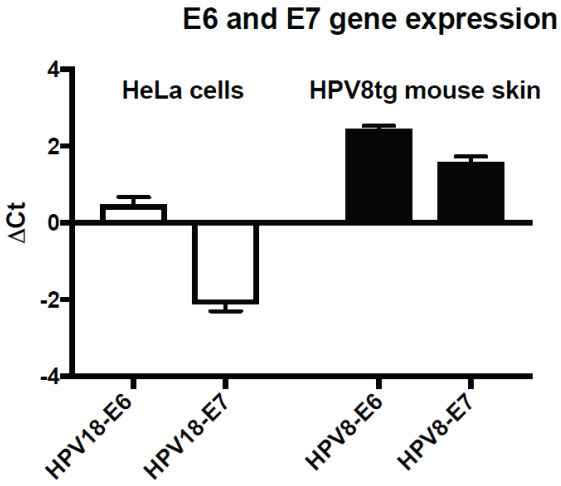

Figure 14: **Expression of E6 and E7 genes of HPV8 and HPV18 in HPV8tg mouse skin and HeLa cells respectively.**
qRT-PCR of E6 and E7 genes from RNA isolated from Hela cells and HPV8tg mouse skin, relative to β-Actin, with mean +/- SD.

Together these findings suggested that HPV8 early region genes induce a proliferative epidermal hyperplasia, notably in the HF. HPV8 induced keratinocyte proliferation was

greatest in the HF and immediately adjoining IFE, as determined by Ki67 expression, even though keratin 14 promoter driven HPV8 early region genes were uniformly expressed.

The Lrig1 KSC population is expanded in HPV8tg mice

Within the HF, the mean area of the infundibulum was markedly increased in HPV8tg compared to WT mice (Figure 15A), while there was no difference in HF length (Figure 15B).

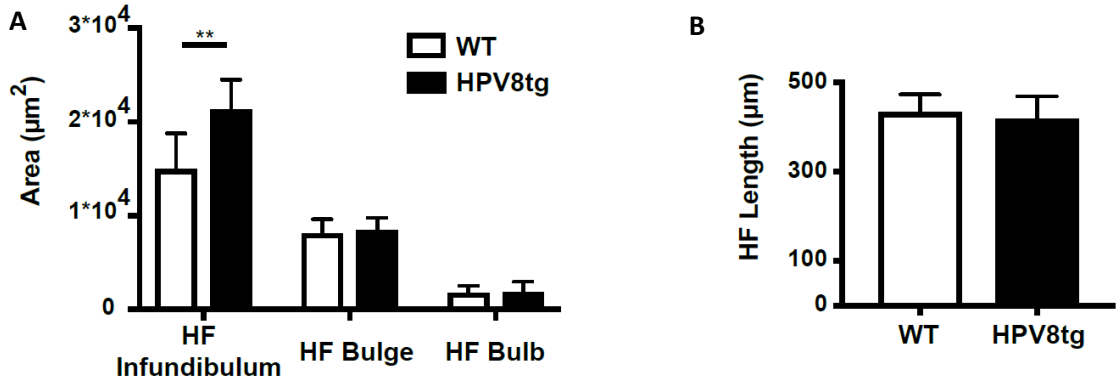

Figure 15: HPV8 transgenes induce hair follicle changes in HPV8tg mice.
A, B, Adult mice whole mount skin were photographed and analyzed for the area of HF regions and length, WT and HPV8tg were compared, with mean+/-SD, using an unpaired t-test (n=20, ** $p<0.01$).

To determine which hair follicle keratinocyte population become expanded in HPV8tg mice compared to wild type littermates, we labelled skin sections in whole mount analysis with a set of stem cell markers. Consistent with the observed HF infundibulum expansion, keratinocyte proliferation was evident within the Lrig1+ KSC population (69 vs 55%, $p<0.001$, n=6), and not in the CD34+ (1 vs 1%), LGR5+ (1 vs 3%) and LGR6+ (29 vs 40%) KSC populations (n=7, Figure 16). Flow cytometric analysis of dissociated skin confirmed a 2.8-fold increase in Lrig1+ keratinocytes in the HPV8tg mice (7.4% +/- 2.2% vs 2.7% +/- 0.8%, n=6, $p < 0.05$), but no difference in CD34+ KSC numbers (0.81% +/- 0.24% vs 0.73% +/- 0.37%) (Figure 16B).

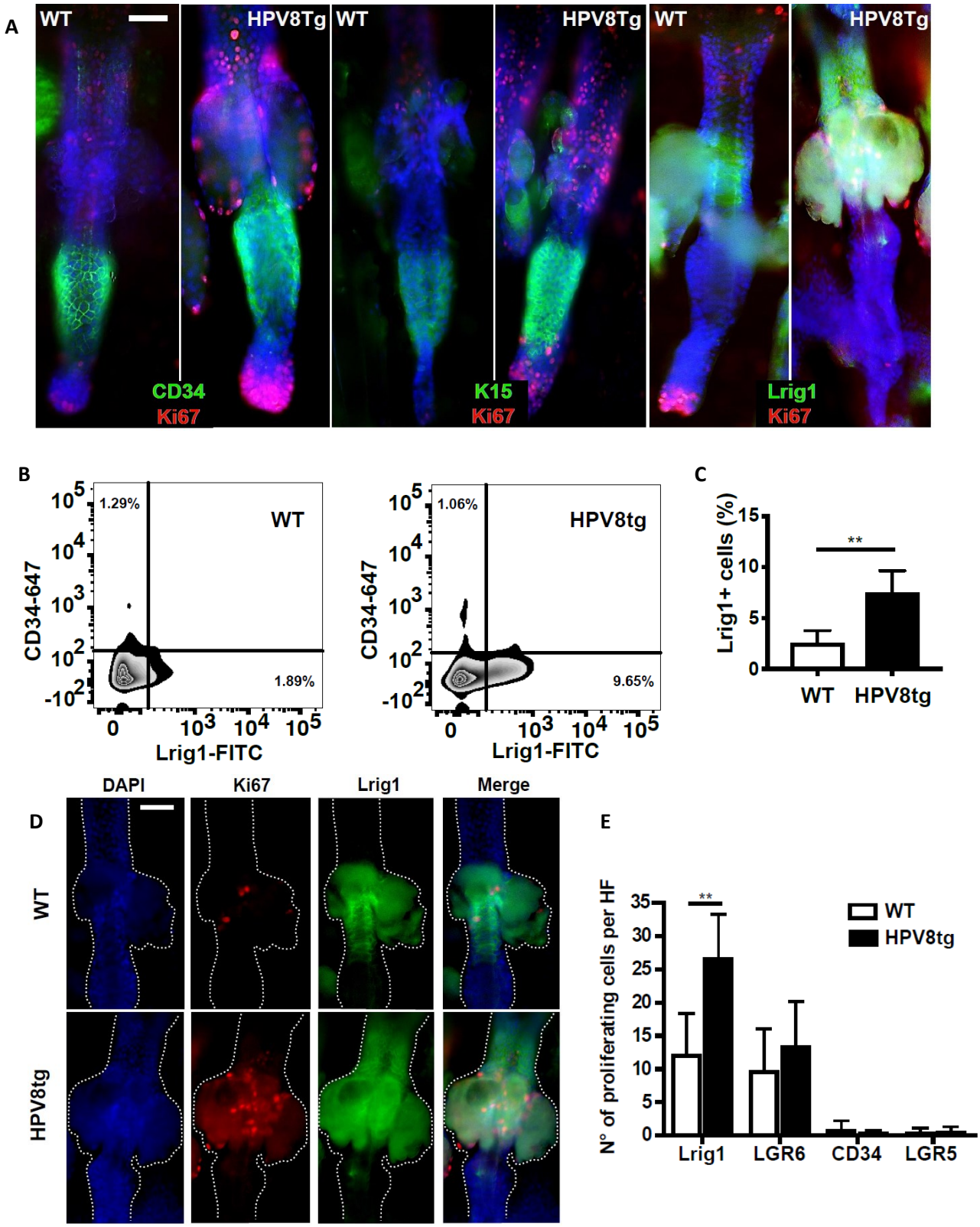

Figure 16: Lrig1 keratinocyte stem cell proliferation in HPV8tg

A, Whole mount immunofluorescence of adult WT and HPV8tg tail skin for Ki67 (red) and HF-KSC markers (green). **B,** FACs analysis WT and HPV8tg mice skin keratinocyte isolates (n=6), labelled with Lrig1-FITC and CD34-647 antibodies, with DAPI to select live cells. **C,** The number of Lrig1 positive cells determined by FACs (n=6). (**, $p<0.01$; unpaired t test),

with mean+/-SD. **D,** Whole mount adult WT and HPV8tg (n=6) skin sections labelled with Ki67 (red), Lrig1 (green) antibodies and DAPI (blue). **E,** Number of proliferating cells within KSC populations (Lrig1, LGR6, CD34, and LGR5) was enumerated, with mean+/-SD, in WT and HPV8tg tissue sections (n=7); (** $p<0.01$). All the images were processed using ImageJ software (NIH, USA). All scale bars = 100 µm

Flow sorted Lrig1+ and CD34+ keratinocyte sub-populations had similar levels of K14 promoter driven early region genes mRNA expression (Figure 17A), despite the observed difference in proliferation. To exclude any difference in the EVER 1 and 2 gene expression levels in HPV8tg mice versus control, qRT-PCR analysis was performed with the RNA extracted from Lrig1+ sorted cells and found comparable levels as shown in Figure 17B.

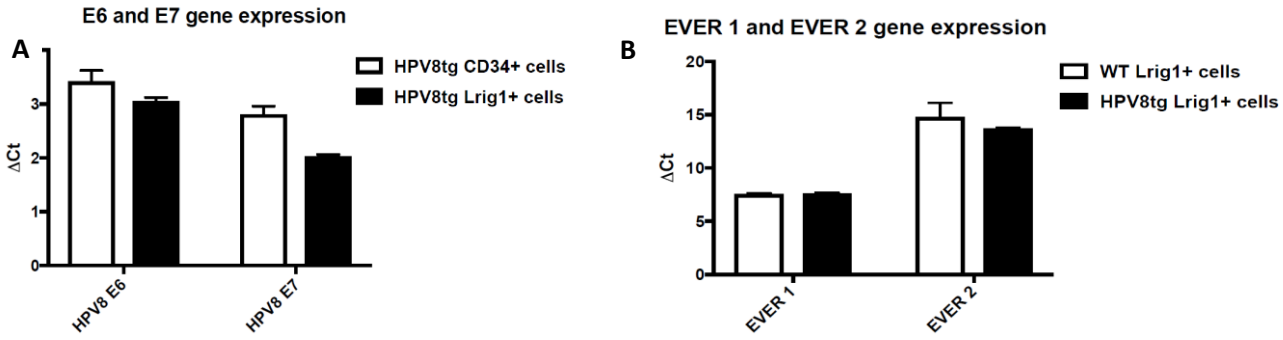

Figure 17: HPV8 transgenes are uniformly expressed in the epidermis of HPV8tg mice. **A,** qRT-PCR of early region genes of WT and HPV8tg mouse skin isolated KSC populations, with mean+/-SD. **B,** qRT-PCR of murine homologues of EVER1 (TMC6) and EVER2 (TMC8) genes of WT and HPV8tg mouse skin isolated Lrig1+ KSC populations, with mean+/-SD.

Flow sorted Lrig1+ keratinocytes from HPV8tg mice also demonstrated a 3.8 fold increased colony forming efficiency (Figures 18A&B), hence Lrig1+ cells retain KSC function. There was no significant difference in colony forming efficiency from flow sorted Lrig1 negative keratinocytes from HPV8tg versus WT mice (Figure 18C).

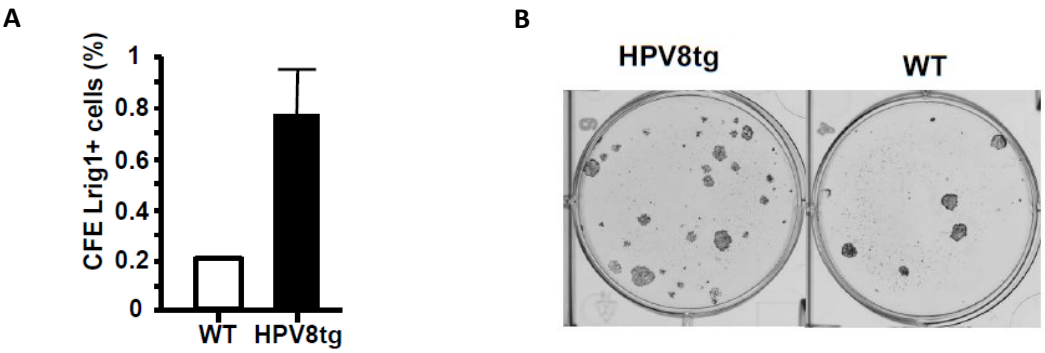

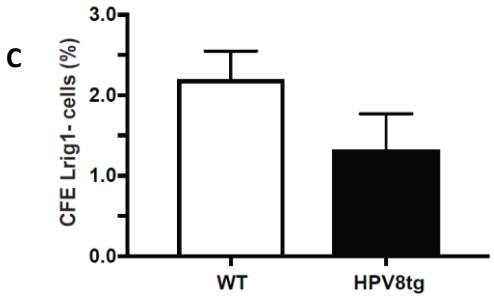

Figure 18: Lrig1+ cells retain KSC function
A, Keratinocyte colony forming assays from flow sorted Lrig1 cells from WT and HPV8tg (n=6) skin dissociates, with mean+/-SD and **B,** A representative image. **C,** Keratinocyte colony forming assays from flow sorted Lrig1 negative cells from WT and HPV8tg (n=6) skin dissociates, with mean+/-SD.

In keeping with Lrig1+ expansion and proliferation, we observed nuclear p63 expression throughout this population and the emanating keratinocytes of HF infundibulum and adjoining IFE (Figure 19A). RT-PCR and western blotting analysis confirmed the switch from p63 TA isoforms to ΔNp63 isoforms in HPV8tg skin (Figures 19B-D), consistent with earlier reports indicating HPV8 early proteins induce p63 expression (Meyers *et al*., 2013). Thus Lrig1+ KSC proliferation through induction of ΔNp63 in HPV8tg skin resulted in KSC expansion into the overlying infundibulum and adjoining IFE.

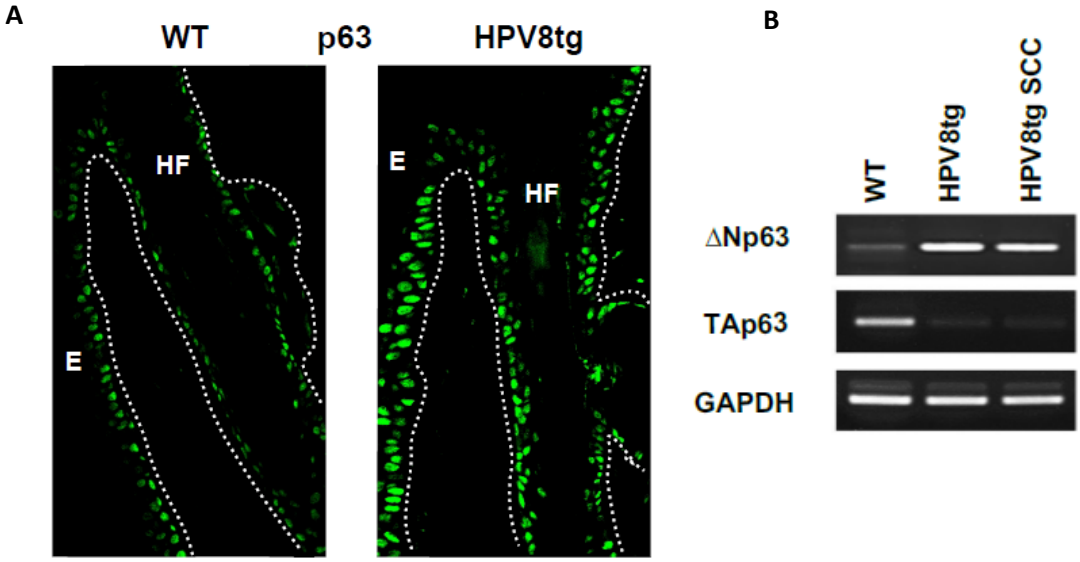

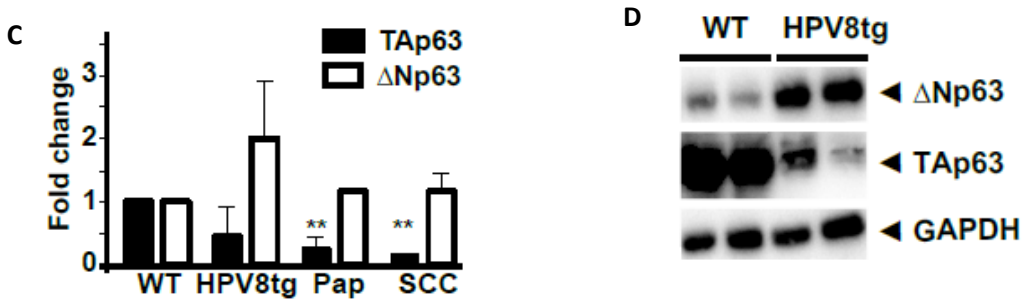

Figure 19: **Switch from TAp63 to ΔNp63 isoforms expression in HPV8tg skin**
A, p63 labelled frozen sections from adult WT and HPV8tg mice (n=3), the broken line indicates the basal layer. Immuno-labelled tissue sections were visualized and photographed by fluorescent microscope with x20 magnification then processed using ImageJ software (NIH, USA). **B&C,** RT-PCR with mean+/-SD (**, $p<0.01$) and **D,** Western blot gels of p63 isoforms from RNA and protein isolates respectively from WT, HPV8tg skin, papilloma (pap) and SCC (n=6).

β-HPV associated expansion of the HF junctional zone KSC population in human skin field cancerization

The dilated HF infundibulum with increased keratinocyte layers and the crowded perifollicular epidermis with hyperkeratosis were consistently observed in the HPV8tg mice, and resembled Freudenthal's funnel, the pathognomonic histological finding in actinic keratosis (n=28 mice, Figure 20).

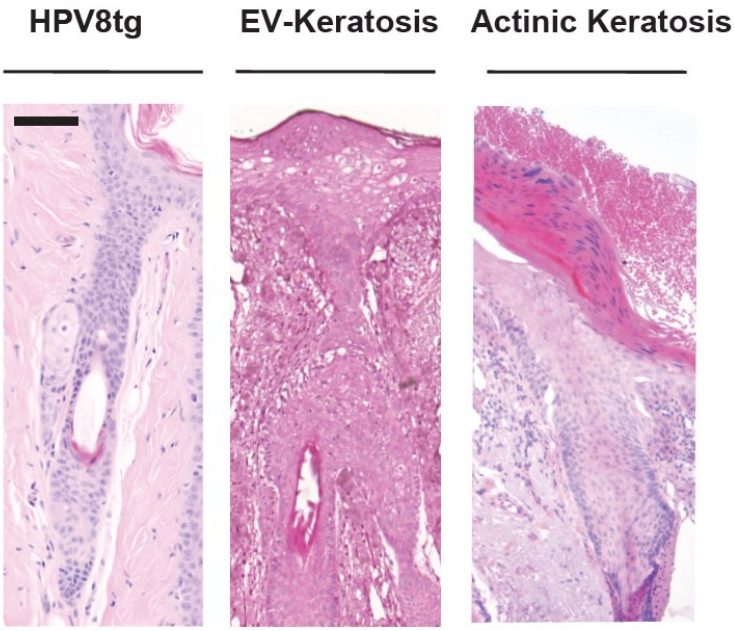

Figure 20: H&E staining on HPV8tg mouse skin, EV-Keratosis and Actinic Keratosis

Hematoxylin and eosin staining of paraffin embedded skin sections from HPV8tg mouse, EV-Keratosis and Actinic Keratosis corresponding to figure 21A. Scale bar is 100μm.

EV keratosis uniformly demonstrated similar histology associated with β-HPV virus reactivation and nuclear p63 expression within the HF infundibulum and perifollicular epidermis (Figure 21A, 6 patients with 44 lesions, Table 1). Likewise, in some cases of actinic keratosis from non-EV patients, we were able to detect nuclear p63 expression within the infundibulum and perifollicular epidermis in areas where β-HPV virus reactivation was well evident, as detected by expression of the viral marker E4 (Figure 21A, n=2 of 25). Hence, our findings suggest that similar to HPV8 mice, EV and some patients with AK demonstrate expansion of a novel junctional zone HF KSC population identified by p63 labelling. These findings would suggest that β-HPV field cancerization arises from the HF infundibulum and predispose to SCC. Indeed, we observed p63 positive cells in HPV8tg and human SCC (Figure 21B, n=5); the latter were from immunocompetent patient from sun-exposed sites. Hence, we propose that β-HPV early region genes initiate proliferation of Lrig1+ KSC causing their expansion into the HF infundibulum and overlying epidermis. β-HPV driven KSC proliferation results in EV keratosis and occasionally non-EV AK, which are predisposed to transformation into SCC whereupon the β-HPV episome and so gene expression is lost (see Figure 34 in Conclusion).

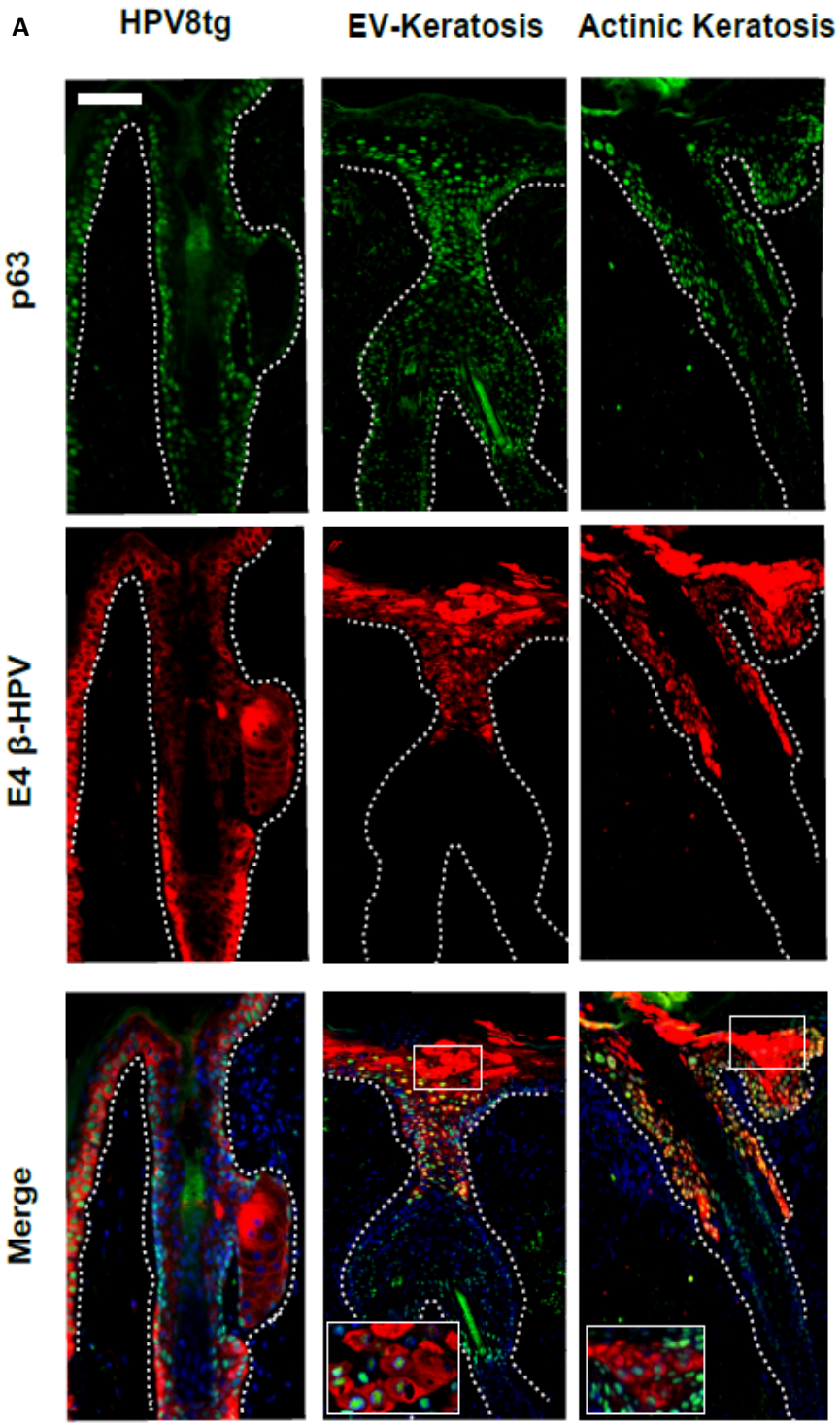
A
HPV8tg
EV-Keratosis
Actinic Keratosis
p63
E4 β-HPV
Merge

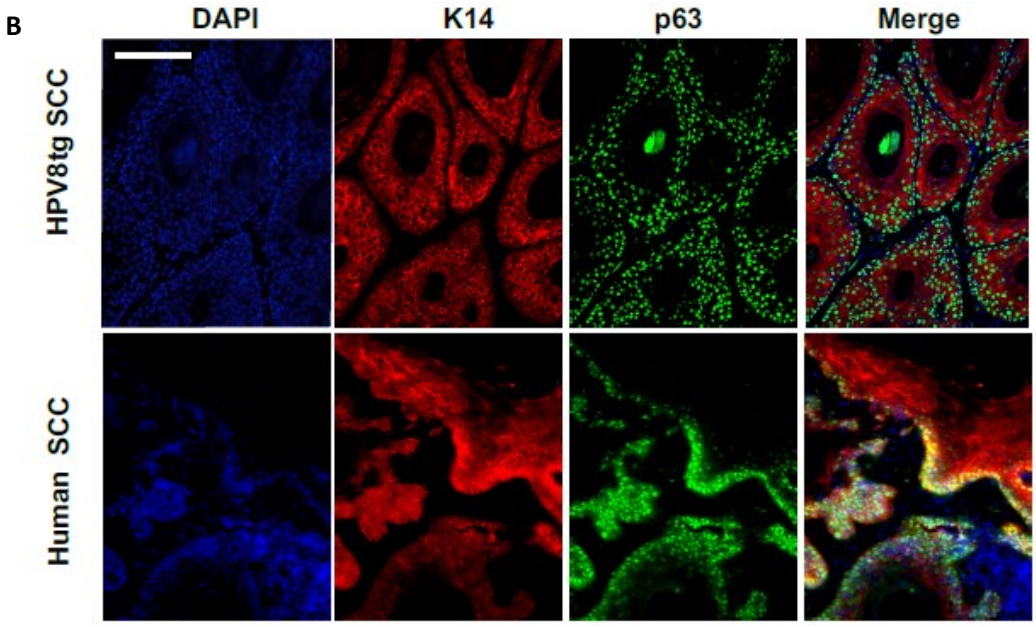

Figure 21: β-HPV induced keratinocyte stem cell expansion results in keratosis that are predisposed to SCC

A, Images of tissue sections of HPV8tg mouse skin, human EV keratosis, and AK labelled with p63 (green), β-HPV E4 (red) specific antibodies, and DAPI (blue). **B,** Images of tissue sections of HPV8tg mouse and human SCCs labelled with K14 (red), p63 (green) specific antibodies and DAPI (blue). Immuno-labelled tissue sections were visualized and photographed by fluorescent microscope with x20 magnification then processed using ImageJ software (NIH, USA). All scale bars are 100μm.

Table 1: summary of EV patient lesions

EV patient	EVER 1/2 genetics	T-Cell phenotype[1]	Year of birth	Nature of lesion[2]	Anatomic site	Year of lesion excision	References
1	WT	Slightly low CD3 Normal CD4 Low CD8	1967	Wart-like lesion	forearm	2003	1,2
				SCC	temple	2003	
				SCC	forehead	2003	
				AK	elbow	2003	
				Bowenoid lesion	forehead	2003	
2	WT	Normal CD3 Slightly low CD4 Normal CD8	1947	Wart-like lesion	forearm	2005	2,3
3	WT	Low CD3 Low CD4 Normal CD8	1969	SCC	temple	1999	2
				Bowenoid lesion	temple	1999	
				Wart-like lesion	forearm	1999	
4			1948	Bowenoid lesion	back	1990	2,4,5
				SCC	eyelid	1993	

	EVER 2 mutation (p.Y109fsX118)	Normal CD3 Normal CD4 Normal CD8		BCC	eyelid	2007	
				SCC/AK	cheek bone	2007	
				SCC	temple	2008	
				SCC	eyelid	2008	
				SCC	nose	2008	
				SCC	nose	2008	
				AK	eyelid	2008	
				SCC	nose	2008	
5	EVER 2 mutation (p.V191fsX226)	Normal CD3 Normal CD4 Normal CD8	1952	Bowenoid lesion	temple	2005	4,5
				Bowenoid lesion	ear	2005	
				Bowenoid lesion	forehead	2007	
				Keratosis	lower lip	2007	
				SK	back	2007	
				Keratosis	back	2007	
				AK	scalp	2007	
				SCC	scalp	2008	
				Bowenoid lesion	neck	2008	
				SCC	scalp	2008	
				SCC	nose	2008	
				SCC	ear	2008	
				Bowenoid lesion	lower lip	2008	
6	WT	Normal CD3 Low CD4 Normal CD8	1958	Wart-like lesion	leg	1991	6
				Wart-like lesion	dorsum of hand	1991	
				Wart-like lesion	leg	1991	
				Skin fibroma	armpit	1997	
				Wart-like lesion	elbow	2003	
				Wart-like lesion	elbow	2005	
				AK	temple	2006	
				Bowenoid lesion	scapula	2008	
				SCC	forehead	2010	
				SCC	forehead	2010	
				Bowenoid lesion	temple	2010	
				AK	temple	2010	

[1]Slightly low = greater than 20% but less than 50% reduction in total count; low = less than 50% reduction in total count

[2]SCC (Squamous Cell Carcinoma), BCC (Basal Cell Carcinoma), AK (Actinic Keratosis), SK (Seborrheic Keratosis).

1) Azzimonti B, Mondini M, De Andrea M, Gioia D, Dianzani U, Mesturini R et al. CD8+ T-cell lymphocytopenia and lack of EVER mutations in a patient with clinically and virologically typical epidermodysplasia verruciformis. Arch Dermatol. 2005 Oct;141(10):1323-5
2) Dell'Oste V, Azzimonti B, De Andrea M, Mondini M, Zavattaro E, Leigheb G, et al. High beta-HPV DNA loads and strong seroreactivity are present in epidermodysplasia verruciformis. J Invest Dermatol. 2009 Apr;129(4):1026-34
3) Zavattaro E, Azzimonti B, Mondini M, De Andrea M, Borgogna C, Dell'Oste V, et al. Identification of defective Fas function and variation of the perforin gene in an epidermodysplasia verruciformis patient lacking EVER1 and EVER2 mutations. J Invest Dermatol. 2008 Mar;128(3):732-5.
4) Landini MM, Zavattaro E, Borgogna C, Azzimonti B, De Andrea M, Colombo E, et al. Lack of EVER2 protein in two epidermodysplasia verruciformis patients with skin cancer presenting previously unreported homozygous genetic deletions in the EVER2 gene. J Invest Dermatol. 2012 Apr;132(4):1305-8
5) Borgogna C, Zavattaro E, De Andrea M, Griffin HM, Dell'Oste V, Azzimonti B, et al. Characterization of beta papillomavirus E4 expression in tumours from Epidermodysplasia Verruciformis patients and in experimental models. Virology 2012;423:195–204
6) Borgogna C, Landini MM, Lanfredini S, Doorbar J, Bouwes Bavinck JN, Quint KD, et al. Characterization of skin lesions induced by skin-tropic α- and β-papillomaviruses in a patient with epidermodysplasia verruciformis. Br J Dermatol 2014;171:1550-4

MATERIAL AND METHODS

Transgenic Mouse Model

HPV8tg and wild type litter mates were housed and managed under conditions approved by the Italian Animal Care Committee. Age and sex matched mice ear thickness and tail width were measured using Vernier caliper.

Whole mount skin preparation

Tail and back skin was cut into 0.5 cm^2 pieces and dissociated using 2.5 U/ml Dispase (Roche, UK) over night at 4°C. The epidermis was gently removed and fixed in 10% neutral buffered formalin for 2 hours at room temperature, tissue was labelled and mounted as previously described (Braun K *et al.,* 2003).

Immunofluorescence labelling

Immunofluorescence on whole mount, frozen and paraffin embedded section was performed using standard techniques as previously described (Borgogna *et al*. 2012). For the list of antibodies used see the following table:

Antibody	Cat.No	Company	Technique
K15	MA1-90929	ThermoFisher Scientific	WM
Ki67	ab16667	Abcam	WM
LGR6	ab12747	Abcam	WM
LGR5	NLS1236	Novus Biologicals	WM
CD34 (RAM34)	553731	BD Pharmingen	WM
CD34	560230	BD Pharmingen	FACS
Lrig1 (C2C3)	GTX119485	GeneTex	IF
Lrig1	AF3688	R&D Systems	WM
Lrig1	FAB3688G	R&D Systems	FACS
p63 (BC4A4)	ab735	Abcam	IF
K14	ab130102	Abcam	IF
β-HPV E4		*	IF
p63 (ΔN)	619002	Biolegend	WB
p63 (TA)	618902	Biolegend	WB
GAPDH	MAB374	Millipore	WB

*E4 β-HPV antibody was kindly provided by John Doorbar, University of Cambridge-UK.

Single cell suspension for flow cytometry and colony forming efficiency

Tail and back skin was cut into 0.5 cm^2 pieces and dissociated using 2.5 U/ml Dispase (Roche, UK) over night at 4°C. The epidermis was gently removed and further dissociated with TrypLE™ Express Enzyme (ThermoFisher, UK), and the supernatant passed through a 70 μm cell strainer (BD bioscience, UK). Enzymes were inactivated with DMEM with 10% FBS and keratinocytes cell suspension were re-suspended as required.

Flow cytometry, cell sorting and colony forming efficiency assay

Samples were analysed and flow sorted using BD LSRFORTESSA and BD FACSAria™ Fusion (BD Biosciences, USA). The data were analyzed using Flowjo software (Tree Star Inc). Keratinocytes were flow sorted for CD34-/Lrig1+ population and 3000 cells per well were seeded in 6-well plate and cultured for 15 days. Rheinwald and Green Media was changed every 3 days. The colonies were stained with crystal violet 0.05%, scanned with GelCount™ (Oxford Optronix), and analyzed using ImageJ software (NIH, USA).

RT-PCR

Mouse skin was homogenized in Trizol (ThermoFisher Scientific, UK). RNA isolation from sorted cells and homogenized tissues was performed with RNeasy kit and cDNA was synthetized using QuantiTect Reverse Transcription Kit (Qiagen, UK). Semi-quantitative reverse transcription-PCR (RT-PCR) reactions were carried out using GoTaq® G2 Green Master Mix (Promega, UK) and specific primers sequence are listed below. Real-time quantitative reverse transcription analysis (qRT-PCR) was performed on QuantStudio™ 7 Flex Real-Time PCR System (ThermoFisher Scientific UK). For the determination of E6 and E7 gene expression levels, SyGreen (PCRBIOSYSTEM, UK) was used. Cycling condition were previously described in Schaper et al., 2005, De Andrea et al., 2010. Total mouse-specific β-Actin was used as the housekeeping gene.

EVER1, EVER2, TAp63 and ΔNp63 transcription levels were analyzed with Taqman probes at standard conditions. Total mouse-specific GAPDH was used as the housekeeping gene. Primers details are described in the following table:

RT-PCR primers:

mΔNp63 fw	5’ ATGTTGTACCTGGAAAACAATG 3’
mΔNp63 rev	5’ GATGGAGAGAGGGCATCAAA 3’
mTAp63 fw	5’ AGACAAGCGAGTTCCTCAGC 3’
mTAp63 rev	5’ TGCGGATACAATCCATGCTA 3’
HPV8-E6 fw	5’ GCGGCTTTAGGTATTCCATTGC 3’
HPV8-E6 rev	5’ GCTACACAACAACAACGACAACACG 3’
HPV8-E7 fw	5’ CCTGAAGTGTTACCAGTTGACCTGC 3’

HPV8-E7 rev	5’ CAGTTGCGTTGACAAAAAGACG 3’
mβ-actin fw	5’ CCAGAGCAAGAGAGGTATCCTGAC 3’
mβ-actin rev	5’ CATTGTAGAAGGTGTGGTGCCAG 3’
mGAPDH fw	5’ TGTCAGCAATGCATCCTGCA 3’
mGAPDH rev	5’ TGTATGCAGGGATGATGTTC 3’
HPV18-E6 fw*	5’ GTGCCAGAAACCGTTGAATC 3’
HPV18-E6 rev*	5’ TTGTGTTTCTCTGCGTCGTT 3’
HPV18-E7 fw*	5’ TGAAATTCCGGTTGACCTTC 3’
HPV18-E7 rev*	5’ CACGGACACACAAAGGACAG 3’

*Lo Cigno I, De Andrea M, Borgogna C, Albertini S, Landini MM, Peretti A, Johnson KE, Chandran B, Landolfo S, Gariglio M. The Nuclear DNA Sensor IFI16 Acts as a Restriction Factor for Human Papillomavirus Replication through Epigenetic Modifications of the Viral Promoters. J Virol. 2015 Aug;89(15):7506-20.

Taqman primers:

ΔNp63	Mm01169470_m1
TAp63	Mm01150797_m1
Tmc6- EVER1	Mm00520751_m1
Tmc8- EVER2	Mm01241000_m1
β-actin	Mm02619580_g1
GAPDH	Mm99999915_g1

Western blotting

100 mg of shaved back skin was homogenized in 1 ml of RIPA buffer containing 1% Triton X-100, 1% Sodium Deoxycholate, 0.1% SDS, 1 mM EDTA, 160 mM NaCl, 20 mM Tris-HCl (pH 7.4) and 25 μl/ml Protease Inhibitor Cocktail (Sigma, UK). Protein concentrations were analyzed using Pierce BCA Protein Assay (ThermoFisher, UK). Thirty μg of protein lysate was loaded on 8% SDS-PAGE, and transferred to polyvinylidene difluoride membranes (Millipore, UK). For the list of antibodies used see “Immunofluorescence labelling”.

Human tissue samples

EV patients’ keratosis formalin-fixed and paraffin embedded (FFPE) tissue sections were analyzed according to the protocol approved by the ‘‘Maggiore Hospital’’ Research Ethics Committee, Italy. Non-EV actinic keratosis (14-NW-1272) and squamous cell carcinoma (09-WSE-02-1) tissues were obtained after UK NHS R&D and Local Research Ethics Committee approval.

Statistical analysis

Paired t-tests were used to compare HPV8 and wild type litter mates, using GraphPad software (Prism).

4.2 Understanding the natural history of β-HPV infection in skin lesions and their malignant progression using tumourgraft models

A major limitation in skin cancer research is the small size of these tumours that are usually formalin-fixed and paraffin embedded for routine pathology, thus decreasing the chance to get fresh material for further analysis. In this context, the orthotopic xenograft model may be an essential technique to increase the availability of tumour material and investigate the molecular mechanisms underlying skin tumorigenesis. Following the xenograft procedure described by Patel et al. (Figure 22, see material and methods "*In vivo* tumorigenicity assays of tumours" for details), a total of 37 skin tumours were xenografted into athymic nude mice.

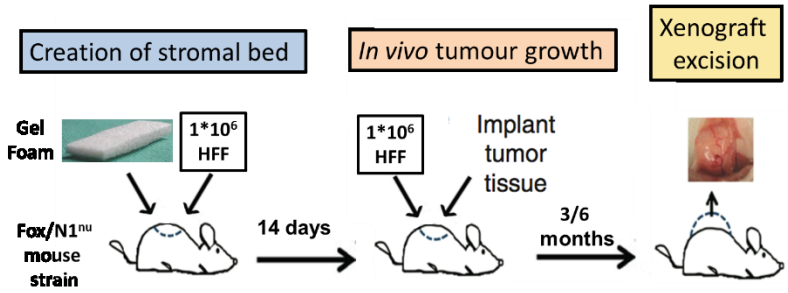

Figure 22. Procedure for establishing *in vivo* orthotopic xenograft with creation of humanized stromal bed (modified from Patel et al., 2012).

They were derived from 24 organ transplant recipients (OTRs) enrolled since 2013 at the University-Hospital in Novara. Most of the patients were older than 60 years (22 out of 24) when the skin tumour was diagnosed and the majority were males (20 out of 24). Most of the patients developed lesions within 10 years from transplantation, and 5 patients had a very long history of immunosuppression; the tumours were removed 30 years or later since transplant (Table 2A). The rate of lesions affecting sun-exposed skin areas (head, hands, forearms and shoulders) was 29 out of 37 (78.4%), confirming sun exposure as a major contributor to epithelial transformation. Histologically, the cutaneous lesions included high-grade tumours such as basal cell carcinoma (BCC, n = 15) and squamous cell carcinoma (SCC, n = 4); precancerous lesions like actinic keratosis (AK, n=13) and keratoacanthoma (KA, n=1) and benign lesions such as seborrheic keratosis (SK, n=3) and lichenoid keratosis (n=1) (Table 2B).

A

SEX	Male	20	31
	Female	4	6
AGE at surgery	>60	22	31
	≤ 60	2	6
Years from transplantation at surgery	≤ 10	13	19
	10-20	6	10
	20-30	0	0
	>30	5	8

B

SCC	4	4	0	4	
BCC	15	7	8	13	2 (BCC)
KA	1	0	1	1	
AK	13	8	5	11	1 (AK) 1 (SCC+ metastasis)
SK	3	2	1	3	
Lichenoid Keratosis	1	0	1	1	

Table 2. (A) Donors' clinical features. (B) Histopathologic features of original tumours and tumourgrafts.

Out of the 37 lesions engrafted, 32 tumourgrafts were collected because a mouse died after surgery and in 4 cases no tumour growth was detected. After tumourgraft removal, the lesions were formalin fixed and paraffin embedded (FFPE). If possible, a small piece of the tumourgraft was stored in RNA LATER for other analysis. At the beginning, the tumours were removed after 6 months from the graft (16 out of 37). Macroscopically, growing tumour masses were detected onto the back of the mice, but histologically, they were not resembling the original tumour. In most of the cases the lesions observed were epidermal cysts (Figure 23). They were characterized by a massive amount of keratin surrounded by dying epithelium. Based on this negative experience, we decided to harvest the tumourgraft earlier, approximately three months after the graft.

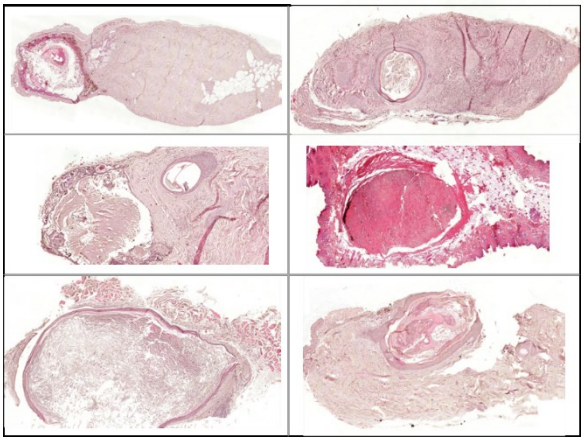

Figure 23. Representative Haematoxylin and Eosin (H&E) staining of epidermal cysts.

Successful growth of the tumour mass was obtained in four cases. In two cases, the original tumours were diagnosed as BCC. The first BCC was derived from a male patient born in 1949. He underwent two kidney transplantations: the first occurred in 1982, the second in 1997 and the BCC appeared 31 years after the first transplantation. The second BCC was removed from a male patient born in 1946. He underwent kidney transplant in 2009 and the lesion appeared 5 years later. As shown in the representative H&E images reported below (Figure 24), strong retention of the overall tumour histology including cell morphology, stromal component architecture, and grade of differentiation of the epithelia was observed between original patients' tumours and tumourgrafts. Both the original tumours were negative for the presence of the viral markers of β-HPV infection (e.g. E4 and L1 expression), as well as the tumourgrafts.

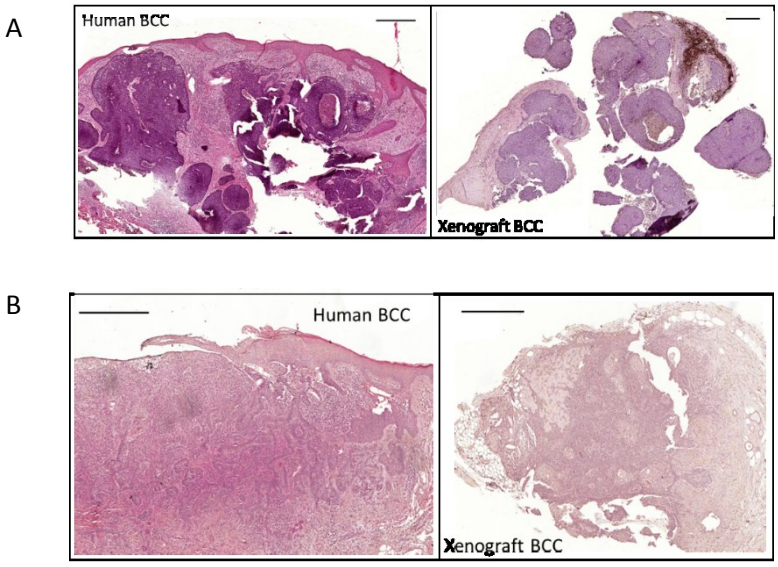

Figure 24. Histopathologic features (H&E staining) of two patients' tumours (left panels) and tumourgrafts (right panels). The BCC in panel A was removed from the shoulder of the male KTR born in 1949. The BCC in panel B was removed from the nose of the male KTR born in 1946. All scale bars are 500 µm.

The other 2 tumourgraft cases that showed a growing tumour mass were named case A and case B (Table 2B) and in both cases, they were derived from β-HPV-positive skin lesions. The case A tumourgraft was obtained from a lesion removed from a female patient with a long history of immunosuppression, as she was transplanted in 1980. Due to her long lasting status of immunosuppression, the patient developed an EV-like phenotype with many wart-like lesions. Consistent with her clinical picture, she developed more than 15 skin cancers and they

were diagnosed as SCC (n=7), BCC (n=4), KA (n=4) and AK-SCC (n=1) (figure 25A). To detect the presence of β–HPV infection, tissue specimens from the available FFPE blocks were costained using immunofluorescence analysis with anti-E4 and anti-L1 antibodies to detect viral antigen expression, and with MCM7 (mini chromosomal maintenance protein 7), a marker of cellular proliferation. β–HPV viral protein expression was found in 4 blocks corresponding to 3 KA from the left and right leg, and an AK-SCC from the right hand. Plucked eyebrows were collected from this patient and β-HPV genotyping revealed the presence of HPV 5, 8, 23, 24, 75, 93 and 96. From this patient, 3 different tumours were grafted into nude mice. Two of them were diagnosed as BCC and SCC in the original specimens, but unfortunately they failed to grow as tumourgrafts. The third tumour grafted into the nude mouse was an AK with some area displaying the histological features of well differentiated SCC (named case A) that was removed from the right hand (Figure 25B). This tumour turned out to be positive for the β-HPV late capsidic protein (L1) in the upper layers of the epithelium where some differentiation was still occurring, indicating the presence of productive viral life cycle in this infected epithelium (Figure 25C).

A

	Case A	
Sex	**Female**	
Date of birth	**8.12.1950**	
Transplant date	**1980**	
Years from transplantation at xenograft	**35**	
Skin tumour develop since transplant	**4 BCC 7 SCC**	**4 KA 1 AK-SCC**

B

C

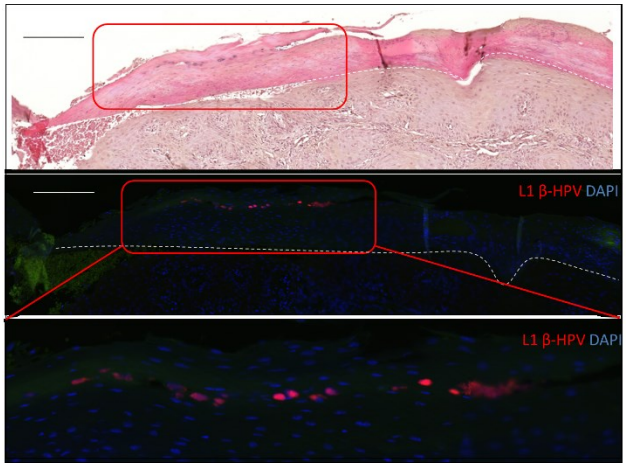

Figure 25. (A) The table summarizes the clinical features of the case A patient. (B) A clinical picture of the original tumour removed from the hand. The black arrow indicates the tumour area. (C) **(**Top panel) H&E staining of a tissue section from the paraffin-embedded AK-SCC (case A) (hand). (Middle panel) A serial section of the AK-SCC stained with antibodies to β-HPV L1 (red). The region shown in the lower panel corresponds to the red square highlighted in the upper pictures. The white dotted line indicates the basal layer. Immunofluorescence sections were counterstained with DAPI (blue) to visualize cell nuclei. All scale bars are 200 μm.

Three months after the engraftment onto the nude mouse, the tumourgraft mass was removed. Histologically, it was diagnosed as AK with some area resembling the original tumour (Figure 26A). To visualize β-HPV infection in the tumourgraft, we performed immunofluorescence analysis to detect β-HPV E4 protein expression and FISH analysis using a HPV5 DNA probe to detect the viral genome. We were able to detect some E4-positive cells as well as HPV DNA FISH-positive signal in some nuclei of the disorganized hyperplastic epithelium. Unfortunately, the overall architecture of the epithelium was not well preserved and the quality of the FFPE tissues was poor very likely due to the fixation procedure (Figure 26 B and C).

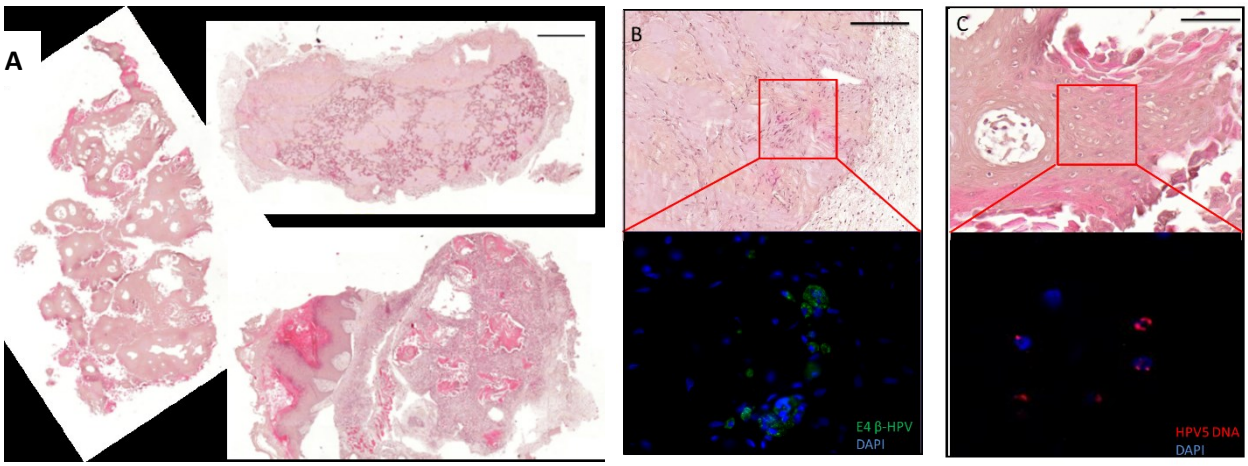

Figure 26. (A) H&E staining of the tumourgraft obtained from the AK-SCC (case A) (Figure 25C). The scale bar is 1000 µm. (B) H&E staining of the area positive for β-HPV E4 (panel B; upper part). Immunofluorescence analysis shows β-HPV E4 cytoplasmic staining in some cells (green) (panel B; bottom part). (C) Magnification of the histological area positive for the presence of viral genome (panel C; upper part). FISH (Fluorescence In Situ Hybridisation) analysis, using HPV5 DNA probe to detect the presence of viral genome, shows some positive nuclei (red) (panel C; bottom part). All sections were counterstained with DAPI (blue) to visualise cell nuclei. The scale bars for panel B and C are 200 µm.

Case B is a skin tumour that was removed from a male patient born in 1960. He underwent kidney transplantation twice. The first kidney transplant occurred in 1996 and was rejected after 11 years. The second transplant was carried out in 2011. From 2012 onwards, the patient developed several proliferative skin cancers in different areas, particularly shoulders and forearm, and they were diagnosed as BCC (n=1), AK (n=1), AK-BCC (n=1) and SK (n=1) (Figure 27A). All these tumours were examined for the presence of the viral markers and

positivity for β-HPV E4 was found in 2 blocks corresponding to an AK and a SK that were removed from the back and the left forearm respectively. These two β-HPV positive tumours were xenografted in nude mice. The AK displayed highly keratotic epithelium with clear signs of β-HPV-related cytopathic effects (Figure 27 B&C). Immunofluorescence analysis showed large areas of β-HPV E4 expression in the more superficial layers of the epithelium. As expected for β–HPV-infected tissues, the cellular proliferation marker MCM7, whose expression is normally restricted to the basal layer, was strongly increased in the E4-positive area compared with the adjacent epithelium, and was apparent in the basal and suprabasal layers, indicating that cells were stimulated to enter the cell cycle (Figure 27D).

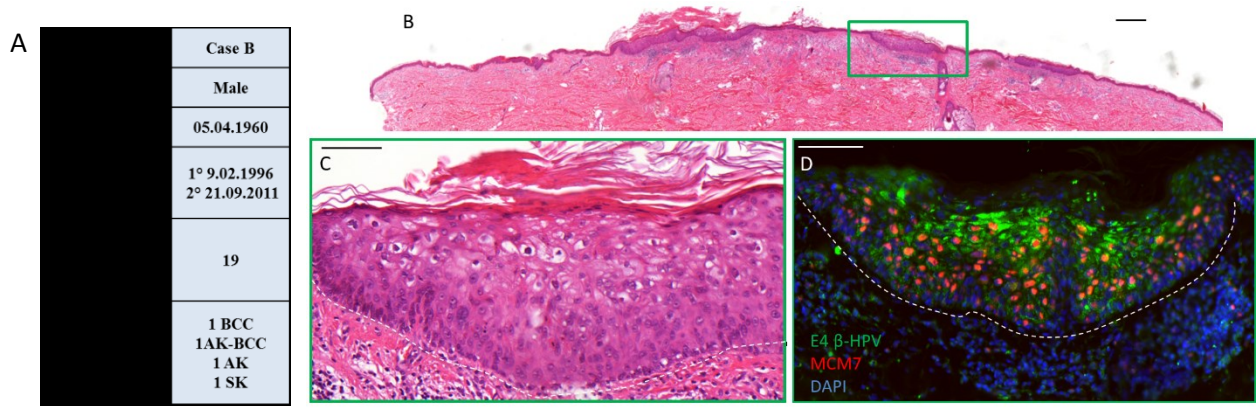

Figure 27. (A) The table summarizes the clinical features of the case B patient. (B) H&E staining shows the histology of the AK (case B as tumourgraft). The green box indicates the area of interest. The scale bar is 500 µm. (C) Magnification of the area in the green box that clearly shows the β-HPV related cytopathic effect. (D) The section was double stained with antibodies to E4 of β-HPV (green) and to the proliferation marker MCM7 (red). The section was counterstained with DAPI (blue) to visualise cell nuclei. The white dotted line indicates the basal layer. The scale bars for panel C and D are 100 µm.

The tumourgraft derived from the AK (case B) was removed after three months from the engraftment into the nude mouse. It showed a high grade of vascolarization. While removing the tumour mass from the back of the mouse, we noticed another tumour mass localized between the neck and the left leg. Both tumour masses were collected and processed by FFPE. H&E staining and immunofluorescence analysis were performed on these tissue sections. Histologically, (Figure 28 A&B) the tumourgraft case B was diagnosed as well differentiated SCC. The tumour from the neck region was diagnosed as lymph node metastasis and morphologically displayed the same cell types as the main tumour, suggesting that the

metastasis was generated from the primary tumour cells that migrated towards the lymph node vessels and recreated a tumour mass in lymph node. In order to investigate whether viral infection was still present in both SCC and metastasis of case B, immunofluorescence analysis to detect β-HPV E4 protein expression was performed. As expected for high-grade tumours, β-HPV E4 expression was absent in the SCC and metastasis of case B, while the proliferation rate was very high and widespread, as shown by the massive expression of the proliferation marker MCM7 (Figure 28). Of note, this case B tumourgraft allowed us to demonstrate in vivo the progression from a pre-malignant lesion, specifically an AK with transcriptionally active β-HPV infection, into a squamous cell carcinoma. Half of the SCC and lymph node metastasis were collected and stored in RNA LATER for further characterization of the transcriptome and proteome profile.

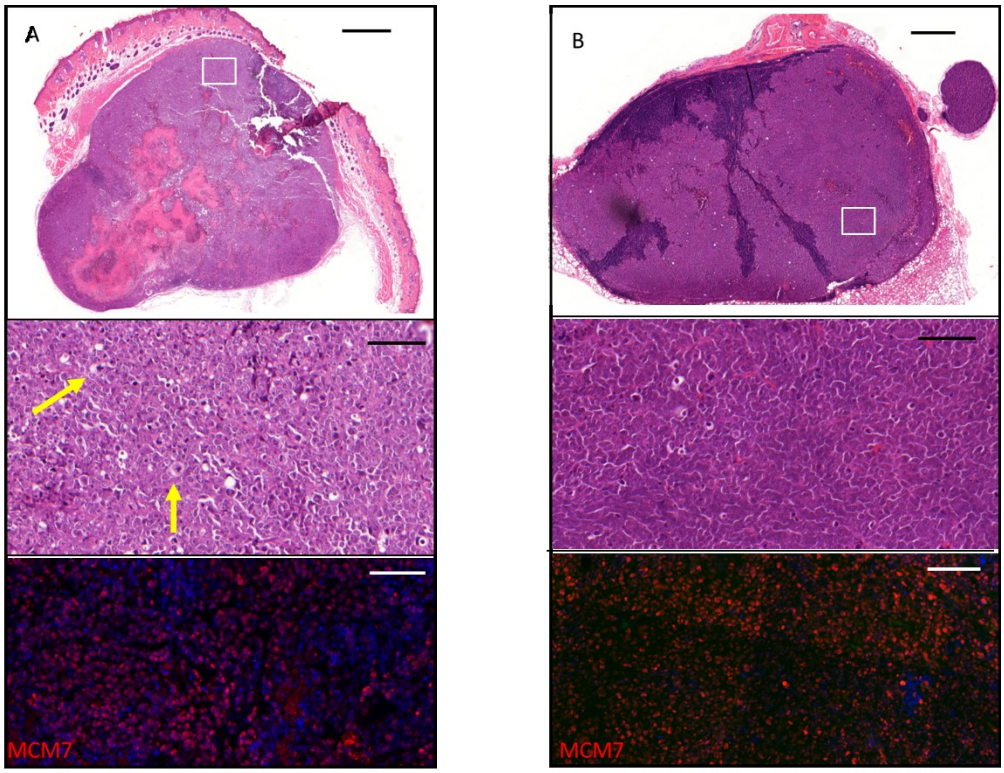

Figure 28. (A, first panel) Histopathologic features (H&E staining) of the main tumour of the tumourgraft case B diagnosed as SCC. Scale bar 1000 µm. (A, second panel) Magnification of the area enclosed by the white square shows cells in mitotic phase (yellow arrows). (A, third panel) The area shows the nuclei stained with the proliferation marker MCM7 (red). (B, first panel) H&E staining of tissue sections from the lymph node metastasis removed from the neck of the mouse. Scale bar is 500 µm. (B, second panel) Magnification of the area of interest highlighted with a white square. (B, third panel) Proliferation marker MCM7 (red) staining. The immunofluorescence sections were counterstained with DAPI (blue) to visualize cell nuclei. Scale bars of the magnifications are 100 µm.

A SK was also excised from case B patient and engrafted into the nude mouse. This lesion was positive for the presence of the viral protein E4 of β-HPV and displayed a widespread expression of the proliferation marker MCM7 (Figure 29). Unfortunately, it didn't grow in the nude mouse.

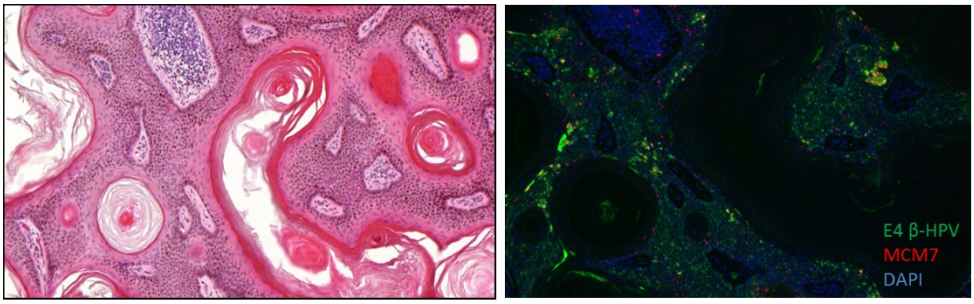

Figure 29. (Left panel) H&E staining of the Seborrheic keratosis (SK) removed from the case B patient (Right panel) Cytoplasmic staining for β-HPV E4 (green) was strongly detected together with diffuse nuclear MCM7 (red). The section was counterstained with DAPI (blue) to visualize cell nuclei.

Although the rate of successful engrafment for skin tumours is not very high, the two β-HPV-infected tumourgraft described in this study represent a promising system by which to investigate molecular alterations underlying β-HPV-induced skin carcinogenesis. Of note, the β-HPV-positive AK that progressed to SCC in the nude mouse provides a powerful system for understanding the role of β-HPV in the development of skin cancer.

MATERIAL AND METHODS

Collection of skin tumour

All fresh samples as well as the formalin-fixed and paraffin-embedded (FFPE) blocks used in this study were retrieved from the University-Hospital in Novara.

Mouse strain

The immunodeficient mice used for tumourgraft development were male athymic Nude-Foxn1^{nu} (Envigo). The two main defects of mice homozygous for the nude spontaneous mutation (*Foxn1^{nu}*, formerly *Hfh11^{nu}*) are abnormal hair growth and defective development of the thymic epithelium. They lack T cells and suffer from a lack of cell-mediated immunity. Homozygous nude mice show partial defect in B cell development probably due to the absence of functional T cells. Athymic nude mice were used instead of SCID mice, because they are reported to give the highest success rate in this animal model (Patel et al., 2012). Mice were housed in accordance with The Guide for the Care and Use of Laboratory Animals.

In vivo tumorigenicity assays of tumours

Athymic nude Foxn1^{nu} mice were anesthetized and a stromal reaction was induced 2 weeks earlier by implanting a piece of 0,5 cm3 of sterilized gelfoam (Johnson & Johnson, New Brunswick, NJ) into the dorsal subcutaneous space together with 10^6 primary human fibroblasts suspended in 100 µl of Matrigel (BD Biosciences). Wounds were closed with surgical suture (Ethicon). After 14 days, the mice were anesthetized and selected tumours were xenografted into the stromal bed in the form of intact tumour tissue (~0.5 cm^3) together with 10^6 primary human fibroblasts suspended in 100 µl of Matrigel (Patel et al., 2012). After 3 or 6 months, the mice were killed via CO_2 inhalation, the tumours were removed and formalin fixed-paraffin embedded blocks were prepared by the Pathology Unit at the University-Hospital in Novara. When it was possible, half of the tumour was stored in RNA LATER for further analysis.

Haematoxylin and Eosin staining

Consecutive 5-µm thick tissue sections were cut from FFPE blocks onto pre-coated microscope slides, incubated at 60°C for 30 min to increase adhesion on slide surface, dewaxed and rehydrated as follows: twice in xylene for 15 min each, twice in 100% ethanol for 10 min each, followed by a series of graded ethanol (95%, 90%, 70%) for 5 min each and finally 1X PBS for 5 min. The slides were incubated in haematoxylin for 10 min, washed in tap water for 5-10

min, than soaked in eosin for 5 min, and washed again quickly in tap water. Tissue sections were than dehydrated in a series of graded ethanol (75% for 20 sec, 95% for 2 sec , 100% for 2 min), diaphanized twice in xylene for 2 min each and finally mounted with a mounting medium for immunohistochemistry (VectaMount Permanent Mounting Medium, Vector Laboratories).

Immunofluorescent analysis

Consecutive 5-µm thick tissue sections were cut from FFPE blocks onto pre-coated microscope slides, incubated at 60°C for 30 min to increase adhesion on slide surface, dewaxed and rehydrated as follows: twice in xylene for 15 min each, twice in 100% ethanol for 10 min each, followed by a series of graded ethanol (95%, 90%, 70%) for 5 min each and finally 1X PBS for 5 min. To quench endogenous peroxidase, tissue sections were incubated with 3% hydrogen peroxide diluted in 1X PBS for 15 min at room temperature with shaking and then rinsed in 1X PBS for 5 min. For antigen unmasking, slides were placed in a glass slide holder and pre-soaked for 5 min in 1X Antigen Unmasking Solution (Vector Laboratories) diluted in bidistilled water, then heated for three times in microwave oven at 750W for 4:30 min each with 1 min intervals inside a pressure cooker and finally cooled for 20 min and washed for 5 min in 1X PBS. All the subsequent incubation steps performed in the staining procedures described below were carried out putting the slides inside a dark humidified box.

For immunofluorescent detection of β-HPV E4 coupled to MCM7, tissue sections after antigen retrieval were blocked with 10% NGS / 1X PBS for 1 h at room temperature. After blocking, primary mouse monoclonal anti-MCM7 antibody (NeoMarkers) was 1:200 diluted in 5% NGS / 1X PBS and incubated onto tissue sections overnight at 4°C. The following day, slides were washed in 1X PBS / 0.05% Tween-20 for 5 min at room temperature with shaking and tissue sections were incubated with the Avidin/Biotin Blocking Kit (Vector Laboratories; 3.6 µl Avidin Solution + 3.6 µl Biotin Solution in 400 µl 50 mM Tris-HCl pH 7.5) for 30 min at room temperature for signal amplification. After a 5 min wash in 1X PBS, tissue sections were incubated with secondary biotinylated universal antibody (Vector Laboratories) for 30 min at room temperature. After a 5 min wash in 1X PBS, streptavidin-HRP (TSA™ Tetramethylrhodamine System, PerkinElmer) 1:100 diluted in 1X PBS was added onto tissue sections for 1 h at room temperature. After another 5 min wash in 1X PBS, TSA fluorescent substrate (TSA™ Tetramethylrhodamine System, PerkinElmer) prepared according to the supplier's specifications was added for 10 min at room temperature, followed by a further 5 min wash in 1X PBS. Tissue sections were subsequently incubated overnight at 4°C with

primary rabbit polyclonal anti E4 antibody (Kindly provided by John Doorbar, University of Cambridge) 1:1000 diluted in 5% NGS / 1X PBS. On the third day, after a 5 min wash in 1X PBS/ 0.05% Tween-20 at room temperature with shaking, FITC-labelled secondary anti-rabbit antibody (Invitrogen) 1:600 diluted in 1X PBS was added onto tissue sections and slides were incubated for 1 h at room temperature. After a 5 min wash in 1X PBS, tissue sections were counterstained with DAPI 1:600 diluted for 10 min at room temperature, then washed again in 1X PBS for 5 min and finally mounted with a mounting medium for fluorescence (VectaShield Antifade Mounting Medium, VECTOR laboratories).
For immunofluorescent detection of β-HPV L1, tissue sections after antigen retrieval were blocked with 10% NGS / 1X PBS for 1 h at room temperature. After blocking, tissue sections were incubated overnight at 4°C with primary rabbit polyclonal anti L1 antibody (Kindly provided by John Doorbar, University of Cambridge) 1:1000 diluted in 5% NGS / 1X PBS. The following day, after a 5 min wash in 1X PBS / 0.05% Tween-20 at room temperature with shaking, TexasRed-labelled secondary anti-rabbit antibody (Invitrogen) 1:600 diluted in 1X PBS was added onto tissue sections and slides were incubated for 1 h at room temperature. After a 5 min wash in 1X PBS, tissue sections were counterstained with DAPI for 10 min at room temperature, then washed again in 1X PBS for 5 min and finally mounted with a mounting medium for fluorescence.

For immunofluorescent detection of DNA-FISH, DNA probe consisting of complete cloned β-HPV HPV5 genome was biotin-labelled using the Biotin-Nick Translation Mix (Roche) according to the manufacturer's instructions. Biotinylated probe was then 1:25 diluted in hybridization buffer (50% formamide, 5X SSC, 0.1% Tween-20, 0.2 ng/µl yeast tRNA) and the probe mix was added to tissue sections previously allowed to air dry after antigen unmasking. After lowering a cover-slip onto tissue sections, slides were heated on a hot block for 5 min at 95°C for DNA denaturation and then cooled on ice and finally incubated overnight at 37°C for probe annealing. The following day, stringent washes with pre-warmed SSC solutions at decreasing concentrations were performed for 10 min each as follows: 2X SSC (allowing also loosening of cover-slips), formamide wash buffer (50% formamide, 2X SSC, 0.05% Tween-20), 1X SSC, 0.5X SSC. Next, a solution containing 1:100 diluted streptavidin-HRP (TSA™ Tetramethylrhodamine System, PerkinElmer) was added onto tissue sections and slides were incubated for 1 h at room temperature. After a 5 min wash in 1X PBS, TSA fluorescent substrate (TSA™ Tetramethylrhodamine System, PerkinElmer) prepared according to the supplier's specifications was added for 10 min at room temperature, followed

by a 5 min wash in 1X PBS and nuclear counterstaining with DAPI diluited 1:600 for 5 min at room temperature. After a final 5 min wash in 1X PBS, slides were mounted with a mounting medium for fluorescence.

Images were acquired using a digital scanner (Pannoramic MIDI, 3D Histech Kft) allowing overlay of immunofluorescent and H&E staining patterns.

β-HPV DNA genotyping

9-10 eyebrows containing hair follicles were plucked from case A patient. DNA was isolated using a QIAamp DNA Mini Kit according to the manufacturer's instructions and eluted in 70 µl AE buffer (Qiagen, Milan, Italy). β-HPV DNA analysis was carried out using broad spectrum PCR (PM-PCR) in combination with a reverse hybridization system (RHA) [Skin β-HPV prototype research assay; Diassay BV, Rijswijk, The Netherlands] as previously described (de Koning et al., 2006). The method was designed to identify the 25 established β-HPV types (i.e., HPV 5, 8, 9, 12, 14, 15, 17, 19, 20, 21, 22, 23, 24, 25, 36, 37, 38, 47, 49, 75, 76, 80, 92, 93, 96). PM-PCR amplification, generating a biotinylated amplimer of 117 bp from the E1 region, was carried out following all the precautions indicated by the manufacturer to avoid recurrence of cross-contamination. Briefly, PM-PCR reaction was performed in a final reaction volume of 50 µL, containing 10 µL of the isolated DNA, 2.5 mM MgCl2, 1x GeneAmp PCR buffer II, 0.2 mM deoxynucleoside triphosphates, 1.5 U Amplitaq Gold DNA polymerase and 10 µl of the PM primer mix. The PCR reaction was performed as follows: 9 min pre-heating step at 94 °C; 35 amplification cycles; 30 s at 94 °C; 45 s at 52 °C; 45 s at 72 °C; 5 min final elongation step at 72 °C. As a positive PCR control, a β-HPV plasmid clone was included. Identification of the amplified β-HPV types was performed by reverse hybridization analysis of the amplimers on genotyping strips provided by the manufacturer. In each strip a probe line contains a mix of "universal" β-HPV probes.

4.3 Establishment of an immunodeficient HPV8tg mouse model that recapitulates the events occurring in OTR.

Findings to date suggest that the immunosuppressive therapies administered to organ transplant recipients promote β-HPV replication, which, in turn, is associated with skin keratosis or field cancerization. However, it remains to be determined whether immunosuppression also facilitates carcinogenesis by inhibiting tumour immune surveillance and killing. To test this hypothesis, a mouse model that recapitulates the events occurring in OTR (Organ Transplant Recipient) has been generated. HPV8 transgenic mice (HPV8tg) have been crossed with Rag2 deficient mice ($Rag2^{-/-}$) (which lack B and T cells). The Rag2 mutant mice (C57BL/6 genetic background) were kindly provided by the group of Cecilia Garlanda from Humanitas Research Center, Milan (Italy). Rag2 deficient mice have been selected because their immunophenotype mirrors the effects of the systemic immunosuppressants used in transplant recipients, such as cyclosporine, and their lifespan is long enough to allow the observation of spontaneous SCC growth. The $Rag2^{-/-}$ mice harbour a pan deletion of exon 3 of the targeted locus resulting in a complete deletion of the entire Rag2 protein coding region (Figure 30A). They exhibit hematopoietic and immune system defects including arrested B and T cells development at the pro-B and pro-T cell stage, respectively. Neonatal $Rag2^{-/-}$ mice were healthy, had no gross abnormalities, and they have been maintained in barrier facility (Shinkai et al., 1992; Hao et al., 2001).

The HPV8tg mouse strain (FVB/N genetic background) was kindly provided by the group of Herbert Pfister, University of Cologne (Germany). They express the complete early region of β-HPV8 (E1, E2, E4, E6, E7) under the control of the K14 promoter (Figure 30B). The early region in the HPV8tg mice has been maintained in heterozygosity. While tumours were never observed in transgene-negative mice, papillomas occurred mostly multifocally and disseminated in 91% of HPV8-positive mice. About 25% of the papillomas showed signs of moderate or severe dysplasia such as disturbed stratification, suprabasal and atypical mitotic figures, nucleus hyperchromatosis, and anisonucleosis.

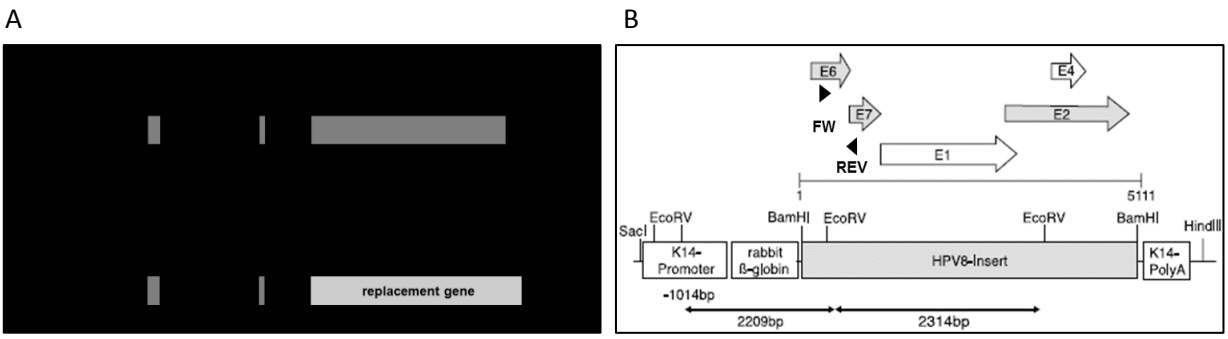

Figure 30. (A) Schematic representation of $Rag2^{+/+}$ and $Rag2^{-/-}$ genes. Black triangles indicate the annealing sites of the primers (FW: forward; wtREV: wild type reverse; mutREV: mutant reverse). In the $Rag2^{-/-}$ gene, the exon 3 is deleted (modified from Hao et al., 2001). (B) Schematic representation of the HPV8tg transgene construct which consists of the promoter of the human cytokeratin-14 gene, intron 2 of the rabbit B-globin gene, all early genes of HPV8 (with schematic overview of the open reading frames), and the K14 polyadenylation signal. Black triangles indicate the annealing sites of the primers (FW: forward; REV: reverse) (modified from Shaper et al., 2005).

If immunosuppression promotes carcinogenesis by inhibiting tumour immune surveillance, we would have expected a great SCC frequency in a short period of time in HPV8tg+:$Rag2^{-/-}$ mice. Thus, the HPV8tg+:$Rag2^{-/-}$ mice may be very useful in this context as they could provide a reliable animal model that closely resembles the immune defects occurring in transplant recipients, thus providing mechanistic insights into this complex clinical problem. The $Rag2^{-/-}$ and HPV8tg+ mouse strains have been mated and the F1 - first filial generation – has been generated. The F1 generation gave rise to HPV8tg+:$Rag2^{+/-}$ and HPV8tg-:$Rag2^{+/-}$ mice with a mixed background (FVB/N-C57BL/6). Mice from the F1 generation (HPV8tg+:$Rag2^{+/-}$ and HPV8tg-:$Rag2^{+/-}$) have been crossed and the F2 generation, including six different genotypes with a mixed background, has been generated as detailed in Table 3. The mice heterozygous for the Rag2 gene ($Rag2^{+/-}$) displayed the same phenotype of the mice homozygous for Rag2 wild type ($Rag2^{+/+}$) (Shinkai et al., 1992). Indeed, the mice with the following genotypes HPV8tg-:$Rag2^{+/+}$ - HPV8tg-:$Rag2^{+/-}$ and HPV8tg+:$Rag2^{+/+}$ - HPV8tg+:$Rag2^{+/-}$ have been considered as controls.

F2 GENERATION GENOTYPES
HPV8tg+:Rag2$^{+/+}$
HPV8tg+:Rag2$^{+/-}$
HPV8tg+:Rag2$^{-/-}$
HPV8tg-:Rag2$^{+/+}$
HPV8tg-:Rag2$^{+/-}$
HPV8tg-:Rag2$^{-/-}$

Table 3. Mouse genotypes obtained in the F2 generation.

The F2 generation has been monitored for 12 weeks to analyse the phenotype of the different genotypes. Soon after birth, the skin of the HPV8tg+:Rag2$^{-/-}$ genotype appeared severely damaged in comparison to the HPV8tg mice (Figure 31 A) or the littermates of the HPV8tg+:Rag2$^{+/+}$ and HPV8tg+:Rag2$^{+/-}$ genotypes (Figure 31 B). In HPV8tg+:Rag2$^{-/-}$ mice, there was evidence of a significant hair loss all over their body (Figure 31 C). Moreover, they developed large lesions that quickly progressed to high-grade malignant tumours. Even though the number of mice from the F2 generation was still limited, we measured the number and area of the skin lesions in HPV8tg+:Rag2$^{-/-}$ versus HPV8tg+:Rag2$^{+/+}$ and HPV8tg+:Rag2$^{+/-}$ mice; the latters served as controls. During the 12 weeks of monitoring, well evident expansion of the lesional areas was observed in HPV8tg:Rag2$^{-/-}$ mice that reduced the number of the countable isolated lesions when compared to the control genotypes. The observed inverse correlation between the number and area of the lesions could be explained by the expansion of the lesional areas that covered all the mouse body. No difference in weight has been detected among the genotypes (Figure 31 D).

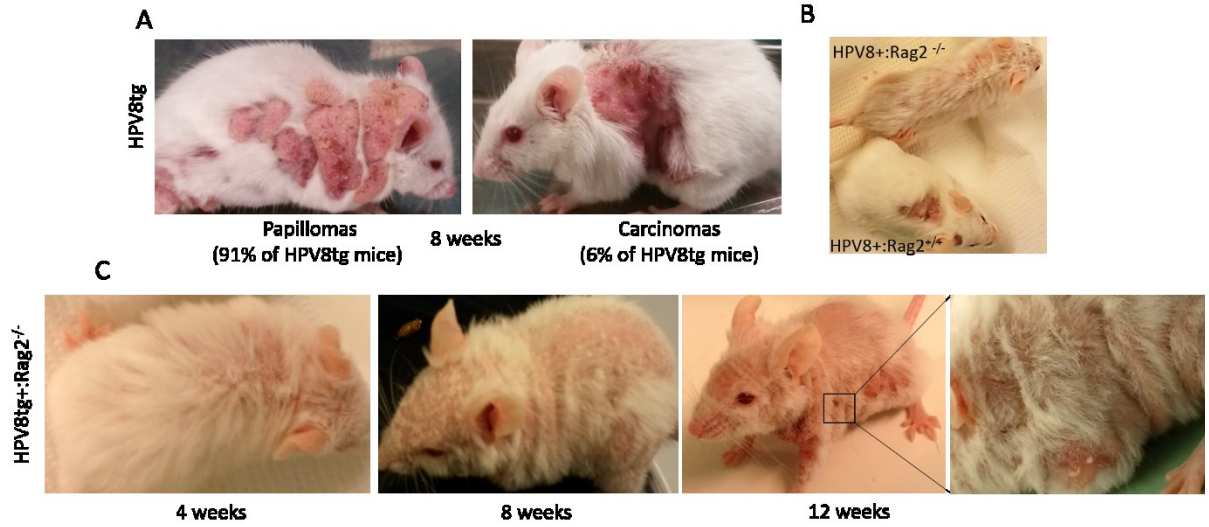

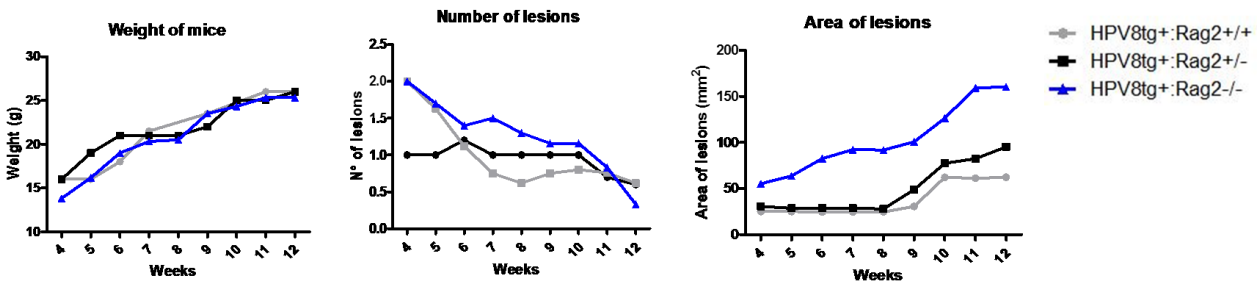

Figure 31. (A) HPV8tg mice shows circumscribed tumours during the 12 weeks of the observation period (left panels). The right picture shows an SCC. (B) Comparison between HPV8tg+:Rag2$^{+/+}$ and HPV8tg+:Rag2$^{-/-}$ phenotypes. (C) The pictures show the phenotype of HPV8tg+:Rag2$^{-/-}$ mouse during the monitoring period of 12 weeks. The left picture shows a magnification of the lesions area. (D) Weight, number and area of the lesions have been analysed and compared in HPV8+:Rag2$^{+/+}$, HPV8+:Rag2$^{+/-}$ and HPV8+:Rag2$^{-/-}$ mice.

Skin biopsies for each mouse genotypes have been collected, formalin fixed and paraffin embedded (FFPE). When we looked at the histology of the skin lesions derived from HPV8tg+:Rag2$^{+/+}$ in comparison to those from HPV8tg+:Rag2$^{-/-}$, some interesting observations were made. While the HPV8tg+:Rag2$^{+/+}$ lesions showed the classical histology of papilloma with acanthosis, hyperkeratosis, and the presence of horn pearls, those from HPV8tg+:Rag2$^{-/-}$ mice were characterized by a higher degree of hyperplasia, a lower grade of differentiation, and the presence of some atypical cells especially in the upper layers (Figure 32).

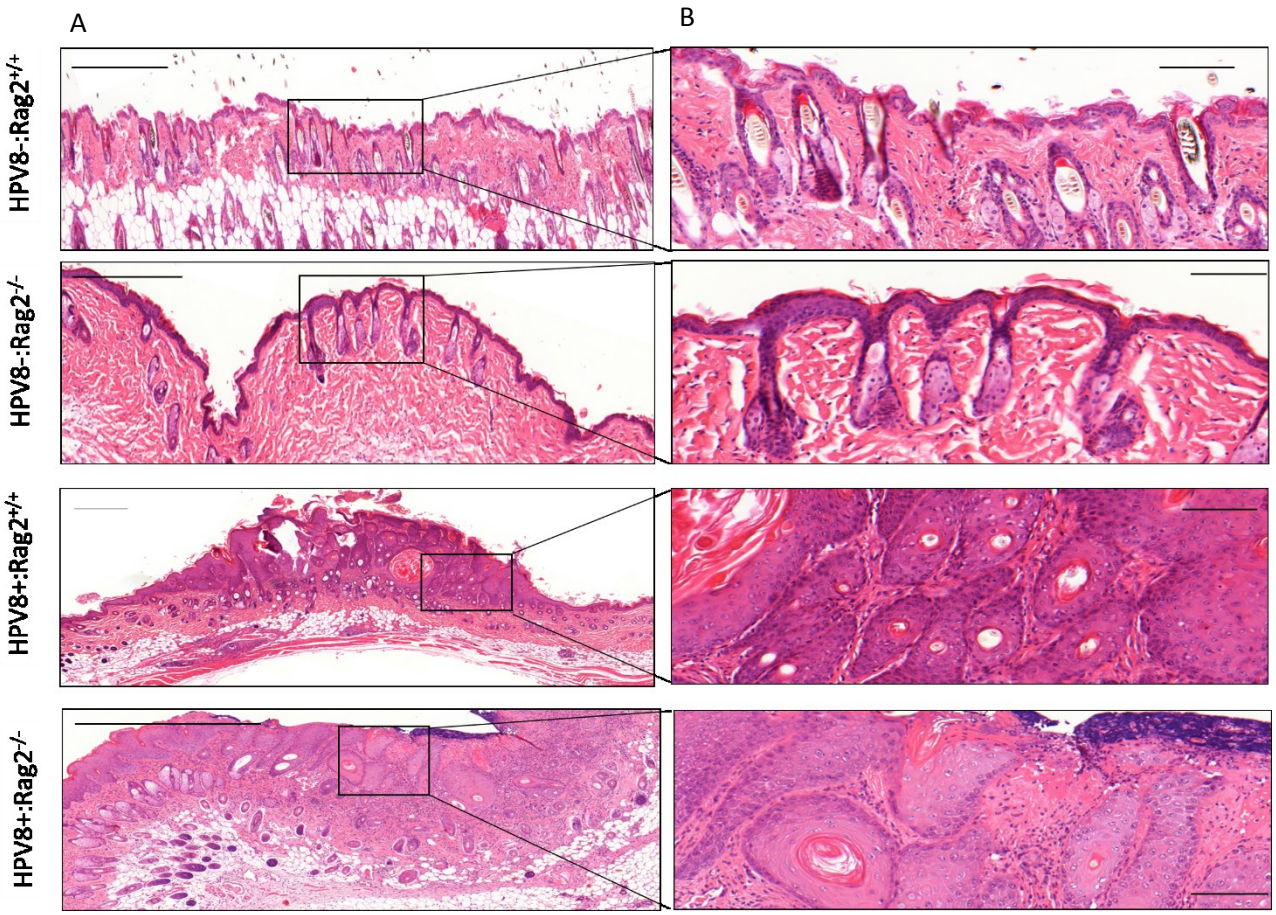

Figure 32. Comparison of the histological features (H&E staining) among the different genotypes. (A). The black squares are enlarged in the right column. (B). Scale bars for the right column are 500 µm and for the left column are 100 µm.

The HPV8tg-:Rag2$^{-/-}$ mice of the F2 generation have been backcrossed with HPV8tg mice to obtain pure FVB/N background. The FVB/N background was chosen because previous studies have shown the susceptibility of the FVB/N in-bred mice to develop epidermal lesions (Shaper et al., 2005; Hennings et al., 1993). We are currently in the third generation of backcrossed mice and we are planning to backcross at least six generations to yield a pure FVB/N background that will be interbred to obtain the genotypes detailed in Table 3.

MATERIAL AND METHODS

Mouse strains

The HPV8tg FVB/N transgenic mice were kindly provided by the group of Herbert Pfister, University of Cologne and have been previously described (Schaper et al., 2005). The Rag2$^{-/-}$ C57BL/6 mice were kindly provided by the group of Cecilia Garlanda from the Humanitas Research Center, Milan and have been previously described (Hao et al., 2001). The mice were housed in the animal facility at the University of Piemonte Orientale, Department of Health Sciences, Novara in accordance with the Guide for the Care and Use of Laboratory Animals. They live in specific pathogen free rooms and in autoclaved, aseptic, and microisolator cages with a maximum of four animals per cage. Food and water were autoclaved and provided *ad libitum*.

Genotyping of progeny

Tail biopsies of 10-day-old mice were cut and put in a microcentrifuge tubes. 400 µl of a solution composed of 125 mM NaCl, 62.5 mM Tris-Cl pH.8, 9.375 mM EDTA pH.8, 0.5% SDS and 1 mg/ml proteinase K were added into each tube and warmed up to 56° for at least 6 hours. At the end of the incubation, 100 µl of 7.5 M NH_4OAc and 600 µl of chloroform were added and mixed. After 15 minutes of incubation on ice, the microcentrifuge tubes were centrifuged at maximun speed for 15 minutes at 4°C. 400 µl of the upper aqueous layer were transferred in a fresh tubes and 750 µl of 100% ethanol were added. The tubes were inverted until white cotton like appeared. After a centrifugation at maximum speed for 5 minutes at 4°C, the supernatant was poured off. Five hundreds µl of 70% ethanol was added and another centrifugation at maximum speed for 5 minutes at 4°C was done. The supernatant was poured off and the pellet kept to dry at room temperature for 10 minutes. Eighty µl of Tris-EDTA pH 7.5 was added to the pellet.

Samples of genomic mouse DNA were analysed by PCR for the presence of the HPV8 transgene using primers that bind the early genes E6 and E7 (see Figure 30B). Forward (FW) primers: 5'-CAATTTTCCTAAGCAAATGGAC-3' and reverse primers (REV): 5'-CACTACATTCAGCTTCCAAAATACA-3'. The PCR reaction conditions consisted of a 4 minutes denaturation step (94°C), 33 cycles of amplification (95°C, 45 seconds; 52°C, 1 minute; 72°C, 1.5 minutes), and a final extension period at 72°C for 7 minutes. PCR products were separated by 1.8% agarose– TAE gel electrophoresis, and SYBR safe DNA gel stain

(Invitrogen) was used to detect the separated bands. HPV8 band sizes were expected to be 842 bp.

For the PCR analysis of the Rag2 gene, 3 sets of primers (1 Forward and 2 Reverse) were used (Rag2 FW 5'–CAAGGACGCTCTAGGAATGCA-3', wtREV 5'-GCTATGTTATGACCCACTGTTAC-3', and mutREV 5'-GCTTTACGGTATCGCCGCTC-3'). The wtREV was specific for exon 3, and the mutREV for the replacement gene (Figure 30A). The PCR protocol was: 4 minutes denaturation step (95°C), 35 cycles of amplification (95°C, 45 seconds; 53°C, 1 minute; 72°C, 1 minutes) and a final extension period at 72°C for 7 minutes. PCR products were separated by 1.5% agarose– TAE gel electrophoresis, and SYBR safe DNA gel stain (Invitrogen) was used to detect the separated bands. Rag2 band sizes were expected to be 324 bp for the wt allele, 419 bp for the mutant allele.

Mice monitoring

All the member of the F2 generation were monitored for 12 weeks once a week. A calliper was used for measuring the size of the two diagonals of the lesions. (D*d)/2 formula was used for calculate the lesional area. Mice weight was calculated with the animal facility scale.

Mice skin biopsy

Mice of F2 generation were sacrified via CO_2 inhalation. The dorsal skin of the mice was shaved and the skin was excised. Formalin fixed and paraffin embedded blocks were prepared for histological analysis by the Pathology Unit at the University-Hospital in Novara.

Haematoxylin and Eosin staining

Consecutive 5-µm thick tissue sections were cut from FFPE blocks onto pre-coated microscope slides, incubated at 60°C for 30 min to increase adhesion on slide surface, dewaxed and rehydrated as follows: twice in xylene for 15 min each, twice in 100% ethanol for 10 min each, followed by a series of graded ethanol (95%, 90%, 70%) for 5 min each and finally 1X PBS for 5 min. The slides were incubated in haematoxylin for 10 min, washed in tap water for 5-10 min, than soaked in eosin for 5 min and washed again quickly in tap water. Tissue sections were than dehydrated in a series of graded ethanol (75% for 20 sec, 95% for 20 sec, 100% for 2 min), diaphanized twice in xylene for 2 min each and finally mounted with a mounting medium for immunohistochemistry (VectaMount permanent mounting medium, Vector Laboratories).

5. CONCLUSIONS

5. Conclusions

Although the role of β-HPV in KC development is not yet fully understood, both experimental and epidemiological evidence suggests a carcinogenic role of β-HPV in this type of skin cancer, especially in the immunocompromised setting. Despite these findings, a causal role of these viruses has been difficult to verify because of their ubiquitous prevalence in the general population, their absence in some cancers, and the lack of experimental models. In this thesis, I report the work we have been doing to provide mechanistic insights into β-HPV-induced skin carcinogenesis in immunosuppressed patients.

During the three year period of my PhD, we have successfully engrafted a series of skin tumour from OTRs using an *in vivo* orthotopic humanized tumourgraft model. The possibility to grow skin tumours in vivo may have important implications in skin cancer research as the main limitation in this field is the small size of the tumours that usually doesn't allow molecular investigations, especially with freshly frozen tissues. In addition, this methodology provides a highly promising *ex vivo* environment in which to study disease progression from pre-malignancy to malignancy e.g. from AK to SCC, which cannot be documented in the human beings (due to the necessary excision of such tumours). Indeed, here we report of an AK excised from a KTR patient with a long history of immunosuppression that gave rise to a tumourgraft that was diagnosis as SCC as well as the lymph node metastatasis found in the neck region of the nude mouse. Worthy of note, the original AK was β-HPV-infected as documented by the presence of intense E4 cytoplasmic staining in the middle and suprabasal layers. Consistent with the "hit and run" mechanism of carcinogenesis describing the cutaneous β-HPV possibly being important for tumour initiation and progression but not necessary for tumour maintenance, the viral proteins were no longer detected in either the SCC or metastasis. Similar results were also obtained with another AK that was removed again from a KTR with a long history of immunosuppression and the development of an EV-like phenotype. In this case the original AK had already some areas with SCC histology. This AK was β-HPV-infected as demonstrated by L1 expression in the more superficial layers of the epithelium. This tumourgraft displayed strong retention of the original AK histology, including cell morphology, stromal component architecture, and grade of differentiation of the epithelia. Although the quality of the FFPE block was not very high, we were able to detect cytoplasmic E4 staining in some cells alongside with HPV DNA FISH signal in some nuclei.

When considering the involvement of β-HPV in the development of KC, it is important to examine where β-HPV is localized in the natural infection. The reservoir for β-HPV is

supposed to reside within long-lived hair follicle keratinocyte stem cells (HF-KSC), since plucked hair consistently demonstrates the presence of β-HPV DNA and KSC characteristics are enhanced by HPV 5 and 8 early region genes (Boxman et al., 1997; Bouwes Bavinck et al., 2008; Hufbauer et al., 2013). However, the precise HF-KSC populations involved in β-HPV latent infection remain to be defined (Kranjec and Doorbar, 2016). To determine the role of HF KSC in β-HPV induced skin carcinogenesis, we utilized a transgenic mouse model in which the entire HPV8 early region genes are expressed under a keratin 14 promoter (HPV8tg) (Schaper et al., 2005; De Andrea et al., 2010). Here, we provide a model of β-HPV-induced skin carcinogenesis that is based on the aberrant expansion of Lrig1+ KSC in the upper hair follicle that spill out into the surrounding epidermis. Different mouse KSC pools are distributed along the HF, defined by the expression of cell surface proteins that facilitate isolation and thus characterization. To date KSC have been identified within four HF regions: upper (Lrig1) and lower (LGR6) junctional zone, the bulge (CD34 and K15) and bulb (LGR5) (Solanas et al, 2013; Kretzschmar et al, 2014). In this study, we have identified the HF Lrig1+ KSC population as the putative target in HPV8tg mice skin carcinogenesis. Lrig1 expression defines a distinct multipotent stem cell population in mammalian epidermis, which resides in the HF junctional zone in mice (Jensen et al., 2009). Although Lrig1 expression defines an IFE KSC population in humans, it is not expressed in the reciprocal HF junctional zone (Figure 33) and so prevented further characterization of the β-HPV target in humans (Jensen et al, 2006).

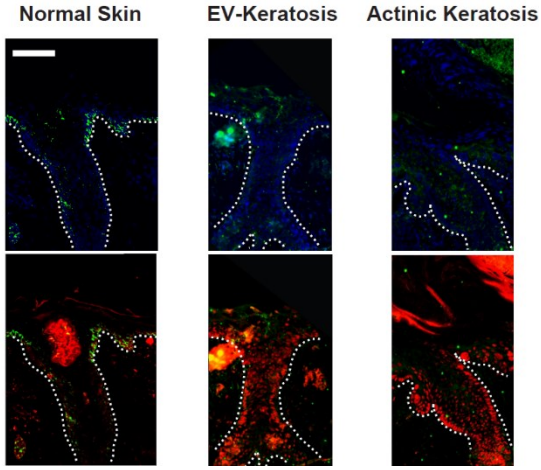

Figure 33: Lrig1 immunolabelling of human skin, EV Keratosis and Actinic Keratosis. Lrig1 (green) and p63 (red) immunofluorescent immunolabelling of formalin fixed paraffin embedded tissue sections from normal human skin, EV Keratosis and Actinic Keratosis corresponding to Figure 21A.The sections were counter stained with DAPI (blue). Scale bar is 100μm.

Reporter mice studies have shown that junctional zone Lrig1 cells give rise to keratinocytes in the infundibulum and adjoining IFE, akin to the expansion of this population in our HPV8tg mice, human EV keratosis and AK.

p63 is a p53 protein family member expressed primarily in epithelia as six distinct isoforms, due to alternative transcription and C terminus splicing (Yang et al., 1998). Three p63 isoforms contain an N-terminal transcriptional activation (TA isoforms) sequence, while the other three do not (ΔN isoforms). All of the p63 isoforms, TA and ΔN, are transcriptionally active and the ΔN isoforms repress TA isoforms as dominant-negative molecules (Koster. 2010). Multiple lines of evidence support the role of p63 in KSC maintenance (Melino et al., 2015): i) p63 null mice demonstrate a terminally differentiated epidermis with no proliferative basal layer containing stem cells (Yang et al., 1999); ii) epidermal p63 knockdown induces differentiation, which is induced by TAp63 (Truong et al., 2006); iii) ΔNp63 expression maintains the proliferative basal layer (Truong et al., 2006); and iv) p63 nuclear accumulation is prominent in KSC and holoclones (Pellegrini et al., 2001). UV directly and via p53 mutation results in p63 downregulation and loss of transcriptional activity (Liefer et al., 2000). Recently it has been proposed that UV induced concomitant activation of oncogenic Ras and TGF-β pathways can restore p63 activity in p53 mutant cells to promote tumor progression (Vasilaki et al., 2016). In keeping with this, UV induced AK and cutaneous SCC frequently demonstrate nuclear p63 (Abbas et al., 2011). The frequency of nuclear p63 positivity is greater in HPV associated SCC of the oral and anogentital regions, promoted by HPV E6 degradation of p53 (Melino, 2011).

β-HPV early region genes E2, E6 and E7 can induce KSC proliferation through inhibition of Notch signaling and subsequent induction of p63 (Hufbauer et al., 2013; Meyers et al., 2013, Pfefferle et al., 2008) providing a putative mechanism for this β-HPV induced field cancerization. Hence, we propose that β-HPV early region genes initiate proliferation of Lrig1+ KSC causing their expansion into the overlying HF infundibulum and overlying epidermis. β-HPV driven KSC proliferation results in EV keratosis and occasionally non-EV AK, which are predisposed to transformation into SCC whereupon the β-HPV episome and so gene expression is lost (Figure 34).

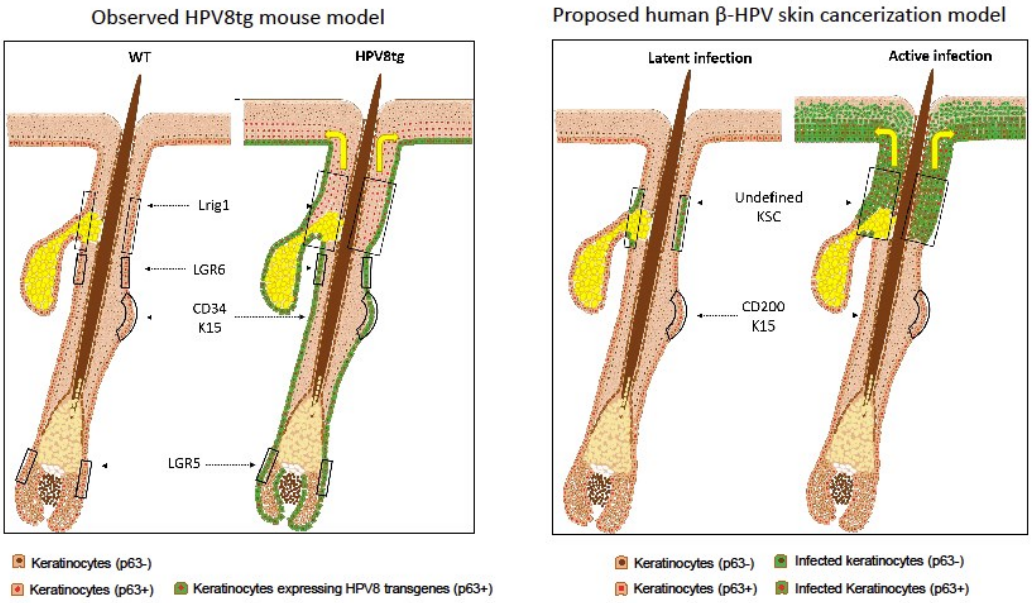

Figure 34: β-HPV Field Cancerization Model
The mouse HF (left image) is composed by at least 4 different KSC populations. In the WT HF, the LGR5 is expressed in the hair bulb, CD34+ and K15+ KSC are located in the bulge, and the Lrig1 and LGR6 KSC are located in the upper and lower junctional zone respectively. In HPV8tg, the Lrig1 KSC population expand beyond the junctional zone niche and no longer express Lrig1 but they maintain KSC function. Similarly, in human β-HPV reactivation (right image), the expanded population occupies the hair follicle infundibulum and adjoining interfollicular epidermis, as shown by the yellow arrow. These changes culminate in the histological phenotype known as Freudenthal's funnel, the pathognomonic finding in actinic keratosis and skin field cancerization.

However, it remains to be determined whether immunosuppression also facilitates carcinogenesis by inhibiting tumour immune surveillance and killing. To test this hypothesis and generate a mouse model that recapitulates the events occurring in OTR, we have crossed the β-HPV8 transgenic mice (FVB/N genetic background) with Rag2 deficient mice (which lack B and T cells; C57BL/6 genetic background). If immunosuppression also facilitates carcinogenesis by inhibiting tumour immune surveillance, we would expect an increased SCC frequency in the HPV8+:Rag2$^{-/-}$ mice compared with the control genotype. The littermates from the F2 generation have been already obtained and are being backcrossed with HPV8tg mice to yield a pure FVB/N background. We are planning to backcross at least six generations to yield a pure FVB/N background that will be then interbred to obtain inbred genotypes. Although the mice are still in a mix genetic background, the phenotype of the HPV8+:Rag2$^{-/-}$ mice seems to be more aggressive in terms of the rate of skin cancer development and progression. There was evidence of a significant hair loss all over the body in these mice, and they developed large skin lesions that quickly progressed to high grade malignant tumours.

When we looked at the histology of the skin lesions derived from HPV8tg+:Rag2$^{-/-}$ mice, some interesting observations were made. While the HPV8tg+:Rag2$^{+/+}$ skin lesions showed the classical histology of papilloma with acanthosis, hyperkeratosis, and the presence of horn pearls, those from HPV8tg+:Rag2$^{-/-}$ mice were characterized by a higher degree of hyperplasia, a lower grade of differentiation, and the presence of some atypical cells especially in the upper layers. Although these data need to be strengthen in the inbred mice, they suggest that the reduced tumour immune surveillance occurring in these mice is increasing the oncogenic activity of the β-HPV early region.

6. REFERENCES

Abbas O, Richards JE, Yaar R, Mahalingam M. Stem cell markers (cytokeratin 15, cytokeratin 19 and p63) in in situ and invasive cutaneous epithelial lesions. Mod Pathol 2011;24(1):90-7

Akgul B, Cooke JC, Storey A. HPV-associated skin disease. J Pathol 2006; 208:165-75

Aldabagh B, Angeles JG, Cardones AR, Arron ST. Cutaneous squamous cell carcinoma and human papillomavirus: is there an association?. Dermatol Surg 2013; 39:1-23

Arron ST, Jennings L, Nindl I, Rosl F, Bouwes Bavinck JN, Seçkin D, et al. Viral oncogenesis and its role in nonmelanoma skin cancer. Br J Dermatol 2011; 164:1201-13

Bergvall M, Melendy T, Archambault J. The E1 proteins. Virology 2013; 445:35-56

Bernard HU, Burk RD, Chen Z van Doorslaer K, zur Hausen H, de Villiers EM Classification of papillomaviruses (PVs) based on 189 types and proposal of taxonomic amendments. Virology 2010; 401:70-9

Bernard HU. Taxonomy and phylogeny of papillomaviruses: an overview and recent developments. Infect Genet Evol 2013; 18:357–61

Borgogna C, Zavattaro E, De Andrea M, Griffin HM, Dell'Oste V, Azzimonti B, et al. Characterization of beta papillomavirus E4 expression in tumours from Epidermodysplasia Verruciformis patients and in experimental models. Virology 2012; 423:195–204

Borgogna C, Landini MM, Lanfredini S, Doorbar J, Bouwes Bavinck JN, Quint KD, et al. Characterization of skin lesions induced by skin-tropic α- and β-papillomaviruses in a patient with epidermodysplasia verruciformis. Br J Dermatol 2014; 171:1550-4

Borgogna C, Lanfredini S, Peretti A, De Andrea M, Zavattaro E, Colombo E, et al. Improved detection reveals β-papillomavirus infection in skin lesions from kidney transplant recipients. Mod Pathol 2014; 27:1101-15.

Bouwes Bavinck JN, Plasmeijer EI, Feltkamp MC. Beta-papillomavirus infection and skin cancer. J Invest Dermatol 2008; 128(6):1355-8

Bouwes Bavinck JN, Neale RE, Abeni D, Euvrard S, Green AC, Harwood CA et al. Multicenter study of the association between betapapillomavirus infection and cutaneous squamous cell carcinoma. Cancer Res 2010; 70: 9777–9786.

Boxman IL, Berkhout RJ, Mulder LH, Wolkers MC, Bouwes Bavinck JN, Vermeer BJ et al. Detection of human papillomavirus DNA in plucked hairs from renal transplant recipients and healthy volunteers. J Invest Dermatol 1997;108:712–5

Braun KM, Niemann C, Jensen UB, Sundberg JP, Silva-Vargas V, Watt FM. Manipulation of stem cell proliferation and lineage commitment: visualisation of label-retaining cells in wholemounts of mouse epidermis. Development. 2003;130(21):5241-55.

Cangkrama M, Ting SB, Darido C. Stem cells behind the barrier. Int J Mol Sci. 2013; 14 (7):13670-86

Ciesielska U, Nowinska K, Podhorska-Okolow M, Dziegiel P. The role of human papillomavirus in the malignant transformation of cervix epithelial cells and the importance of vaccination against this virus. Adv Clin Exp Med 2012; 21:235-44

Connolly K, Manders P, Earls P, Epstein RJ. Papillomavirus-associated squamous skin cancers following transplant immunosuppression: one Notch closer to control. Cancer Treat Rev 2014; 40:205-14

Crequer A, Picard C, Patin E, D'Amico A, Abhyankar A, Munzer M et al. Inherited MST1 deficiency underlies susceptibility to EV-HPV infections. PLoS One 2012; 7(8):e44010

Crequer A, Troeger A, Patin E, Ma CS, Picard C, Pedergnana V, et al. Human RHOH deficiency causes T cell defects and susceptibility to EV-HPV infections. J Clin Invest 2012; 122:3239-47

Crosbie EJ, Einstein MH, Franceschi S, Kitchener HC. Human papillomavirus and cervical cancer. Lancet 2013; 382:889-99

Cubie HA. Diseases associated with human papillomavirus infection. Virology 2013; 445:21-34

De Andrea Marco, Massimo Rittà, Manuela M Landini, Cinzia Borgogna, Michele Mondini, Florian Kern, Karin Ehrenreiter, et al. Keratinocyte-Specific stat3 Heterozygosity Impairs Development of Skin Tumors in Human Papillomavirus 8 Transgenic Mice. Cancer Research 2010; 70 (20): 7938–48.

de Villiers EM, Fauquet C, Broker TR, Bernard HU, zur Hausen H. Classification of papillomaviruses. Virology 2004; 324:17-27

Donati G. and Watt FM. Stem cell heterogeneity and plasticity in epithelia. Cell Stem Cell 2015; 16, 465–476

Doorbar J. Papillomavirus life cycle organization and biomarker selection. Dis Markers 2007; 23:297-313

Doorbar J, Quint W, Banks L, Bravo IG, Stoler M, Broker TR. et al. The biology and life-cycle of human papillomaviruses. Vaccine 2012; 30 Suppl5:F55-70

Doorbar J. The E4 protein: structure, function and patterns of expression. Virology 2013; 445:80-98

Euvrard S, Kanitakis J, Claudy A. Skin cancers after organ transplantation. N Engl J Med 2003; 348: 1681–1691

Feltkamp MC, de Koning MN, Bavinck JN, Ter Schegget J. Betapapillomaviruses: innocent bystanders or causes of skin cancer. J Clin Virol 2008; 43:353-60

Forslund O. Genetic diversity of cutaneous human papillomaviruses. J Gen Virol 2007; 88:2662-9

Hao, Z. & Rajewsky, K. Homeostasis of peripheral B cells in the absence of B cell influx from the bone marrow. 2001 J. Exp. Med. 194:1151–64.

Harwood CA, Proby CM. Human papillomaviruses and non-melanoma skin cancer. Curr Opin Infect Dis 2002; 15:101-14

Hennings H, Glick AB, Lowry DT, Krsmanovic LS, Sly LM, Yuspa SH, FVB/N mice: an inbred strain sensitive to the chemical induction of squamous cell carcinomas in the skin. Carcinogenesis. 1993;14(11):2353-8.

Hufbauer M, Biddle A, Borgogna C, Gariglio M, Doorbar J, Storey A, et al. Expression of betapapillomavirus oncogenes increases the number of keratinocytes with stem cell-like properties. J Virol. 2013; 87(22):12158-65.

Jensen KB, Watt FM. Single-cell expression profiling of human epidermal stem and transit-amplifying cells: Lrig1 is a regulator of stem cell quiescence. Proc Natl Acad Sci U S A. 2006, 8;103(32):11958-63.

Jensen KB, Collins CA, Nascimento E, Tan DW, Frye M, Itami S, et al. Lrig1 expression defines a distinct multipotent stem cell population in mammalian epidermis. Cell Stem Cell 2009; 4:427–39.

Knipe DM, Howley PM, "Fields Virology, 4th edition", 2001; 41:121-32

Knipe DM, Howley PM, "Fields Virology 5th edition", 2007

Koster MI. p63 in skin development and ectodermal dysplasias. J Invest Dermatol 2010;130(10):2352-8.

Kranjec C., Doorbar J. Human papillomavirus infection and induction of neoplasia: a matter of fitness. Curr Opin Virol. 2016; 20:129-136

Kretzschmar K, Watt FM. Markers of epidermal stem cell subpopulations in adult mammalian skin. Cold Spring Harb Perspect Med. 2014; 3; 4(10).

Landini MM, Borgogna C, Peretti A, Colombo E, Zavattaro E, Boldorini R. et al. α- and β-papillomavirus infection in a young patient with an unclassified primary T-cell immunodeficiency and multiple mucosal and cutaneous lesions. J Am Acad Dermatol. 2014; 71(1):108-15

Lazarczyk M, Pons C, Mendoza JA, Cassonnet P, Jacob Y, Favre M. Regulation of cellular zinc balance as a potential mechanism of EVER-mediated protection against pathogenesis by cutaneous oncogenic human papillomaviruses. J Exp Med 2008; 205: 35-42.

Leiding JW, Holland SM. Warts and all: human papillomavirus in primary immunodeficiencies. J Allergy Clin Immunol 2012; 130:1030-48

Liefer KM, Koster MI, Wang XJ, Yang A, McKeon F, Roop DR. Down-regulation of p63 is required for epidermal UV-B-induced apoptosis. Cancer Res 2000;1;60(15):4016-20

McBride AA. The papillomavirus E2 proteins. Virology 2013; 445:57-59

McLaughlin-Drubin M, Meyers J, Munger K. Cancer associated human papillomaviruses. Curr Opinion Virol 2012; 2:459-466

Melino G. p63 is a suppressor of tumorigenesis and metastasis interacting with mutant p53. Cell Death Differ 2011;18(9):1487-99

Melino G, Memmi EM, Pelicci PG, Bernassola F. Maintaining epithelial stemness with p63. Sci Signal 2015;8(387):re9

Meyers JM, Spangle JM, Munger K. The human papillomavirus type 8 E6 protein interferes with NOTCH activation during keratinocyte differentiation. J Virol 2013;87:4762-7

Michel A, Kopp-Schneider A, Zentgraf H, Gruber AD, de Villiers EM. E6/E7 expression of human papillomavirus type 20 (HPV-20) and HPV-27 influences proliferation and differentiation of the skin in UV-irradiated SKH-hr1 transgenic mice. J Virol 2006, 80: 11153–11164.

Moody CA, Laimins LA. Human papillomavirus oncoproteins: pathways to transformation. Nat Rev Cancer 2010; 10:550-60

Nindl I, Gottschling M, Stockfleth E. Human papillomaviruses and non-melanoma skin cancer: basic virology and clinical manifestations. Dis Markers 2007; 23:247-59

Page ME, Lombard P, Ng F, Göttgens B, Jensen KB. The Epidermis Comprises Autonomous Compartments Maintained by Distinct Stem Cell Populations. Cell Stem Cell. 2013; 13 (4):471-482.

Patel G, Yee C, Yuspa S, Vogel J. A humanized stromal bed is required for engraftment of isolated human primary squamous cell carcinoma cells in immunocompromised mice. J Invest Dermatol 2012; 132:284-90

Pellegrini G, Dellambra E, Golisano O, Martinelli E, Fantozzi I, Bondanza S et al. p63 identifies keratinocyte stem cells. Proc Natl Acad Sci U S A 2001;98(6):3156-61

Pfefferle R, Marcuzzi GP, Akgul B Kasper HU, Schulze F, Haase I, et al. The human papillomavirus type 8 E2 protein induces skin tumors in transgenic mice. J Invest Dermatol 2008; 128:2310-5

Pfister H. "Chapter 8: Human papillomavirus and skin cancer." J Natl Cancer Inst Monogr 2003; 52-56

Quint KD, Genders RE, de Koning MNC, Borgogna C, Gariglio M, Bouwes Bavinck JN, et al. Human Beta-papillomavirusinfection and keratinocyte carcinomas. J Pathol. 2015; 235(2):342–54

Roman A, Munger K. The papillomavirus E7 proteins. Virology 2013; 445:138-68

Schaper ID, Marcuzzi GP, Weissenborn SJ. Kasper HU, Dries V, Smyth N. et al. Development of skin tumors in mice transgenic for early genes of human papillomavirus type 8. Cancer Res 2005; 65:1394-400

Shinkai Y, Rathbun G, Lam K, Oltz E, Stewart V, Mendelsohn M, et al. RAG-2- deficient mice lack mature lymphocytes owing to inability to initiate V(D)J rearrangement. Cell. 1992 6;68:855-67.

Singh A, Park H, Kangsamaksin T, Singh A, Readio N, Morris RJ. Keratinocyte Stem Cells and the Targets for Nonmelanoma Skin Cancer. Photochem Photobiol. 2012 88(5):1099-110

Solanas G, Benitah SA. Regenerating the skin: a task for the heterogeneous stem cell pool and sourraunding niche. Nat Rev Mol Cell Biol. 2013 14(11):737-48.

Stanley MA. Epithelial cell responses to infection with human papillomavirus. Clin Microbiol Rev 2012; 25:215-22

Strachan LR, Ghadially R. Tiers of clonal organization in the epidermis: the epidermal proliferation unit revisited. Stem Cell Rev. 2008; 4(3):149-57

Tessari G, Naldi L, Boschiero L, Nacchia F, Fior F, Forni A, et al. Incidence and clinical predictors of a subsequent nonmelanoma skin cancer in solid organ transplant recipients with a first non-melanoma skin cancer: a multicentre cohort study. Arch Dermatol 2010; 146: 294–299.

Tinsley, J. M., C. Fisher, and P. F. Searle. Abnormalities of Epidermal Differentiation Associated with Expression of the Human Papillomavirus Type 1 Early Region in Transgenic Mice. J Gen Virol. 1992,73 (5): 1251–60.

Tommasino M. The human papillomavirus family and its role in carcinogenesis. Semin Cancer Biol 2014, 26:13-21

Truong AB, Kretz M, Ridky TW, Kimmel R, Khavari PA. p63 regulates proliferation and differentiation of developmentally mature keratinocytes. Genes Dev 2006;20(22):3185-97

Van Doorslaer K. Evolution of the papillomaviridae. Virology 2013; 445:11-20

Vasilaki E, Morikawa M, Koinuma D, Mizutani A, Hirano Y, Ehata S, et al. Ras and TGF-β signaling enhance cancer progression by promoting the INp63 transcriptional program. Sci Signal 2016; 9:ra84.

Viarisio D, Mueller-Decker K, Kloz U, Aengeneyndt B, Kopp-Schneider A, Gröne HJ, et al. E6 and E7 from beta HPV38 cooperate with ultraviolet light in the development of actinic keratosis-like lesions and squamous cell carcinoma in mice. PLoS Pathog. 2011; 7(7):e1002125.

Yang A, Kaghad M, Wang Y, Gillett E, Fleming MD, Dotsch V, et al. p63, a p53 homolog at 3q27-29, encodes multiple products with transactivating, death-inducing, and dominantnegative activities. Mol Cell 1998;2: 305–316

Yang A, Schweitzer R, Sun D, Kaghad M, Walker N, Bronson RT et al. p63 is essential for regenerative proliferation in limb, craniofacial and epithelial development. Nature 1999;398(6729):714-8

Watt FM, Jensen KB. Epidermal stem cell diversity and quiescence. EMBO Mol Med. 2009; 1(5):260-7.

Watt, FM. Mammalian skin cell biology: at the interface between laboratory and clinic. Science, 2014; 346:937–940.